รายงานโครงการวิจัยฉบับสมบูรณ์

โครงการ: บทบาทของเอนไซม์เอ็นเอดีพีเอชออกซิเดส ในกระบวนการตายของเซลล์ออสติโอบ ลาสต์เนื่องจากเหล็ก และศักยภาพของสารยับยั้งเอนไซม์เอ็นเอดีพีเอชออกซิเดส ในการรักษาภาวะ กระดูกพรุนในผู้ป่วยธาลัสซีเมียและผู้มีภาวะเหล็กเกิน

The role of NADPH oxidases in iron-mediated osteoblastic cell death and the therapeutic potential of NOXs inhibitors in iron overload and thalassemia-induced osteoporosis

รหัสโครงการ MRG6180268

คณะผู้วิจัย

หัวหน้าโครงการ

ผู้ช่วยศาสตราจารย์ ดร.กรกมล เลิศสุวรรณ ภาควิชาชีวเคมี คณะวิทยาศาสตร์ มหาวิทยาลัยมหิดล

นักวิจัยที่ปรึกษา

ศาสตราจารย์ ดร.นพ.นรัตถพล เจริญพันธุ์ สถาบันชีววิทยาศาสตร์โมเลกุล มหาวิทยาลัยมหิดล

สนับสนุนโดยสำนักงานคณะกรรมการการอุดมศึกษา และสำนักงานกองทุนสนับสนุนการวิจัย (ความเห็นในรายงานนี้เป็นของผู้วิจัย สกอ. และ สกว. ไม่จำเป็นต้องเห็นด้วยเสมอไป)

Project title: บทบาทของเอนไซม์เอ็นเอดีพีเอชออกซิเดส ในกระบวนการตายของเซลล์ออสติโอบลาสต์เนื่องจากเหล็ก

และศักยภาพของสารยับยั้งเอนไซม์เอ็นเอดีพีเอชออกซิเดส ในการรักษาภาวะกระดูกพรุนในผู้ป่วย

ชาลัสซีเมียและผู้มีภาวะเหล็กเกิน

The role of NADPH oxidases in iron-mediated osteoblastic cell death and the therapeutic potential

of NOXs inhibitors in iron overload and thalassemia-induced osteoporosis

Project duration: 2 years (from 2nd July 2018 to 1st July 2020)

Principal investigator: Assistant professor Dr. Kornkamon Lertsuwan, Ph.D.

Mentor: Professor Dr. Narattaphol Charoenphandhu, M.D., Ph.D.

Abstract

The association between iron overload and osteoporosis has been found in many diseases, such as hemochromatosis, β-thalassemia and sickle cell anemia with multiple blood transfusion. One of the contributing factors is iron toxicity to osteoblasts. Herein, ferric ammonium citrate (FAC) and ferrous ammonium sulfate (FAS) were used as ferric and ferrous donors. Our results showed that both iron species suppressed cell survival and proliferation. Both also induced osteoblast cell death consistent with the higher levels of cleaved caspase 3 and caspase 7 in osteoblasts indicating that iron-induced osteoblast apoptosis. By using ferroptosis inhibitor, ferrostatin-1 as well as the determination of glutathione peroxidase 4 expression, our data showed that iron-induced osteoblasts also relied on ferroptosis. Additionally, both iron species could induce G0/G1 cell cycle arrest in osteoblasts with the stronger effects from ferric than ferrous. Downregulation of osteoblast differentiation genes was observed in osteoblasts exposed to ferric and ferrous. Decreased alkaline phosphatase (ALP expression), ALP activity and mineralization in osteoblasts under iron overload were also shown with the stronger effects from ferric than ferrous. Cellular ROS production was significantly increased in osteoblasts exposed to ferric and ferrous, but antioxidant agent (N-acetyl cysteine; NAC) could not alleviate osteoblast cell death. In addition, the expression of NADPH oxidases (NOX1 and NOX4) was also significantly increased in iron treated osteoblasts, but NOX inhibitor (diphenylene iodonium; DPI) failed to rescued iron-osteoblast cell death suggesting that iron-induced osteoblast cell death did not depend on NOX expression or activity. Iron treatments led to the elevated intracellular iron in osteoblasts as determined by flame atomic absorption spectrophotometry. Iron chelator (deferiprone; DFP); however, could not rescue iron-induced osteoblast cell death. As the common treatment for calcium malabsorption, effects of 1,25 dihydroxyvitamin D₃ [1,25(OH)₂D₃] and exogenous calcium on osteoblast cell viability and iron uptake capacity in osteoblasts under iron overload were investigated. While 1,25 dihydroxyvitamin D₃ [1,25(OH)₂D₃] treatment led to increased levels of intracellular iron in osteoblasts exposed to iron, it did not affect osteoblast cell viability under iron overload. These results confirmed the independence of intracellular iron level or iron uptake capacity in iron-induced osteoblast cell death. Interestingly, our results showed that exogenous treatment of calcium improved osteoblast cell viability under iron overload suggesting the potential therapeutic application of exogenous calcium treatment in iron overload-induced osteoporosis. In conclusion, ferric and ferrous differentially compromised the osteoblast functions and viability, which can be alleviated by an increase in extracellular ionized calcium, but not 1,25(OH)2D3 or iron chelator DFP. This study has provided the invaluable information for therapeutic design targeting specific iron specie(s) in iron overload-induced osteoporosis. Moreover, an increase in extracellular calcium could be beneficial for this group of patients. Results from this project have been published and accepted in 2 international peer-reviewed journals including Biometals (impact factor 2.478, Q1) and PLoS One (impact factor 2.776, Q1) Moreover, results have been presented (both oral and poster presentation) and published in 4 international conferences both in Thailand and abroad

บทคัดย่อ

ภาวะกระดูกพรุนถูกพบเป็นภาวะแทรกซ้อนได้มากในโรคหลายชนิดที่เกิดภาวะเหล็กเกิน (iron overload) ร่วมด้วย เช่น โรคธาลัสซีเมียชนิดเบต้า โรค sickle cell anemia ที่อาจมีภาวะเหล็กเกินจากการรับเลือดอย่างต่อเนื่อง หนึ่งในปัจจัยที่ ทำให้เกิดภาวะกระดูกพรุนแทรกซ้อนกับภาวะเหล็กเกินได้แก่ ภาวะที่เหล็กทำให้เกิดการตาย หรือยับยั้งการทำงานของเซลล์ สร้างกระดูก (เซลล์ออสติโอบลาสต์; osteoblast) ในการศึกษานี้เฟอร์ริกแอมโมเนียมซิเตรท และเฟอร์รัสแอมโมเนียมซัลเฟต ถูกใช้เป็นตัวแทนของเหล็กเฟอร์ริกและเฟอร์รัสตามลำดับ ผลการศึกษาพบว่าเหล็กทั้งสองรูปแบบสามารถความสามารถใน การแบ่งเซลล์ และทำให้เกิดการตายของเซลล์ออสติโอบลาสต์ได้ เหล็กทั้งสองชนิดสามารถทำให้เกิดการเพิ่มขึ้นของ cleaved caspase 3 และ cleaved caspase 7 บ่งชี้ว่าภาวการณ์ตายของเซลล์ออสติโอบลาสต์ภายใต้ภาวะเหล็กเกินนั้นเกิดผ่าน กระบวนการอะพอพโตซิส (Apoptosis) นอกจากนี้เมื่อทำการทดลองโดยใช้สารยับยั้งกระบวนการตายแบบเฟอร์รอพโตซิส (Ferroptosis) ได้แก่สาร Ferrostatin-1 ร่วมกับการติดตามการแสดงออกของโปรตีน Glutathione peroxidase 4 (GPX4) ทำ ให้ได้ข้อมูลเพิ่มเติมว่าการตายของเซลล์ออสติโอบลาสต์ภายใต้ภาวะเหล็กเกินยังเกิดผ่านกระบวนการเฟอร์รอพโตซิสอีกด้วย ็นอกจากนี้เหล็กทั้งสองรูปแบบยังทำให้เกิด cell cycle arrest ที่ระยะ G0/G1 ซึ่งนำไปสู่การยับยั้งกระบวนการแบ่งเซลล์และ ทำให้เกิดการตายของเซลล์ได้ การยับยั้งการแสดงออกของยืนที่เกี่ยวข้องกับการพัฒนาของเซลล์ออสติโอบลาสต์ อีกทั้งการ ลดลงของการแสดงออกและกิจกรรมของเอนไซม์อัลคาไลน์ฟอสฟาเตส (Alkaline phosphatase; ALP) และการสะสม แคลเซียมของเซลล์ออสติโอบลาสต์ที่ได้รับเหล็ก บ่งชี้ว่าเหล็กทั้งสองรูปแบบยับยั้งการพัฒนาและความสามารถในการสะสม แคลเซียมของเซลล์ออสติโอบลาสต์ อย่างไรก็ดีผลการทดลองทั้งหมดพบว่าเหล็กในรูปแบบเฟอร์ริกมีความเป็นพิษต่อเซลล์ ออสติโอบลาสต์มากกว่าเฟอร์รัส นอกจากนี้ยังพบว่าเซลล์ออสติโอบลาสต์ที่ได้รับเหล็กมีการสร้าง Reactive oxygen species (ROS) เพิ่มขึ้นในเซลล์ออสติโอบลาสต์ แต่การได้รับสาร antioxidant ได้แก่ N-acetyl cysteine (NAC) ก็ไม่สามารถยับยั้งการ ตายของเซลล์ออสติโอบลาสต์ และการแสดงออกของเอนไซม์เอ็นเอดีพีเอชออกซิเดส (NADPH oxidases; NOXs) ได้แก่ NOX1 และ NOX4 ก็เพิ่มขึ้นในเซลล์กลุ่มนี้ แต่การใช้สารยับยั้งการทำงานของเอนไซม์ดังกล่าวได้แก่ Diphenylene iodonium (DPI) ก็ไม่สามารถป้องกันการตายของเซลล์ออสติโอบลาสต์ได้ นอกจากนี้เมื่อทำการวัดความสามารถในการนำเหล็กเข้า เซลล์ (Iron uptake) ของเซลล์ออสติโอบลาสต์ในภาวะเหล็กเกิน พบว่าเซลล์ออสติโอบลาสต์มีการนำเหล็กเข้าสู่เซลล์ที่เพิ่มขึ้น ในภาวะเหล็กเกิน แต่การลดระดับของเหล็กภายในเซลล์โดยใช้ Iron chelator ได้แก่ Deferiprone (DFP) ก็ไม่สามารถช่วย ้ป้องกันการตายของเซลล์ออสติโอบลาสต์ภายใต้ภาวะเหล็กเกินได้ เป็นการยืนยันว่าการตายของเซลล์ออสติโอบลาสต์ภายใต้ ภาวะเหล็กเกินไม่ขึ้นกับปริมาณของเหล็กที่เซลล์ออสติโอบลาสต์นำเข้าสู่เซลล์ เนื่องจากวิตามินดี และแคลเซียมเสริมเป็นอีก หนึ่งหนทางในการรักษาผู้ป่วยที่อาจเกิดภาวะกระดูกพรุนได้ ผลของสารทั้งสองต่อการตายของเซลล์ออสติโอบลาสต์ภายใต้ ภาวะเหล็กเกินจึงถูกทำการศึกษา ผลการศึกษาพบว่าวิตามินดีทำให้เกิดการนำเข้าเหล็กสู่เซลล์ออสติโอบลาสต์มากขึ้นแต่ไม่ ้มีผลต่อการตายของเซลล์ออสติโอบลาสต์ภายใต้ภาวะเหล็กเกิน ในขณะที่การให้แคลเซียมในรูปของ CaCl, สามารถป้องกัน การตายของเซลล์ออสติโอบลาสต์ภายใต้ภาวะเหล็กเกินได้ โดยสรุปแล้ว ผลการศึกษาครั้งนี้พบกว่าเหล็กทั้งรูปแบบเฟอร์ริก และเฟอร์รัสสามารถทำให้เกิดการตาย และยับยั้งการทำงานของเซลล์ออสติโอบลาสต์ได้ โดยกระบวนการดังกล่าวไม่ถูก ยับยั้งได้โดยการใช้ DFP หรือวิตามินดี แต่จะถูกยับยั้งได้โดยการใช้แคลเซียมเสริม ผลการศึกษานี้ได้ให้ข้อมูลสำคัญเพื่อ ประกอบการออกแบบการรักษาผู้ป่วยที่มีภาวะกระดูกพรุนจากการมีเหล็กเกิน (Iron-induced osteoporosis) เช่นผู้ป่วยธาลัส-ซีเมียได้ ผลที่ได้การศึกษาได้ถูกเผยแพร่ (Published) และได้รับการตอบรับ (accepted) ใน international peer-reviewed journals 2 เรื่องในวารสาร Biometals (Impact factor 2.478, Q1) และวารสาร PLoS One (Impact factor 2.776, Q1) นอกจากนี้ผลการศึกษาที่ได้ยังได้ถูกเผยแพร่ทั้งในรูปแบบของโปสเตอร์ การบรรยาย และ proceedings ในงานประชุม วิชาการระดับนานาชาติทั้งสิ้น 4 งานทั้งในและต่างประเทศ

Keywords: osteoblasts, iron overload, osteoporosis คำสำคัญ: ออสติโอบลาสต์, ภาวะเหล็กเกิน, โรคกระดูกพรุน

Executive Summary

Contract number: MRG6180268

Project title: บทบาทของเอนไซม์เอ็นเอดีพีเอชออกซิเดส ในกระบวนการตายของเซลล์ออสติโอบลาสต์เนื่องจากเหล็ก

และศักยภาพของสารยับยั้งเอนไซม์เอ็นเอดีพีเอชออกซิเดส ในการรักษาภาวะกระดูกพรุนในผู้ป่วยธาลัสซี เมียและผู้มีภาวะเหล็กเกินThe role of NADPH oxidases in iron-mediated osteoblastic cell death and

the therapeutic potential of NOXs inhibitors in iron overload and thalassemia-induced osteoporosis

Project duration: 2 years (from 2nd July 2018 to 1st July 2020)

Principal investigator: Dr. Kornkamon Lertsuwan, Ph.D.

Mentor: Professor Dr. Narattaphol Charoenphandhu, M.D., Ph.D.

1. Introduction to the research problem and its significance

It has been shown that more than 50% of ß-thalassemia patients develop osteoporosis and osteopenia, which can lead to patients' immobility, morbidity and even mortality Haidar (2011), De Sanctis (2013). Similar phenomenon could be seen in thalassemic mouse models Charoenphandhu (2013), Kraidith (2016), Thongchote (2011), Thongchote (2014), Thongchote (2015). In addition to osteoporosis, iron overload is another complication commonly found in thalassemia patients. Iron has been shown to have negative effects on osteoblast differentiation and function, which could contribute to iron overload-induced osteoporosis Diamond (1991), Chen (2015), Tsay (2010), Zhao (2014). Corresponding to other studies, results from our group also showed the negative effects of iron on osteoblast survival (Lertsuwan, et al., unpublished data). Knowing the underlying mechanism of iron-induced osteoblast cell death will provide the critical data for therapeutic method for iron overload-induced osteoporosis. However, the signaling involving in iron-induced osteoblastic cell death has not been elucidated.

Studies in mammalian cells showed that iron exposure leads to increased intracellular reactive oxygen species (ROS) accumulation from the reduced level of antioxidant, glutathione. Enzymes that play a crucial role in iron-mediated cell death is a group of ROS-producing enzymes called NADPH oxidases (NOXs) Dixon (2012). Previous studies showed that overactivated NOXs contributed to high level of oxidative stress associated with osteoporosis Schroder (2015), Schroder (2009), Leboff (2009), and ROS production from NOXs caused osteoblast damage and dysfunction Nojiri (2011). Therefore, the involvement of ROS and NOX in osteoblast toxicity under iron overload was investigated. Since iron chelator has been widely used to prevent iron overload in patients with thalassemia and other iron overload causing diseases, the association of iron uptake capacity and the effects of iron chelator in iron-induced-cell death were also demonstrated.

In summary, this study provided the information about mechanisms behind iron-induced osteoblast cell death and the potential involvement of NOXs in this mechanism were investigated. In addition, effects of iron overload on osteoblast differentiation and mineralization as well as osteoblast cell proliferation and cell cycle progression under iron overload were examined. The potential therapeutic properties of NOX inhibitor (diphenylene iodonium; DPI), iron chelator (deferiprone; DFP) and antioxidant agent (N-acetyl cysteine; NAC) in iron-induced osteoblast cell death were tested. Last but not least, the effects of the commonly used calcium absorption enhancer (vitamin D₃) and exogenous calcium treatment on osteoblast cell death under iron overload were also demonstrated. This study provided an

important data for the identification of novel therapeutic target(s) and methods for iron-mediated osteoporosis in iron overload and/or thalassemia patients.

Results from this project has been published and accepted in 2 international peer-reviewed journals including Biometals (impact factor 2.478, Q1) in the topic of "Ferrous and ferric differentially deteriorate proliferation and differentiation of osteoblast-like UMR-106 cells" and PLoS One (impact factor 2.776, Q1) in the topic of "Differential effects of Fe²⁺ and Fe³⁺ on osteoblasts and the effects of 1,25(OH)₂D₃, deferiprone and extracellular calcium on osteoblast viability under iron-overloaded conditions". Moreover, results have been presented and published in 4 international conferences both in Thailand and abroad.

2. Objectives

- 2.1 To investigate the underlying mechanism iron-induced osteoblast cell death
- 2.2 To examine the effects of iron overload on osteoblast differentiation and mineralization
- 2.3 To elucidate and compare the involvement reactive oxygen species (ROS) production and NADPH oxidases (NOXs) in ferric (FAC) and ferrous (FAS)-treated osteoblast cells
 - 2.4 To involvement of iron uptake capacity of osteoblasts in iron-induced osteoblast cell death
- 2.5 To examined the potential therapeutic properties of NOX inhibitor (diphenylene iodonium; DPI), iron chelator (deferiprone; DFP) and antioxidant agent (N-acetyl cysteine; NAC) in iron-induced osteoblast cell death
- 2.6 To elucidate the effects of vitamin D₃ and exogenous calcium treatment on osteoblast cell survival under iron overload
- 2.7 To investigate the effects of ferric and ferrous on cell cycle progression in osteoblasts under iron overload.

3. Methodology

- 3.1 The underlying mechanisms involving iron-induced osteoblast cell death by ferric and ferrous were performed by investigating the alteration of apoptotic markers and ferroptosis markers including cleaved caspase 3, cleaved caspase 7, poly (ADP-ribose) polymerase-1 (PARP-1) by western blot analysis. The dependence of ferroptosis in iron-induced osteoblast cell death was tested by using ferroptosis inhibitor, ferrostatin-1. Osteoblast cell viability was determined by MTT assay
- 3.2 Effects of iron overload from ferric and ferrous on osteoblast differentiation was determined by the expression of osteoblastic genes by qRT-PCR and alkaline phosphatase (ALP) activity assay. Mineralization of osteoblasts was determined by alizarin red staining of calcium deposition in osteoblast cells and extracellular matrices.
- 3.3 The level of cellular ROS was determined by using a commercially available ROS detection kit. The potential involvement of NOXs was determined by the expression alteration of NOXs in osteoblasts treated with ferric and ferrous. Gene expression alteration was examined by qRT-PCR.
- 3.4 To study the correlation of iron uptake capacity of osteoblast cell death under iron overload, intracellular iron in osteoblasts treated ferric and ferrous was measured by using flame atomic absorption spectrometry (FAAS)
- 3.5 The potential therapeutic properties of NOX inhibitor (diphenylene iodonium; DPI), iron chelator (deferiprone; DFP) and antioxidant agent (N-acetyl cysteine; NAC) in iron-induced osteoblast cell death were

examined by osteoblast cell viability assay of osteoblasts cells treated with ferric and ferrous in the presence or absence of these agents.

3.6 As the common treatment for calcium malabsorption, effects of vitamin D and exogenous calcium on osteoblast cell viability and iron uptake capacity in osteoblasts under iron overload were investigated. Osteoblast cell viability under iron overload with ferric or ferrous in the presence or absence of vitamin D or exogenous calcium treatment. In addition, intracellular iron in osteoblasts treated with iron in the presence and absence of vitamin D was also investigated by using FAAS.

3.7 Effects of ferric and ferrous on cell cycle progression in osteoblasts under iron overload were determined by flow cytometry analysis.

4. Key findings from this project

- 4.1 The alteration of apoptotic markers was clearly observed, especially in ferric treated osteoblasts. Ferrostatin could significantly rescued osteoblasts from iron-induced osteoblast cell death indicated the involvement of ferroptosis mechanism in iron-induced osteoblast cell death. This speculation was later confirmed by the downregulation of the ferroptosis downregulated marker, glutathione peroxidase 4. Hence, iron-induced osteoblast cell death replied on both apoptosis and ferroptosis mechanisms.
- 4.2 The downregulation of osteoblast differentiation genes was observed in osteoblasts exposed to ferric and ferrous. Decreased ALP expression, activity and mineralization in osteoblasts under iron overload were also shown.
- 4.2 Results showed that cellular ROS production was significantly increased in osteoblasts exposed to ferric and ferrous. In addition, the expression of NOX1 and NOX4 was also significantly increased in iron treated osteoblasts. These indicated the correlation between cellular ROS level and iron-osteoblast cell death and the potential role of NOX1 and NOX4 in iron-induced osteoblast cell death.
- 4.3 Intracellular iron in osteoblasts was significantly increased after being exposed to both ferric and ferrous. This result showed the potential correlation between iron uptake capacity and iron-induced osteoblast cell death. More experiments on intracellular level and iron-induced osteoblast cell death were conducted using several treatments that affected intracellular iron including iron chelator and vitamin D. These results have been discussed later in this section.
- 4.4 The results showed that DPI, DFP and NAC could not rescue osteoblasts from iron-induced osteoblasts cell death. Some of these agents also showed its toxicity in osteoblasts itself; hence, they were not the good candidates for therapeutic agents for iron-induced osteoblast cell death. While iron chelator, DFP, was shown to effectively lower intracellular level of iron in osteoblasts under iron overload, it could not suppress iron-induced osteoblast cell death indicating that this phenomenon might not depend on iron uptake capacity or intracellular iron level in osteoblasts.
- 4.5 Our results showed that while vitamin D treatment led to increased levels of intracellular iron in osteoblasts exposed to ferric and ferrous, it did not affect osteoblast cell viability under iron overload. These results confirmed the independence of intracellular iron level or iron uptake capacity of osteoblasts in iron-induced osteoblast cell death. Interestingly, our results showed that exogenous treatment of calcium improved osteoblast cell viability under iron overload suggesting the potential therapeutic application of exogenous calcium treatment in iron overload-induced osteoporosis.
- 4.6 Effects ferric and ferrous on cell cycle progression in osteoblasts under iron overload were studied. The results showed that iron significantly induced G0/G1 cell cycle arrest leading to the suppression of osteoblast cell viability and proliferation.

5. Research output

International publication

Results from this project has been published in 1 international peer-reviewed article in Biometals (impact factor 2.478, Q1), and another manuscript is accepted to be published in PLoS One (impact factor 2.776, Q1) as follows. More output summary could be found in Table 2.

Lertsuwan K, Nammultriputtar K, Nanthawuttiphan S, Phoaubon S, Lertsuwan J, Thongbunchoo J, Wongdee K, Charoenphandhu N (2018) Ferrous and ferric differentially deteriorate proliferation and differentiation of osteoblast-like UMR-106 cells. Biometals 31(5):873-889. (Attached document)

Lertsuwan K, Nammultriputtar K, Nanthawuttiphan S, Tannop N, Teerapornpuntakit J, Thongbunchoo J, Charoenphandhu N (2020) Differential effects of Fe²⁺ and Fe³⁺ on osteoblasts and the effects of 1,25(OH)2D3, deferiprone and extracellular calcium on osteoblast viability under iron-overloaded conditions. PLoS One (Accepted) (Attached document)

Presentation in international and national conferences

- 1.1 Being a speaker in the topic: "Targeting Molecular Mechanism for Osteoporosis in Thalassemia and Iron Overload" in COCAB-moving forward for food and drug translational research (August 2018)
- 1.2 Parts of results from this project has been presented and published (conference proceeding) in the topic: "Comparative Effects of Ferric and Ferrous on Osteoblast Cell Survival and Function" in Pure and Applied Chemistry International Conference 2019 (February 2019).

Nanthawuttiphan S, Charoenphandhu N, **Lertsuwan**, **K**. (2019, February) *Comparative Effects of Ferric and Ferrous on Osteoblast Cell Survival and Function* presented at Pure and Applied Chemistry International Conference 2019, Bangkok, Thailand.

- 1.3 Parts of results from this project has been presented as a poster in a topic of: "Differential effects of Fe^{2+} and Fe^{3+} on the proliferation and differentiation of osteoblasts"
- Nammultriputtar K., **Lertsuwan K.** and Charoenphandhu N. (2019, March) Differential effects of Fe2+ and Fe3+ on the proliferation and differentiation of osteoblasts. Poster presented at the 9th Federation of the Asian and Oceanian Physiological Societies Congress (FAOPS), Kobe, Japan.
- 1.4 Oral presentation at 27th FAOBMB & 44th MSBMB Conference and IUBMB Special Symposia, Kuala Lumpur, Malaysia in a topic of "Unveiling underlined molecular mechanisms of Thalassemia-induced osteoporosis" Lertsuwan K, Nammultriputtar K, Nammultriputtar K, Phoaubon S and Charoenphandhu N. (2019, August) Unveiling underlined molecular mechanisms of Thalassemia-induced osteoporosis. Oral presentation at 27th FAOBMB & 44th MSBMB Conference and IUBMB Special Symposia, Kuala Lumpur, Malaysia
- 1.5 Parts of results from this project has been presented and published (conference proceeding) in the topic: "Investigating the Involvement of Ferroptosis in Osteoblast Cell Death under Iron Overload"

Tannop N, Charoenphandhu N. and **Lertsuwan K.** (2020, February) Investigating the Involvement of Ferroptosis in Osteoblast Cell Death under Iron Overload. Poster presented at Pure and Applied Chemistry International 2020 (PACCON 2020), Bangkok, Thailand

Table 2 Outputs from this project were illustrated as follows

Output	Detail	First / Corresponding author	
		First author	Corresponding author
Research articles			
Lertsuwan K, Nammultriputtar K, Nanthawuttiphan	manuscript is under	Lertsuwan K.	Charoenphandhu N
S, Phoaubon S, Lertsuwan J, Thongbunchoo J,	preparation.		
Wongdee K, Charoenphandhu N (2018) Ferrous and	manuscript is submitted.		
ferric differentially deteriorate proliferation and	manuscript is under revision.		
differentiation of osteoblast-like UMR-106 cells.	manuscript is accepted/ in		
Biometals 31(5):873-889. (IF 2.478, Q1)	Press.		
	☑ manuscript is published.		
Lertsuwan K, Nammultriputtar K, Nanthawuttiphan	☐ manuscript is under	Lertsuwan K	Charoenphandhu N
S, Tannop N, Teerapornpuntakit J, Thongbunchoo J	preparation.		
Charoenphandhu N (2020) Differential effects of Fe ²⁺	manuscript is submitted.		
and Fe³⁺ on osteoblasts and the effects of	manuscript is under revision.		
1,25(OH)2D3, deferiprone and extracellular calcium	☑ manuscript is accepted/ in		
on osteoblast viability under iron-overloaded	Press.		
conditions. PLoS One (IF 2.776, Q1) (Accepted)	manuscript is published.		
International conference			
Nanthawuttiphan S, Charoenphandhu N and	☑ results are presented.	Nanthawuttiphan S	Lertsuwan K.
Lertsuwan, K. (2019, February) Comparative Effects	proceeding is accepted.	•	
of Ferric and Ferrous on Osteoblast Cell Survival	proceeding is published.		
and Function presented at Pure and Applied			
Chemistry International Conference 2019, Bangkok,			
Thailand.			
Nammultriputtar K., Lertsuwan K. and	☑ results are presented.	Nammultriputtar K	Charoenphandhu N
Charoenphandhu N. (2019, March) Differential	proceeding is accepted.		
effects of Fe ²⁺ and Fe ³⁺ on the proliferation and	proceeding is published		
differentiation of osteoblasts. Poster presented at			
the 9th Federation of the Asian and Oceanian			
Physiological Societies Congress (FAOPS), Kobe,			
Japan.			
Lertsuwan K, Nammultriputtar K, Nammultriputtar K	results are presented.	Lertsuwan K	Charoenphandhu N
Phoaubon S and Charoenphandhu N. (2019, August)	<u>_ </u>		
Unveiling underlined molecular mechanisms of	proceeding is published		
Thalassemia-induced osteoporosis. Oral			
presentation at			
27th FAOBMB & 44th MSBMB Conference and			
IUBMB Special Symposia, Kuala Lumpur, Malaysia			
Tannop N, Charoenphandhu N. and Lertsuwan K.	results are presented.	Tannop N	Lertsuwan K
(2020, February) Investigating the Involvement of	proceeding is accepted.		
Ferroptosis in Osteoblast Cell Death under Iron	proceeding is published.		
Overload. Poster presented at Pure and Applied			
Chemistry International 2020 (PACCON 2020),			
Bangkok, Thailand			

6. Schedule for the entire project

Schedule/year	Year 1		Year 2	
	Month	Month	Month	Month
	1-6	7-12	1-6	7-12
Investigate the involvement of apoptosis and ferroptosis in iron-induced osteoblast cell death	1			
Determine the involvement of ROS production and the expression of NADPH oxidases	1			
including NOX1 and NOX4 upon iron exposure to osteoblastic UMR-106 cells				
Manuscript #1 submission				
Determine the effects of extracellular iron exposure on iron uptake ability into UMR-1106 cells		1		
Manuscript #1 published				
Examine the effects of ferric and ferrous on osteoblast differentiation and mineralization		1		
Evaluate effects of NOX inhibitor (diphenylene iodonium; DPI), iron chelator (deferiprone; DFF			1	
and antioxidant agent (N-acetyl cysteine; NAC) on iron uptake ability and osteoblast cell death				
under iron overload				
Examine effects of vitamin D ₃ on iron uptake ability and osteoblast cell death under iron			1	
overload				
Manuscript #2 preparation/submission				
Examine effects of both iron species on cell cycle progression of osteoblasts				1
Manuscript #2 accepted				
Full report submission				1

7. Budget details

	Year 1 (Baht)	Year 2 (Baht)	Sum
			(Baht)
1. Honorarium	156,000	156,000	312,000
- Honorarium for principal investigator			
2. Materials			
- Chemicals and disposables for cells tissue culture and	35,000	35,000	70,000
treatments			
- Chemicals and consumables for molecular techniques,	99,000	89,000	188,000
such as qRT-PCR, Western blot, ROS assay, glutathione			
assay, CRIPSR/Cas9 construction			
- Experimental animals and related chemicals and			
consumables	10,000	20,000	30,000
3. Expenses	-	=	-
4. Hiring	-	-	-
Total	300,000	300,000	600,000

Research results from the project

Objective 1: To investigate the alteration of apoptotic markers upon iron-induced osteoblast cell death

1.1 Rationale

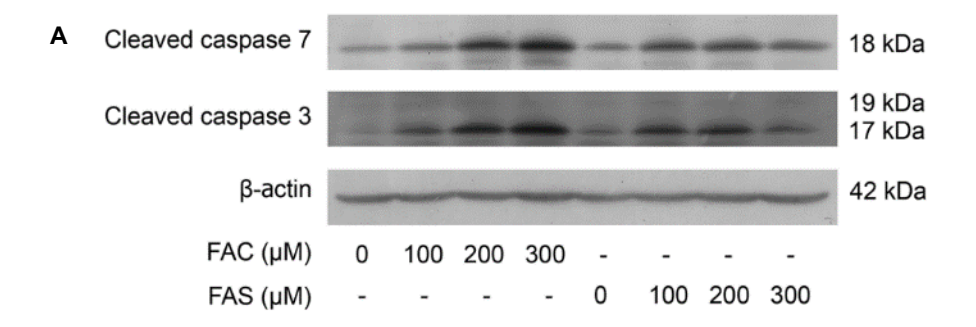
Previous studies from our and other groups showed that iron could induce osteoblast cell death, so the primary program cell death, apoptosis, was investigated to verify and compare the potential mechanism of osteoblast cell death under iron overload by ferrous and ferric species.

1.2 Experimental procedures

UMR-106 cells were seeded at 4.2x10⁵ cells/well in 6-well tissue culture plate. Then, the cells were treated with ferric ammonium citrate (FAC) or ferrous ammonium sulfate (FAS) at 0, 100, 200 or 300 μM. After 72 hours of treatment, cell pellet was collected by scraping, and protein samples were extracted by using modified radioimmunoassay precipitation (RIPA) buffer containing 50 mM Tris–HCl pH 7.4, 1% Triton X-100, 0.25% deoxycholate, 150 mM NaCl. Protein concentration in each sample was determined by using BCA protein assay kit (Roche, USA). Twenty-five micrograms of proteins were used for SDS-PAGE and western blot analysis for the expression of cleaved caspase-3, cleaved caspase-7, poly (ADP-ribose) polymerase-1 (PARP-1) and actin (housekeeping control). The relative protein expression was determined by pixel density of each protein band normalized by its own actin.

1.3 Results

As caspase 3 and caspase 7 function as the executive caspases in apoptosis pathway, they are commonly used as apoptotic markers. Our results showed that FAC induced the increased level of cleaved caspase 3 and cleaved caspase 7 significantly in dose-dependent fashion (Figure 1A). While the change is not significant in FAS treated groups, the increasing trends of cleaved caspase 3 and cleaved caspase 7 were also observed. The semi-quantitative value of cleaved caspase 3 and cleaved caspase 7 upon FAC and FAS treatment on UMR-106 cells normalized to control was also shown in Figure 1B and 1C. These results suggested that FAC and FAS induced osteoblast cell death via apoptosis.



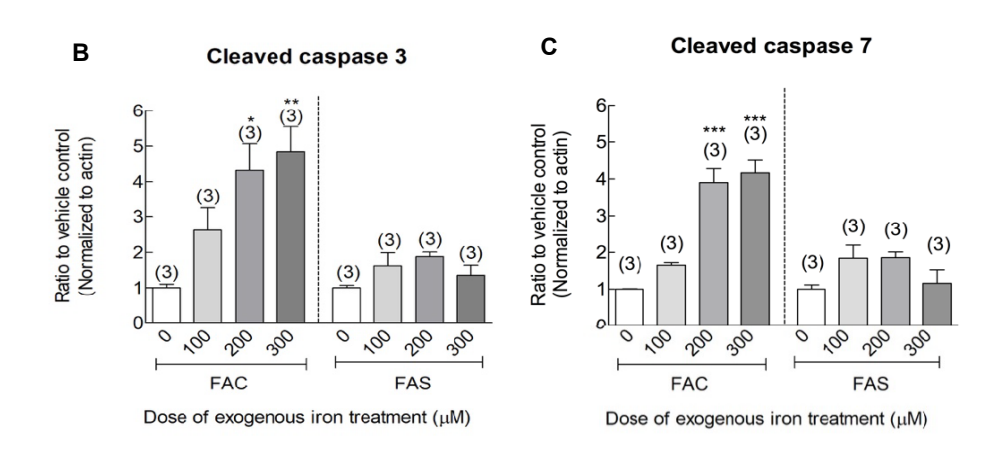


Figure 1 Both FAC and FAS induced the increased level of cleaved caspase 3 and cleaved caspase 7 in UMR-106 cells. (A) western blot of cleaved caspase 3 and 7 from UMR-106 cells treated with FAC and FAS, (B and C) quantitative analysis of cleaved caspase 3 and 7 from western blot normalized to β-actin (* P < 0.05; ** P < 0.01, *** P < 0.001)

In addition to cleaved caspases, the alteration of total and cleaved Poly (ADP-ribose) polyemerase-1 (PARP-1), which is the protein functioning in DNA repair and is known to be the primary caspases target during apoptosis, was also investigated. The expression of PARP-1 and cleaved PARP-1 was shown in Figure 2A. Even though they are not statistically significant, our quantified results showed that the full length of PARP-1 was notably decreased in UMR-106 cells treated with FAC, while this effect could not be seen in FAS treated groups (Figure 2C). Similar trend was also shown in cleaved PARP-1 level upon FAC and FAS treatment (Figure 2B). When the level of cleaved PARP-1 was normalized to the full length PARP-1 to yield the relative level of cleaved PARP-1 to full length PAR-1, the results showed that the ratio between cleaved PARP-1 to full length PARP-1 was increased significantly in osteoblastic cells, UMR-106 cells, treated FAS at 300 µM (Figure 2D).

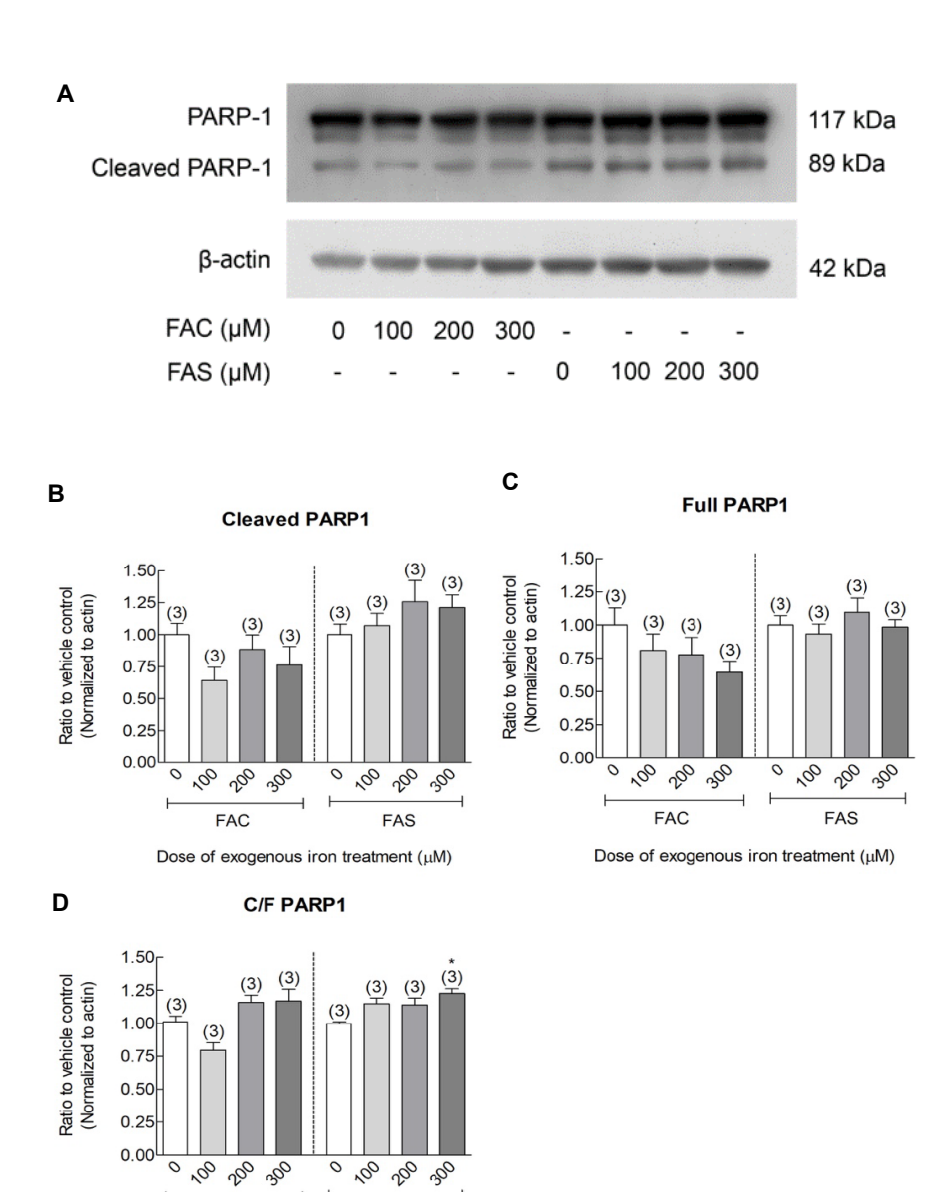


Figure 2 The expression of full length PARP-1 and cleaved PARP-1 in UMR-106 cells upon ferric (FAC) and ferrous (FAS) treatments was shown in this figure. (A) western blot showed that expression alteration of full length and cleaved PARP-1 upon FAC and FAS treatments, (B) and (C) quantified data from western blot, (D) relative level of cleaved PARP-1 and full length PARP-1 (* P < 0.05; ** P < 0.01)

Dose of exogenous iron treatment (μM)

Objective 2: To investigate the involvement of ferroptosis mechanism in iron-induced osteoblast cell death

2.1 Rationale

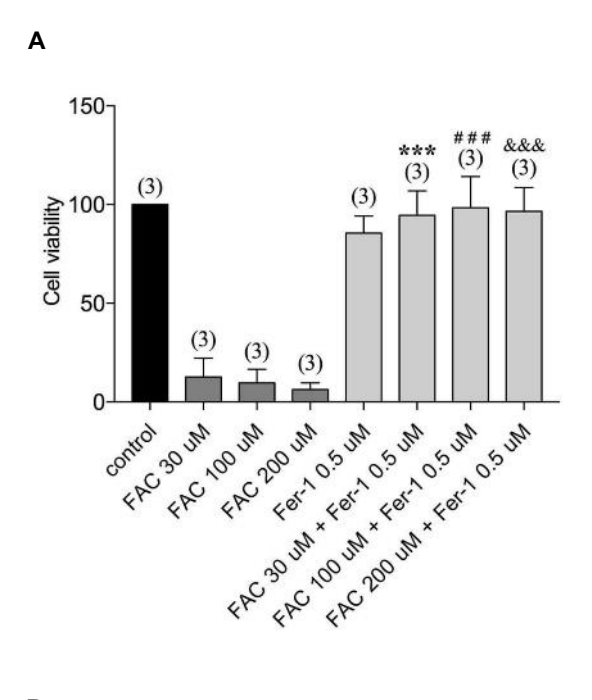
Our results from objective 1 showed that FAC could significantly induce apoptotic marker processing, while FAS could not. With the relative similar EC50 of both iron species on UMR-106 cell death, other alternative cell death pathway(s) was also considered to be a potential cell death mechanism in UMR-106 cell death under iron overload.

2.2 Experimental procedures

UMR-106 cells were seeded at 2500 cells/well in 96-well tissue culture plate. Then, the cells were treated with ferric ammonium citrate (FAC) or ferrous ammonium sulfate (FAS) at 0, 100, 200 or 300 μM with or without 0.5 μ M ferroptosis inhibitor (ferrostatin-1). After 72 hours of treatment, cell viability was measured by MTT assay. Tetrazolium dye, 3- (4,5-dimethylthiazol- 2- yl) -2,5- diphenyltetrazolium bromide (MTT) was reduced by metabolic enzymes in mitochondria of living cells. The reducing activity can change the color of yellow tetrazole (MTT dye) to purple formazan. After the end of the experiments, the culture media were removed followed by adding 100 μL of 0.5 mg/mL MTT dye in culture media in each well and incubating at in 37°C for 3 hours. The background of culture medium was subtracted by the empty well contained only 0.5 mg/mL MTT solution. After incubation, 100 μL of 5% (w/v) sodium dodecyl sulfate (SDS) in 50% (v/v) N, N-Dimethylformamide in purified water was added in each well. The MTT formazan was completely dissolved by mixing with 200P micropipette. The absorbance was measured with microplate reader at 540 nm. For data analysis, the absorbance was subtracted from culture medium background and normalized to control group. Then, the absorbance was calculated as a percentage of cell viability.

2.3 Results

Ferroptosis is a novel iron-dependent non-apoptotic cell death. As FAS does not induce significant change in apoptotic markers in UMR-106 cells, the alternative cell death pathway was investigated. In this experiment, ferroptosis-specific inhibitor, ferrostatin-1 was used. Our results showed that FAC dramatically decreased osteoblast cell survival in dose-dependent manner. While ferrostatin-1 alone did not negatively affect UMR-106 cell viability, cells treated with both FAC and ferrostatin-1 was shown to be resistant to FAC-induced osteoblast cell death (Figure 3A). Similar results were shown in FAS-treated groups. As FAS markedly induced osteoblast UMR-106 cell death, ferrostatin-1 could also suppress FAS-induced cell death (Figure 3B). These results indicated that iron also induced osteoblast cell death via ferroptosis pathway.



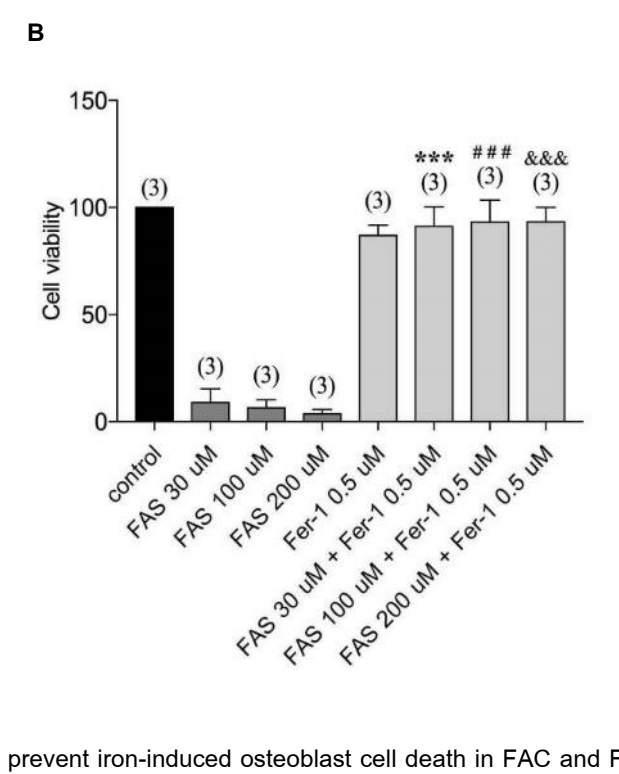


Figure 3 Ferrostatin-1 could prevent iron-induced osteoblast cell death in FAC and FAS-treated UMR-106 cells. (A) UMR-106 cells treated with FAS, (B) UMR-106 cells treated with FAS with or without ferrostatin-1 (*** P < 0.001 compared to the treatment at 30 μ M, **## P < 0.001 compared to the treatment at 100 μ M, *&& P < 0.001 compared to the treatment at 200 μ M)

Objective 3: To examine the effects of FAC and FAS on glutathione peroxidase 4 (GPX4) level in osteoblasts

3.1 Rationale

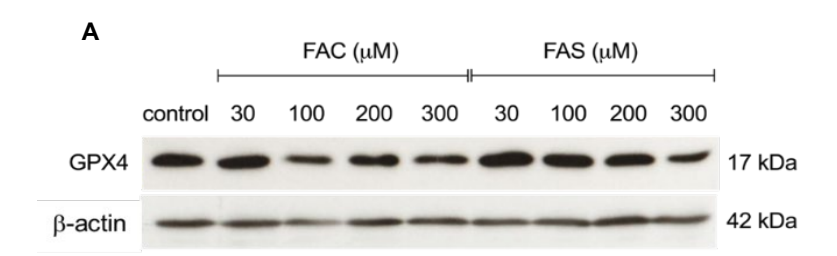
Inactivation of glutathione peroxidase 4 (GPX4) can increase intracellular lipid peroxides, resulting in ferroptosis. Therefore, we would like to examine if treating osteoblast cells with FAC and FAS at different concentration would affect the level of GPX4 protein in osteoblasts. Moreover, GPX4 down-regulation is one of the hallmarks for ferroptosis. This experiment would confirm the involvement of ferroptosis in iron-induced osteoblast cell death.

3.2 Experiment procedures

UMR-106 cells were seeded at 1.0×10^5 cells/well in 6-well plate (Corning, NY, USA). Cells were treated with 0, 30, 100, 200 and 300 μ M of FAC or FAS for 72 hours. The treatments were changed every day. After that, cell pellets were collected by scraping and washed twice with 1X cold phosphate buffer saline (PBS). Proteins were extracted by radioimmunoassay precipitation (RIPA) buffer containing 10% protease inhibitor for 1 hour on ice. Cell lysates were centrifuged at 7,500 rpm for 30 minutes and supernatants were collected. Protein concentration was measured by using BCA protein assay kit (Thermo scientific, USA). Thirty-five microgram of protein were separated through 8-15% acrylamide gel at 100 volts for 100 minutes and transferred to nitrocellulose membrane at 12 volts for 120 minutes. Membranes were blocked for 2 hours at room temperature in blocking solution (Capricorn Scientific, USA). After that, membranes were washed 3 times with TBST and incubated with specific antibody for GPX4 (Abcam, USA) and β -actin (Abcam, USA) overnight at 4°C. Then, membranes were wash 3 times with TBST and incubated with anti-rabbit IgG secondary antibody (Cell Signaling, USA). Protein was visualized by enhanced chemiluminescence (ECL) (Millipore, USA) and exposed to X-ray film (GE Healthcare, UK). The band intensity was quantified by using Image J software.

3.3 Results

Even though the results were not statistically significant, the expression level of GPX4 protein was notably decreased after UMR-106 cells were treated with FAC or FAS in a dose-dependent manner (Figure 4A and B). These results suggested that both FAC and FAS reduced GPX4 level in osteoblasts resulting in ferroptosis cell death.



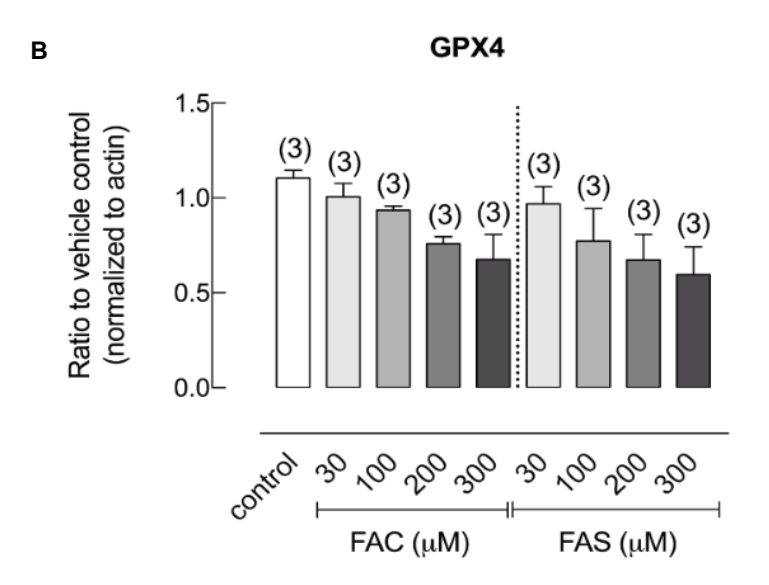


Figure 4 The effects of FAC and FAS on glutathione peroxidase 4 (GPX4) level in osteoblasts (A) The expression level of GPX4 protein (B) The quantified data of (A).

Objective 4: To elucidate and compare the involvement reactive oxygen species (ROS) production activity in ferric (FAC) and ferrous (FAS)-treated osteoblast cells

4.1 Rationale

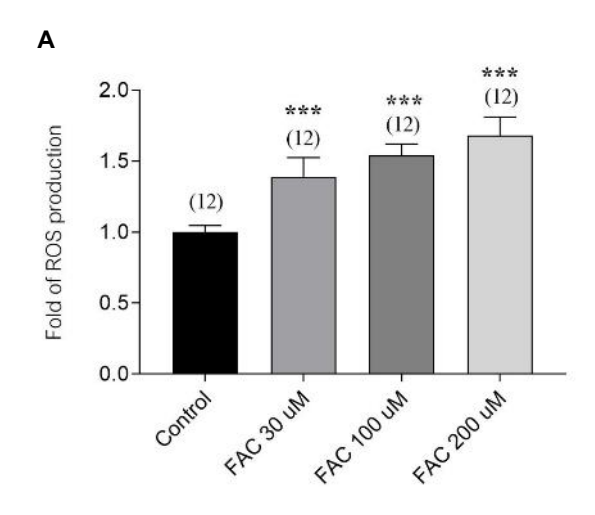
Since ROS production was shown to play an important role in both apoptosis and ferroptosis, cellular ROS production in UMR-106 cells upon FAC and FAS treatment was investigated and compared. These results would lead to the potential prevention for iron toxicity in osteoblast by using antioxidants in the future experiments.

4.2 Experimental procedures

UMR-106 cells were seeded at 2.5×10^4 cells/well in 96-black well plate. After 24 hours, ROS production was measured by using DCFDA cellular ROS detection assay kit (ab113851, Abcam, USA). In brief, the cells were washed with 1X buffer. Then, DCFDA solution was added 100 μ L/well, and the cells were incubated for 45 minutes. They were washed with 1X buffer again; then iron treatment was added at 0, 30, 100 and 200 μ M and incubated for 6 hours. ROS production was measured with fluorescence microplate reader at Ex/Em: 485/535 nm. The levels of ROS production in each treatment were normalized to control.

4.3 Results

Our results showed that FAC at 30, 100 and 200 μ M significantly increased cellular ROS production (Figure 5A). Similarly, FAS was shown to induce ROS production significantly in UMR-106 cells at 100 and 200 μ M (Figure 5B). Even though both iron species could induce ROS production significantly in osteoblast UMR-106 cells, the cells showed to be more sensitive for FAC than FAS. In general, these results showed that ROS might involve in iron-induced osteoblast cell death in UMR-106 cells with both ferric and ferrous exposure.



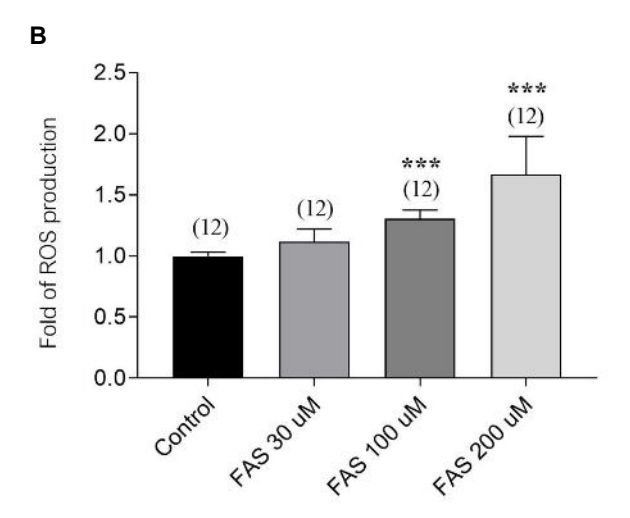


Figure 5 ROS production was increased in osteoblast UMR-106 cells after FAC and FAS exposure. (A) FAC increased ROS production significantly at 30, 100 and 200 μ M, (B) FAS induced ROS production significantly at 100 and 200 μ M (*** P < 0.001 compared to control)

Objective 5: To elucidate and compare the expression of NADPH oxidases in osteoblast UMR-106 cells under iron overload

5.1 Rationale

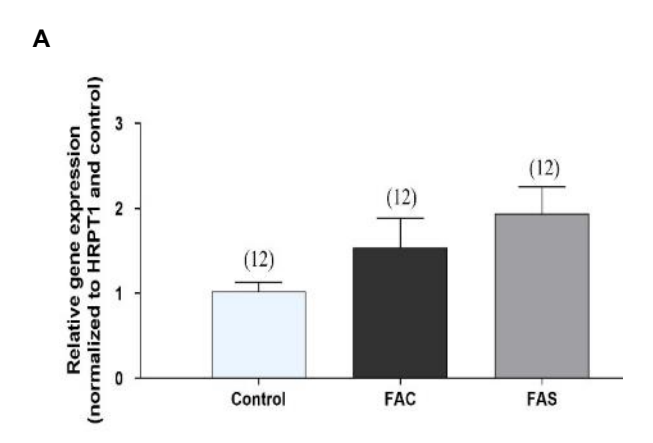
NADPH oxidases (NOXs) were the ROS-producing enzymes. Previous studies showed that the inhibition of NOXs pharmacologically and genetically led to the prevention of alcohol- and ovariectomy-induced osteoporosis. The basal expression of NOXs in UMR-106 cells were investigated in the previous studies from ours and others. NOX1 and NOX4, expressed in UMR-106 cells, were selected for this study. Here, the expression alteration of NOX1 and NOX4 in UMR-106 cells under iron overload was investigated.

5.2 Experimental procedures

UMR-106 cells were plated in 6-well plate at seeding density 4.2 x 10^5 cells/well. Twenty-four hours after plating, cells were treated FAC or FAS with EC₅₀ at 200 μ M for 72 hours. The cells were collected by washing with 1X PBS 2 times and resuspended in TRIzol reagent to extract total RNA. The RNA was purified and measured with NanoDrop-2000c spectrophotometer with OD at 260 and 280 nm. The ratio of which ranged between 1.8 and 2.0 was considered acceptable. Then, one microgram of RNA was converted to complementary DNA (cDNA) with iScript cDNA synthesis kit (Bio-rad, CA, USA). The quantitative real–time PCR (qRT-PCR) was performed by QuantStudio 3D Digital PCR System (Thermo Fisher Scientific, MA, USA) with SsoFast EvaGreen Supermix (Bio-rad, Hercules, CA, USA) for 40 cycles at 95 °C for 60 seconds, 55-60 °C annealing temperature for 30 seconds, and 72 °C for 30 seconds. Fold change values were calculated from the threshold cycles (CT) based on the standard Δ CT method. Relative expression was expressed as the $2^{-\Delta\Delta_{CT}}$ method normalized to control.

5.3 Results

Previous study showed that NADPH oxidases (NOXs) 1 and 4 were expressed in UMR-106 cells, while NOX2 and NOX3 were not. The expression alteration of NOX1 and NOX4 after both iron exposure was investigated. Even though the expression alteration of NOX1 was not statistically significant in UMR-106 cells under iron exposure, the increasing trend of NOX1 was noticeable in both FAC and FAS treated cells with the stronger effects from FAC (Figure 6A). In the other hand, NOX4 was significantly increased in FAC-treated UMR-106 cells for 24 and 72 hours (Figure 6B). These data showed that NOX4 could be a contributor for ROS production in UMR-106 cells under iron overload.



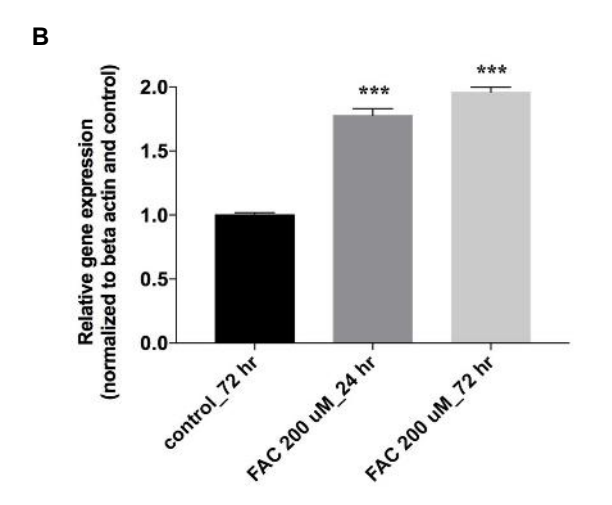


Figure 6 Gene expression alteration of NOX1 and NOX4 in UMR-106 cells upon FAC and FAS exposure was illustrated. (A) NOX1 showed non-significant increase in UMR-106 cells treated with FAC and FAS, (B) NOX4 showed a statistically significant increase in UMR-106 cells after being treated with FAC at 24 and 72 hours (** P < 0.01 and *** P < 0.001 as compared to control)

Objective 6: To investigate the effects of NOX inhibitor on UMR-106 cell survival in normal condition and under iron overload

6.1 Rationale

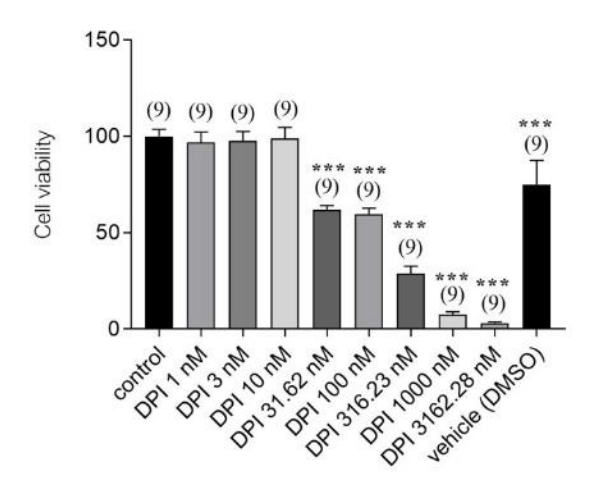
As the ROS-producing enzymes, NOXs inhibition was used to prevent several ROS-related cell toxicity in many models. However, the dosage and length of the treatment of NOXs inhibitor still needed to be compromised because NOXs also participated in electron transport within mitochondria. In this experiment, dose-dependent effects of NOX pan inhibitor, Diphenyleneiodonium (DPI), on UMR-106 cells in normal condition and under iron overload will be tested.

6.2 Experimental procedures

UMR-106 cells were seeded at 2500 cells/well in 96-well tissue culture plate. Then, the cells were treated with DPI at varied doses ranging from 0 to 3.162 μ M. After 72 hours of treatment, cell viability was measured by MTT assay as discussed in the previous experiment (objective 2). For data analysis, the absorbance was subtracted from culture medium background and normalized to control group. Then, the data was calculated as a percentage of cell viability.

6.3 Results

Our results showed that high doses of DPI could negatively affect UMR-106 cell survival leading to the significantly decreased percent cell survival of UMR-106 cells treated with 31.62 nM, 100 nM, 316.23 nM, 1000 nM (1 μ M) and 3162.28 nM (3.162 μ M). However, low concentration of DPI at 1 nM, 3 nM and 10 nM did not affect UMR-106 cell survival (Figure 7). Therefore, the low concentration of DPI will be selected for the future experiment.



***p < 0.001 compared with control

Figure 7 DPI toxicity on UMR-106 cells was shown. Significant decreased of percent cell viability was observed in the concentration greater than 31.26 nM, while the lower concentration did not affect UMR-106 cell survival. (*** P < 0.001 as compared to control)

Objective 7: To evaluate the effects of diphenyleneiodonium (DPI) on iron-induced osteoblast cell death under iron overload with FAC and FAS

7.1 Rationale

As the ROS-producing enzymes, NADPH oxidases (NOXs) inhibition was used to prevent several ROS-related cell toxicities in many models. However, the dosage and length of the treatment of NOXs inhibitor still needed to be compromised because NOXs also participated in electron transport within mitochondria. Our preliminary data found that NOXs were overexpressed, and ROS was increased in osteoblasts treated with FAC and FAS. A pan NOXs inhibitor, diphenylene iodonium (DPI) was selected as the potential therapeutic agent for iron-induced osteoblast cell death under iron overload. Thereby, the effects of DPI on iron-induced osteoblast cell death are examined.

7.2 Experiment procedures

UMR-106 cells were plated at 1,000 cells/well in 96-well tissue culture plate. Twenty-four hours after plating, the cells were treated with 0, 250 or 1,000 μ M of FAC for 48 hours with or without DPI (1.0 nM) or DMSO (vehicle control). After the treatment period, cell viability was measured by using MTT assay. The absorbance of each well representing cell viability was determined at 595 nm by a microplate reader as mentioned earlier.

7.3 Results

The results showed that treating cells with only FAC decreased osteoblastic cell viability in a concentration-dependent manner comparing to the control. Whereas, increasing of cell viability were not statically significant in FAC and DPI-treated groups, and DMSO as a vehicle control did not affect cell viability (Figure 8). Therefore, this result suggested that DPI at 1 nM could not improve osteoblastic cell viability under iron overload.

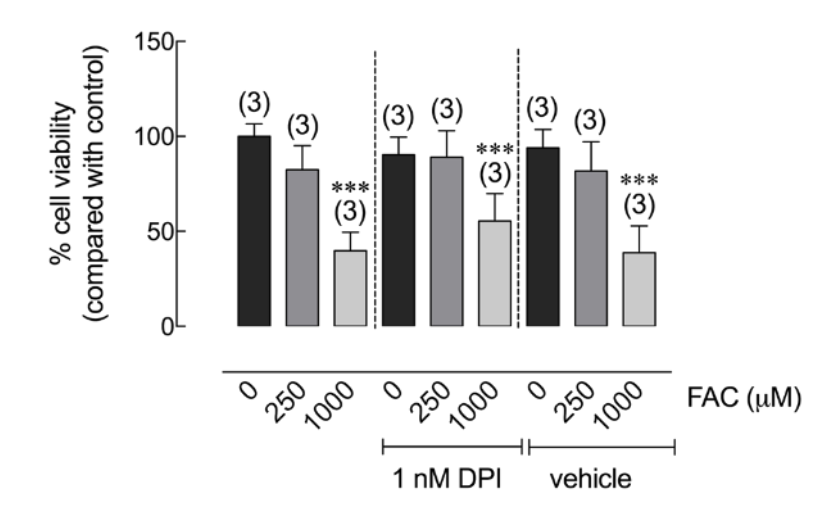


Figure 8 Osteoblast cell viability after iron exposure with FAC in the presence of DPI or vehicle control. ***P < 0.001 as compared to control group (0 μM) without DPI

Objective 8: To verify the potential capacity of osteoblast to uptake different iron species, ferric (FAC) and ferrous (FAS) in iron overload condition by flame atomic absorption spectrometry (FAAS)

8.1 Rationale

In intestinal cells, the two iron forms can use different transport routes into the cells. Previous studies showed that osteoblast also expresses transporter proteins from both transport systems. Therefore, this experiment is aimed to elucidate whether exogenous iron exposure could lead to the increased iron uptake capacity by measuring intracellular iron concentration by FAAS.

8.2 Experimental procedures

UMR-106 cells were plated in 12-well plate at 2.1×10^5 cells/well. Twenty four hours after plating, cells were treated with iron treatments (FAC or FAS) at 0, 100, 200 and 300 μ M for 24 hours. The cells were collected by washing twice with 1X phosphate buffered saline (PBS) before gently scraped with cell scraper in PBS. After centrifugation at 7,000 rpm for 15 minutes, the pellet was resuspended in 250 μ L of ultrapure water for a brief sonication. Then, the samples were digested with 65% nitric acid (HNO₃) and 30% hydrogen peroxide (H₂O₂) by Ethos UP MAXI-44 microwave digester (Milestone, CT, USA). After digestion, the samples were adjusted to 25 mL with ultrapure water. Intracellular iron concentration was measured by FAAS (PinAAcle 900T Atomic Absorption Spectrometer, PerkinElmer, Waltham, MA, USA). The system was calibrated with blank solution (2% HNO₃) to subtract background and start analyzing. The working standard in optimum range at 0, 0.04, 0.4, 0.8, 1.6, and 3 μ g/mL that were diluted from 1,000 μ g/mI Fe certified standard solution with 2% HNO₃ were used to construct the standard curve. Then, the samples were analyzed and 0.8 μ g/mL standard concentration was re–analyzed after every 8 samples for the accuracy. Intracellular iron concentration was normalized to protein concentration that can measured by bicinchoninic acid assay (BCA assay) as previously described.

8.3 Results

The experiment aimed to measure the intracellular iron concentration of UMR-106 cells under the different iron treatment using FAAS. After 24-hours treatment with either FAC or FAS at concentration 0, 100, 200 and 300 μ M, cells were collected and prepared for FAAS measurement. UMR-106 osteoblast-like cells showed the increased intracellular iron concentration after being exposed to FAC from 0.18 mg/mg protein (in a control group) to 0.43, 0.65 and 1.03 mg/mg protein in FAC treatment at 100, 200 and 300 μ M, respectively. The intracellular iron concentration of cells that were exposed to FAS also showed the same trend from 0.17 mg/mg protein (in a control group) to 0.56, 0.50 and 0.51 mg/mg protein in FAS treated groups at 100, 200 and 300 μ M, respectively. These results demonstrated that both iron species could increase intracellular iron in UMR-106 cells. In addition, our results showed that FAC could induce higher intracellular iron uptake into UMR-106 cells (Figure 9).

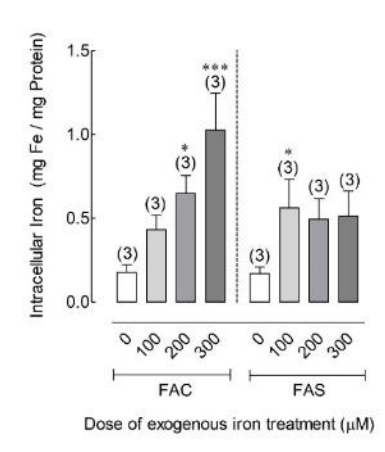


Figure 9 The potential capacity of osteoblast to uptake different iron species, ferric (Fe^{3+}) and ferrous (Fe^{2+}) in iron overload condition by flame atomic absorption spectrometry (FAAS) showing increased intracellular iron concentration upon iron exposure. FAC showed the significant higher potent to influx into osteoblast than FAS. (* P < 0.05, *** P < 0.001 as compared to control)

Objective 9: To study effects of 1,25-dihydroxyvitamin D_3 on iron uptake into osteoblast under iron overload condition by flame atomic absorption spectrometry (FAAS)

9.1 Rationale:

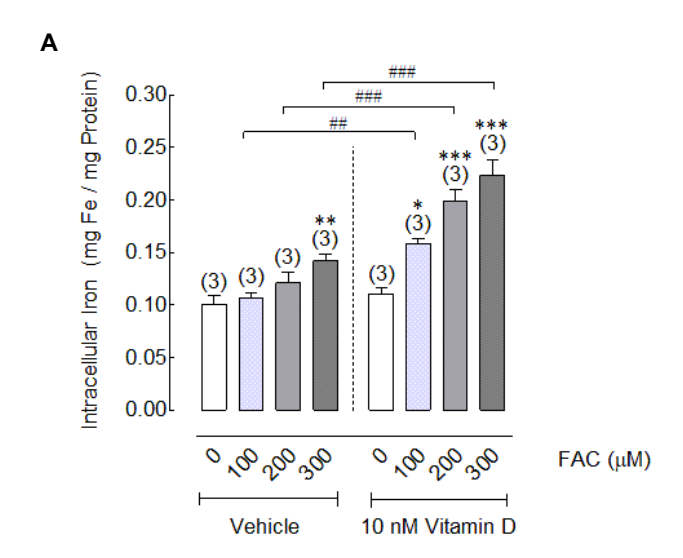
Vitamin D_3 was shown to regulate the genes involved in iron homeostasis at the enterocytes. It downregulated hepcidin expression but upregulated ferroportin expression leading to increased iron excretion. However, in the condition of iron overload the effects of vitamin D_3 on iron uptake into bone cells have not been reported. Therefore, this experiment aimed to test the action of vitamin D_3 on iron influx into osteoblast under enrich iron concentrations and compare the capability of osteoblast to uptake two iron species under vitamin D_3 treatment.

9.2 Experimental procedures

UMR-106 cells were plated in 12-well plate at 2.1×10^5 cells/well. Twenty four hours after plating, cells were treated with 10 nM $1,25(OH)_2D_3$ or 9:1 propylene glycol-ethanol (as a vehicle control) without iron treatment for 72 hours. Then, cells were treated with iron treatments (FAC or FAS) at 0, 100, 200 and 300 μ M containing 10 nM $1,25(OH)2D_3$ or vehicle control for 24 hours. After that, the cells were collected, and intracellular iron was measured by FAAS as mentioned previously (objective 7).

9.3 Results

The results showed that vitamin D_3 significantly increased intracellular iron of UMR-106 cells as compared to the similar concentration of iron with vehicle control. Intracellular iron rose from 0.11 to 0.16 mg/mg protein in 100 μ M of FAC, increased from 0.12 to 0.20 mg/mg protein in 200 μ M of FAC and increased 0.14 to 0.22 mg/mg protein in 300 μ M of FAC (Figure 10A). Likewise, the same condition with FAS treatment demonstrated that vitamin D_3 also enhanced FAS uptake into osteoblast leading to the elevated intracellular iron significantly different from vehicle control at the same concentration of FAS treatments. Intracellular iron increased from 0.10 to 0.14 mg/mg protein in a control group, increased 0.10 to 0.16 mg/mg protein in 100 μ M of FAS, increased 0.11 to 0.18 mg/mg protein in 200 μ M of FAS and increased 0.11 to 0.17 mg/mg protein in 300 μ M of FAS (Figure 10B). The results indicated that 1,25-dihydroxyvitamin D_3 enhanced iron uptake into osteoblasts after FAC and FAS exposure, and FAC still had stronger effects on iron uptake into osteoblasts.



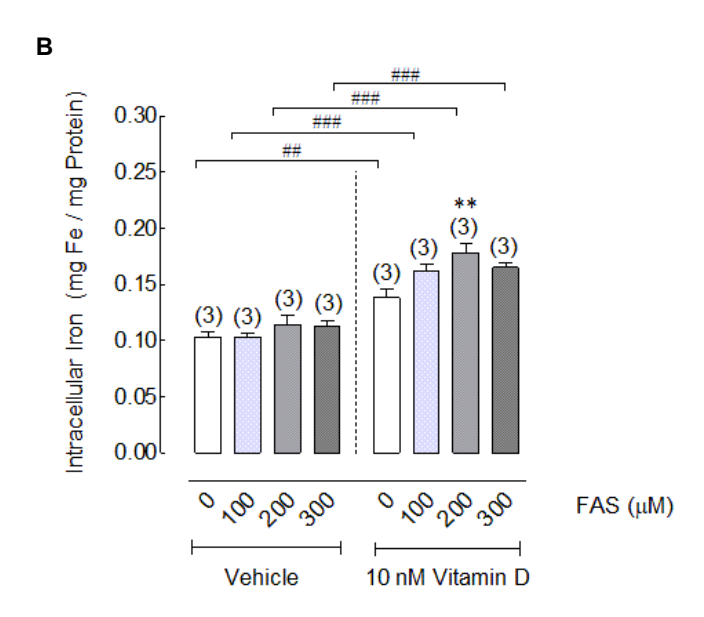


Figure 10 Effects of 1,25-dihydroxyvitamin D_3 on iron uptake into osteoblast under iron overload condition by FAAS. UMR-106 cells were treated with 72-hours vitamin D_3 pre-treatment and 24-hours of FAC (A) or FAS (B) together with vitamin D_3 . (* P < 0.05, ** P < 0.01 *** P < 0.001 as compared to control group (0 μ M); *** P < 0.01, *** P < 0.01 as compared to the same dose in vehicle control treatment)

Objective 10: To examine the effects of 1,25-dihydroxyvitamin D_3 on osteoblast cell viability under iron overload condition

10.1 Rationale

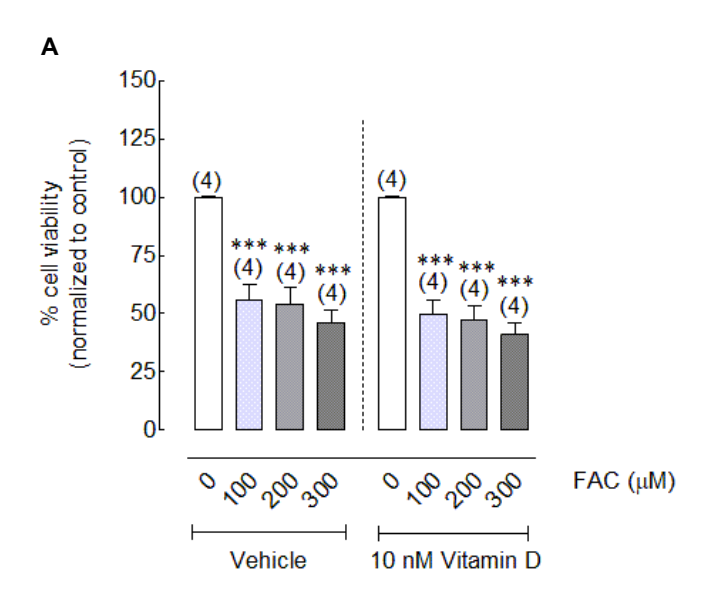
Previous experiments showed that $1,25 \, (OH)_2 \, D_3$ (1,25-dihydroxyvitamin D_3) increased iron uptake into osteoblast UMR-106 cells (Figure 9). Our results indicated that both cytotoxic effects and iron uptake into osteoblast were dose-dependent. Therefore, increased of iron uptake into osteoblast from vitamin D_3 uptake could lead to higher iron-induced cell death. This experiment is aimed to elucidate the effects of vitamin D_3 on osteoblast cell viability under iron overload.

10.2 Experimental procedures

UMR-106 cells were plated in 12-well plate by seeding density at 2.1×10^5 cells/well. Twenty-four hours after plating, cells were treated with 10 nM 1,25(OH)₂D₃ (vitamin D₃) or 9:1 propylene glycol-ethanol (vehicle control) without iron treatment for 72 hours; then, cells were treated iron treatments (FAC or FAS) at 0, 100, 200 and 300 μ M by containing 10 nM vitamin D₃ or vehicle control for 24 hours. After the treatment, cell viability was assayed by MTT assay as previously described.

10.3 Results

The results showed that vitamin D_3 tended to enhance both iron species to suppress UMR-106 cell viability; even though, the differences between vitamin D_3 and vehicle control in each concentration of iron treatment could not reach to statistical significantly different. The comparison between cell viability in vehicle control and vitamin D_3 treatment at the same concentration of FAC found to decrease from 56.07% to 49.77% in 100 μ M of FAC, decreased 54.23% to 47.13% in 200 μ M of FAC and decreased 45.87% to 41.08% in 300 μ M of FAC (Figure 11A). Similarly, in FAS treatment, vitamin D_3 was showed to promote FAS for suppressing osteoblast cell viability. The comparison between cell viability in vehicle control and vitamin D_3 treatment at the same concentration of FAS found to decrease from 64.89% to 57.01% in 100 μ M of FAS, decreased 60.88% to 55.68% in 200 μ M of FAS and decreased 55.94% to 52.40% in 300 μ M of FAC (Figure 11B). These results suggested that vitamin D_3 could facilitate iron-induced osteoblast cell death from both FAC and FAS exposure. This indicated the potential correlation between iron uptake and osteoblast cell death under iron overload.



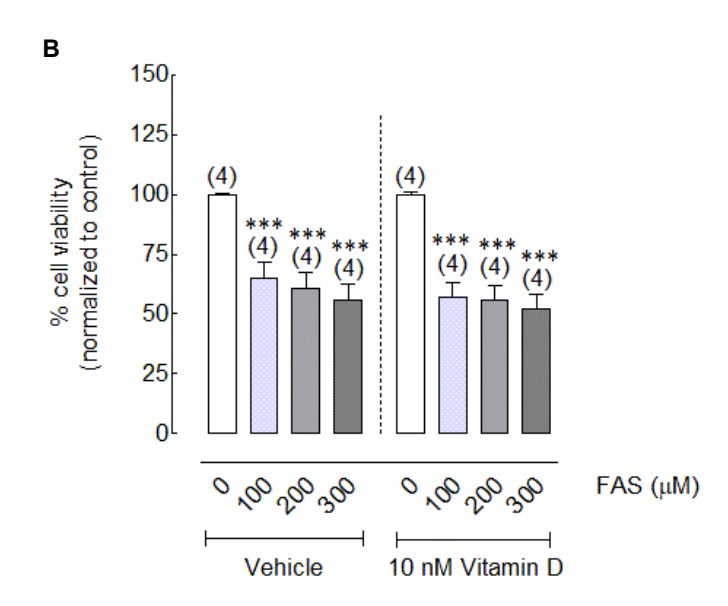


Figure 11 Effects of 1,25-dihydroxyvitamin D_3 (vitamin D_3) on osteoblast cell viability under iron overload condition by MTT assay. UMR-106 cells were treated with 72-hours vitamin D_3 pre-treatment and 24-hours of FAC (A) or FAS (B) treatment together with vitamin D_3 . (*** P < 0.001 as compared to control group (0 μ M))

Objective 11: To elucidate the effects of iron in two forms, ferric (Fe³⁺) and ferrous (Fe²⁺), on osteoblast cell mineralization

11.1 Rationale

Since the previous studies showed that iron overload suppressed the expression of several bone-specific proteins, such as ALP and osteocalcin that are important for bone mineralization. In addition, iron overload might decrease osteoid maturation and bone mineralization by incorporating into hydroxyapatite crystals. However, the comparative effects of two iron species on bone mineralization need to be investigated. Therefore, this experiment was aimed to test the effects of two iron species on bone mineralization by alizarin red staining that refer to bone nodule formation and calcium deposition.

11.2 Experimental procedures

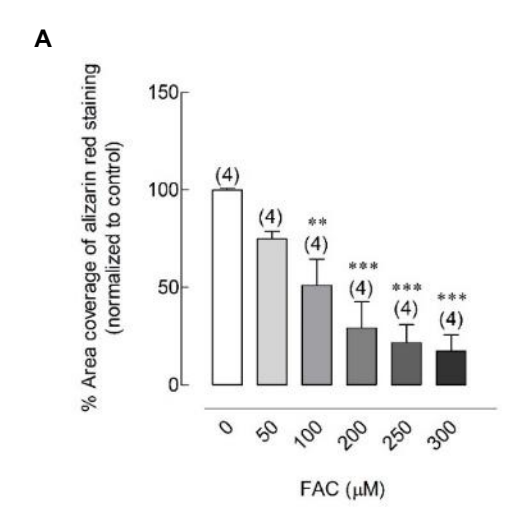
UMR-106 cells were plated in 24-well plate by seeding density at 2 x 10^4 cells/well. Twenty-four hours after plating, the old media was changed to complete media with 50 mM β -glycerophosphate and 50 μ g/ml L-ascorbate 2-phospate in the presence of the treatments including 0, 50,100, 200, 250 and 300 μ M of FAC or FAS. The media was changed every other day for 6 days. At day 6th, the cells were stained for calcium mineralization by alizarin red staining. The culture media was removed, and cells were gently washed with 1x PBS for 3 times. Then, cells were fixed in 70% cold ethanol for 1 hour at 4°C, and after fixing, cells were washed with deionized water for 3 times. The water was completely removed, and cells were stained with 40 mM alizarin red S for 5-10 minutes on the shaker at room temperature. Alizarin red S was removed and 5 times washing with 1x PBS or until the water came out clear. The cells were inspected with microscope and took the pictures. The total area of red nodule formation was quantified by Image J software

11.3 Results

After the osteoblast-like UMR-106 cells were induced for bone nodule formation and treated with either FAC or FAS for 6 days, cells were stained with alizarin red to determine bone mineralization (Table 1). The proportion of alizarin red staining was quantified to area coverage. The results showed that both iron species inhibited bone mineralization by decreasing bone nodule formation (Figure 12). Especially FAC had strong inhibitory effects on bone nodule formation in dose dependent manner (Figure 12A). The comparative effects between two iron forms showed that FAC had a stronger suppressive effect on bone mineralization than FAS, such as at the highest concentration (300 µM) FAC showed a markedly reduced bone mineralization by 82.52% while FAS decreased bone mineralization by 33.21% (Figure 12).

Table 1 Alizarin staining (red color) determined bone mineralization after iron exposure for 6 days.

Alizarin staining	FAC conc. (µM)	Alizarin staining	FAS conc. (μM)
	0		0
	50		50
	100		100
	200		200
	250		250
	300		300



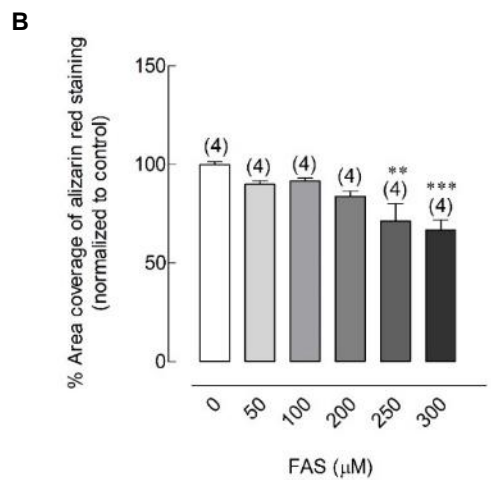


Figure 12 Effects of ferric (Fe³⁺) and ferrous (Fe²⁺) on osteoblast mineralization by alizarin red staining. Bone nodule formation was induced in UMR-106 cells by adding 50 mM β-glycerophosphate and 50 μ g/ml L-ascorbate 2-phospate together with or without iron exposure for 6 days. (A) FAC showed a markedly reduced bone mineralization in dose dependent manner. (B) Similar pattern with lower potency was found in FAS treated groups. (** P < 0.01, *** P < 0.001 as compared to control group (0 μ M))

Objective 12: To evaluate effects of antioxidant (N-acetyl cysteine; NAC) on iron-induced osteoblast cell death under iron overload with FAC and FAS

<u>12.1 Rationale</u> The results from this study showed the increased cellular reactive oxygen species (ROS) production in osteoblast cells exposed to both iron species: Fe³⁺ (from FAC) and Fe²⁺ (from FAS). Therefore, effects of antioxidant (N-acetyl cysteine; NAC) on iron-induced osteoblast cell death is evaluated.

12.2 Experiment procedure

UMR-106 cells will be seeded at 1000 cells/ well in 96-well plates for 24 hours. After that, cells will be treated with either FAC and FAS at 30, 100, 200 or 300 μM in the presence or absence of 0.5 mM NAC for 72 hours. After the treatment, cells in each group are subjected to cell viability assay by MTT assay. At the end of the treatment period, cell viability was determined by MTT assay by adding 0.5 mg/mL thiazolyl blue tetrazolium bromide (MTT dye) (Sigma Chemical Co., St. Louis, MO, USA) in culture media and incubating at in 37°C for 3 hours. After incubation, MTT solvent (5% (w/v) Sodium dodecyl sulfate (SDS) (Vivantis Technologies Sdn. Bhd., Malaysia) in 50% (v/v) N, N-dimethylformamide (VWR international, LLC, OH, USA) in purified water) was added in each well. The absorbance was measured with micro-plate reader (M695+, Metertech Inc., Taiwan) at 540 nm Riss et al (2016). An absorbance was subtracted from culture medium background and normalized to control group. Then the absorbance was calculated as a percentage of cell viability.

12.3 Results

Similar to the inhibitory effects of iron on osteoblast cell viability shown in previous study, increased cellular ROS was shown in osteoblasts treated with both Fe3+ and Fe2+. N-acetyl-L-cysteine (NAC) is a well-known antioxidant that has been shown to effectively reduce cellular ROS. In this experiment, osteoblast cell viability was determined in osteoblasts treated with various doses of FAC or FAS with or without NAC (Figure 13) Osteoblast cell viability decreased significantly down to 88.00%, 65.04%, 47.84 and 19.60% in osteoblasts treated with 30 μ M, 100 μ M, 200 μ M and 300 μ M FAC, respectively (Figure 13A). Similarly, FAS also reduced osteoblast cell viability to 88.89%, 74.18%, 53.40% and 21.67% at 30 μ M, 100 μ M, 200 μ M and 300 μ M FAS, respectively (Figure 13B). Our results showed that NAC did not help protecting osteoblasts from iron-induced osteoblast cell death. Interestingly, osteoblast viability also further reduced from 65.04% to 36.77% in 100 μ M FAC treated groups, from 47.84% to 15.96% in 200 μ M FAC treated groups (Figure 13A) and from 53.40% to 39.09% in 200 μ M FAS treated groups (Figure 13B) in the presence of NAC.

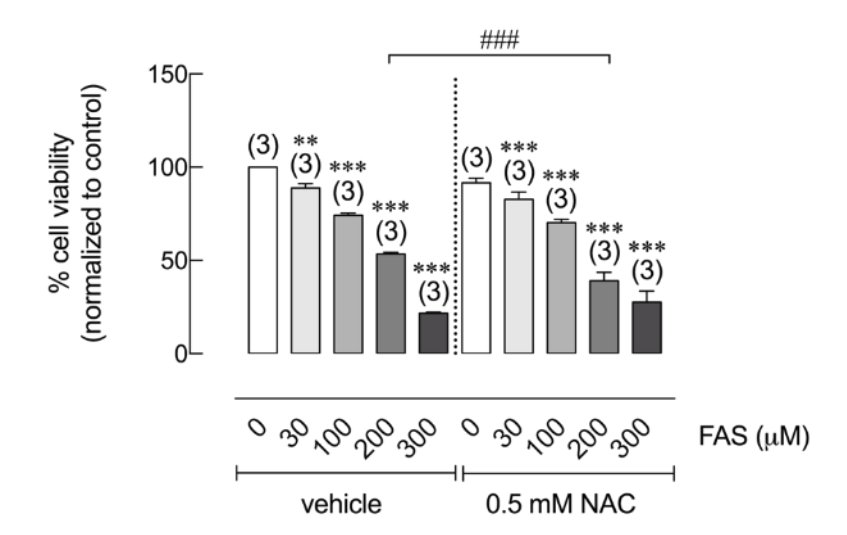


Figure 13 Effects of N-acetyl-L-cysteine (NAC) on osteoblast cell viability under iron overload with (A) FAC and (B) FAS. ***P < 0.001 as compared to control group (0 μ M) with vehicle control; ****P < 0.001 as compared to the same dose of iron between vehicle and NAC treatment.

Objective 13: To examine the effects of iron chelator, deferiprone (DFP), on intracellular iron in osteoblasts and iron-induced osteoblast cell death under iron overload with FAC and FAS

13.1 Rationale

Intracellular iron was increased in osteoblasts treated with both FAC and FAS according to our results reported earlier. Thereby, the correlation between intracellular iron and iron-induced osteoblast cell death is hypothesized, and the effects of iron chelator on intracellular iron in osteoblasts and iron-induced osteoblast cell death during iron overload are examined.

13.2 Experiment procedure

UMR-106 cells were plated in 12 well plate by seeding density 1 x 105 cells/well. Twenty four hours after plating, cells were treated with 10 nM $1,25(OH)_2D_3$ and used 9:1 propylene glycol-ethanol as a vehicle without iron treatment for 72 hours; then cells were treated iron treatments (FAC or FAS) with concentration 0, 100, 200 and 300 μ M by containing 10 nM $1,25(OH)_2D_3$ or vehicle control without $1,25(OH)_2D_3$ for 24 hours.

After treatment, cells were collected by washing twice in cold 1X phosphate buffered saline (PBS) and then the cell were added 100 μ M 3-hydroxy-1,2-dimethyl-4 (1 H)-pyridone (deferiprone; catalog no. 379409 Sigma Chemical Co., St. Louis, MO, USA) in 1X PBS and incubated with slowly shaker at 4 °C for 30 minutes and then the solution was removed and cells are washed again with 1X PBS before gently scraped with cell scraper (Corning In., NY, USA) in 1X PBS. After centrifugation at 7,000 rpm for 15 minutes, the pellet was re-suspended in 250 μ l of ultrapure water for a brief sonication (Li et al., 2016). Then the samples were digested with 65% nitric acid (HNO3) and 30% hydrogen peroxide (H₂O₂) by Ethos UP MAXI-44 microwave digester (Milestone, CT, USA). After digestion the samples were adjusted volume to 25 mL with ultrapure water.

Intracellular iron concentration was measured by FAAS (PinAAcle $9\,0\,0\,T$ Atomic Absorption Spectrometer, PerkinElmer, Waltham, MA, USA). The system was calibrated with blank solution (2% HNO₃) to subtract background and start analyzing the working standard in optimum range at 0, 0.04, 0.4, 0.8, 1.6, and 3 μ g/mL that were diluted from 1,000 μ g/mL Fe certified standard solution with 2% HNO₃. Then the samples were analyzed and 0.8 μ g/mL standard concentration was re-analyzed after every 8 samples for checking the accuracy of working standard. Data analysis, intracellular iron concentration was normalized to protein concentration that can measured by bicinchoninic acid assay (BCA assay) as previously described in Noble et al. (2009).

For the determination of osteoblast cell viability, cells were treated with FAC or FAS in the presence or absence of 100 μ M deferiprone for 72 hours. After that, osteoblast cell viability will be measured by MTT assay as mentioned earlier.

13.3 Results

To further verify whether intracellular iron level relates to iron-induced osteoblast cell death under iron overload or not, effects of iron chelator on intracellular iron in osteoblasts under iron overload with FAC and FAS were tested. Deferiprone (DFP) was an iron chelator used to protect the excess iron in iron overload patients. Therefore, this experiment aimed to study effects of DFP on intracellular iron of osteoblasts under iron overload with or without $1,25(OH)_2D_3$ stimulation. After cells were exposed to vehicle control or $1,25(OH)_2D_3$ and iron treatments, osteoblasts were incubated with DFP prior to intracellular iron measurement by FAAS. Overall, intracellular iron in

osteoblast UMR-106 cells was decreased after the incubation with 100 μ M deferiprone (Figure 14). In the absence of 1,25(OH)₂D₃, only high concentration of FAC at 300 μ M could significantly raise intracellular iron in osteoblasts. No significant change was observed in other FAC or FAS treated groups; hence, the effects of DFP on the level of intracellular iron in these groups (Figure 14A-B). However, intracellular iron level in osteoblasts treated with 300 μ M FAC was decreased significantly from 0.14 mg/mg proteins to 0.10 mg/mg proteins in the presence of DFP (Figure 14A). On the other hand, DFP notably lowered intracellular iron from 0.11 to 0.09 mg/mg proteins in control groups, from 0.16 to 0.11 mg/mg proteins in 100 μ M, from 0.20 to 0.12 mg/mg proteins in 200 μ M and from 0.22 to 0.14 mg/mg proteins in 300 μ M FAC treated groups under 1,25(OH)₂D₃ stimulation (Figure 14C). Similarly, intracellular iron in FAS together with 1,25(OH)₂D₃ treated osteoblasts also decreased from 0.14 to 0.10 mg/mg proteins in control groups, from 0.16 to 0.12 mg/mg proteins in 100 μ M, from 0.18 to 0.12 mg/mg proteins in 200 μ M and from 0.17 to 0.12 mg/mg proteins in 300 μ M FAS treated osteoblasts (Figure 14B). These results demonstrated that iron chelator, DFP, could reduce 1,25(OH)₂D₃-induced intracellular iron in osteoblasts from both iron exposure.

As previous experiment showed that deferiprone (DFP) could reduce intracellular iron in osteoblasts treated with FAC and FAS with and without $1,25(OH)_2D_3$ (Figure 14). Effects of DFP on osteoblast cell survival under iron overload, especially those under $1,25(OH)_2D_3$ stimulation were investigated. As shown in Figure 15A, FAC significantly reduced osteoblast cell survival in dose-dependent manner both in vehicle control and DFP treated groups. While osteoblast cell survival was slightly improved in DFP treated groups: from 92.75% to 99.63%, from 73.54% to 75.66%, from 46.09% to 50.94% in osteoblasts treated with 30 μ M, 100 μ M and 200 μ M FAC, respectively, none of these changes showed statistical significance. This effect could not be seen in osteoblast treated with 300 μ M FAC (Figure 15A). Similarly, dose-dependent inhibitory effects were also seen in FAS treated osteoblasts. However, a nonsignificant improvement of osteoblasts was only seen in osteoblasts cells treated with 30 μ M FAS from 93.83% in vehicle control to 97.89% in DFP treated group. It is worth to note that long-term exposure of DFP also significantly reduced osteoblast cell survival by itself (Figure 15A-B). Thereby, the further reduction in osteoblasts exposed to both iron and DFP was also observed. Osteoblast cell survival further decreased in the presence of DFP from 23.14% to 16.62% in 300 μ M FAC, from 77.13% to 45.03% in 100 μ M FAS and from 28.12% to 14.25% in 300 μ M FAS treated groups (Figure 15A-B).

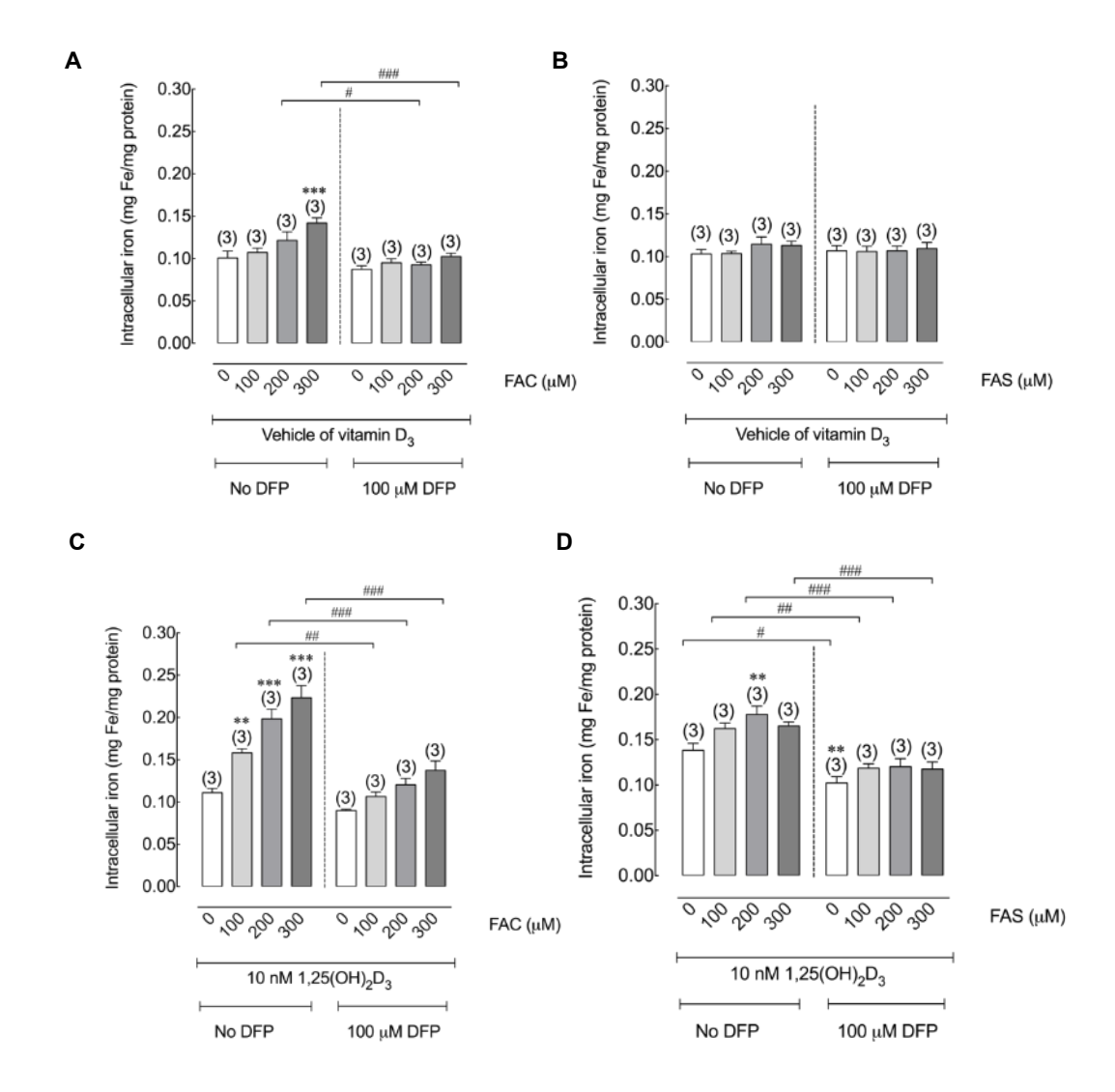
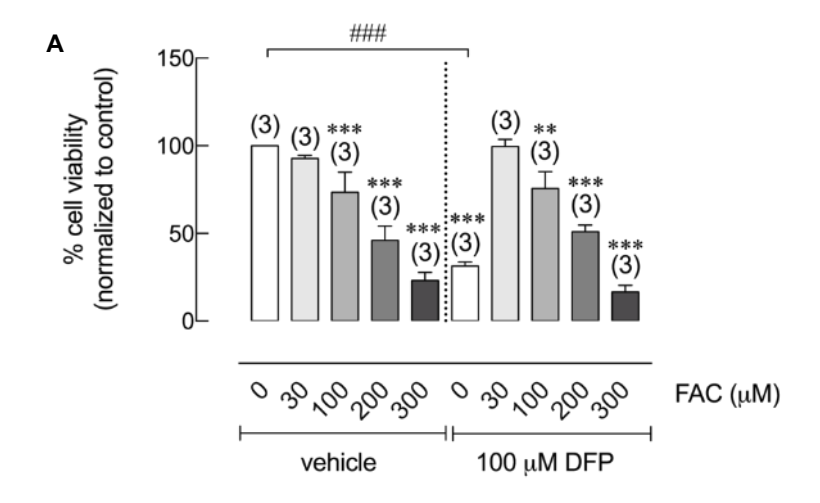


Figure 14 Intracellular iron in osteoblasts after treated with iron under the stimulation of vehicle control (A-B) or $1,25(OH)_2D_3$ (C-D) in the presence or absence of deferiprone (DFP). Both (A&C) FAC and (B&D) FAS were included. *P < 0.05, **P < 0.01 ***P < 0.001 as compared to control group (0 μ M) without DFP. *P < 0.05, **P < 0.01, ***P < 0.01, ***P < 0.001 as compared to the same iron concentration.



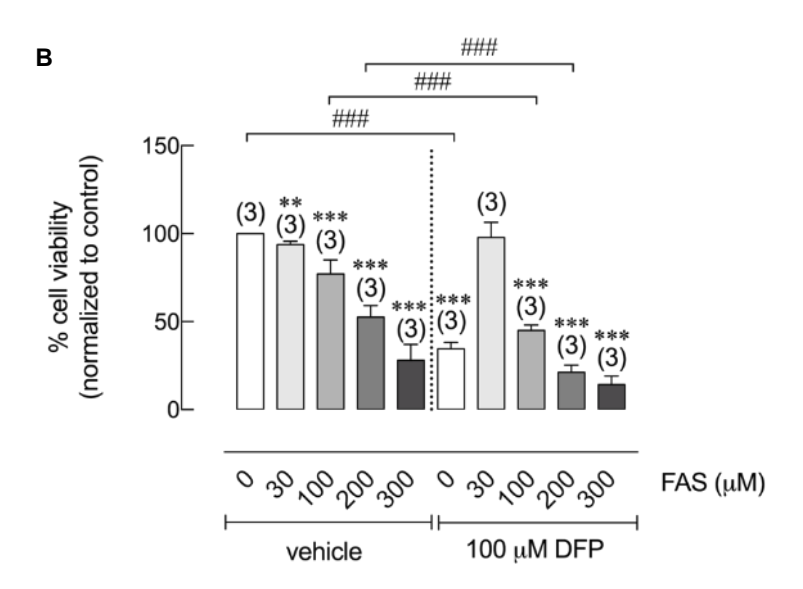


Figure 15 Osteoblast cell viability under iron overload from (A) FAC and (B) FAS in the presence of deferiprone (DFP). *P < 0.05, **P < 0.01 ***P < 0.001 as compared to control group (0 μ M) without DFP. *P < 0.05, **P < 0.01, ***P < 0.001 as compared to the same iron concentration.

Objective 14: To examine the effects of ferric and ferrous on the expression of osteoblast differentiation factors

14.1 Rationale

Osteoblast differentiation was determined by the expression of osteoblast differentiation factors, and iron overload has been reported to contribute to osteoblast differentiation impairment. This study aimed to investigate the effects of two iron species, ferric (Fe³⁺) and ferrous (Fe²⁺), on the expression of osteoblast differentiation factors including runt-related transcription factor 2 (Runx2), alkaline phosphatase (ALP), collagen type 1A and osteocalcin by qRT-PCR. UMR-106 cells were exposed to ferric ammonium citrate (FAC) of ferrous ammonium sulfate (FAS) as Fe³⁺ and Fe²⁺iron donors, respectively for 24, 48 and 72 hours before subjected to qRT-PCR.

14.2 Experiment procedures

Cells were plated at 4.2×10^5 cells/well in 6-well plate (Corning, NY, USA). After seeding, cells were exposed to Fe³⁺ or Fe²⁺ iron donors (FAC and FAS) at 0, 100, 200 and 300 µM for 24, 48, and 72 hours. Several studies showed that the expression alteration of osteoblast differentiation markers in different osteoblast cell lines including UMR-106 cells could be observed since 12 to 96 hours of extracellular treatments, and the alteration of mRNA and protein expression was significantly correlated Accordingly, 24 to 72-hour exposure period should be sufficient to see the mRNA expression alteration in iron treated osteoblasts. Moreover, this short exposure time will minimize the effects of Fe²⁺ and Fe³⁺ on osteoblast viability; while, the iron overload condition can still be represented. The cells were collected by washing twice with phosphate buffered saline (PBS) solution and dissolved in TRIzol reagent (Invitrogen, Carlsbad, CA, USA) to extract total RNA. RNA was purified then measured the OD with NanoDrop-2000c spectrophotometer (Thermo Fisher Scientific, Waltham, MA, USA) at 260 and 280 nm. The ratio of which ranged between 1.8 and 2.0 was considered acceptable. Then, 1 µg of RNA was converted to complementary DNA (cDNA) with iScript cDNA synthesis kit (Bio-rad, Hercules, CA, USA) according to the manufacturer's instruction.

The quantitative real-time PCR (qRT-PCR) was performed by QuantStudio 3D Digital PCR System with SsoFast EvaGreen Supermix (Bio-rad, Hercules, CA, USA) for 40 cycles at 95 °C for 60 seconds, 55–60 °C annealing temperature (S1 Table) for 30 seconds and 72 °C for 30 seconds. Fold change values were calculated from the threshold cycles (C_T) based on the standard ΔC_T method. Relative expression was expressed as the $2^{-\Delta\Delta CT}$ method.

14.3 Results

Twenty-four, 48 and 72 hour-treatments of Fe³⁺ or Fe²⁺ did not significantly change Runx2 mRNA expression level (Figure 16A–B). On the other hand, high concentration of both iron treatments significantly decreased ALP mRNA level at 24 hours (Figure 16C–D). For 48- and 72-hour exposure, the significant reduction of ALP mRNA level was found in only Fe³⁺ iron treatment but not Fe²⁺ (Figure 16C–D). Ferric treatment also had stronger effects on the expression of collagen type 1A at 24 hours than Fe²⁺ iron. Interestingly, Fe³⁺ treatment at 200 and 300 μM triggered collagen type 1A mRNA expression (Figure 16E), but neither Fe³⁺ nor Fe²⁺ changed collagen type 1A mRNA level at 48 and 72-hour (Figure 16E–F). Similar trend could be seen in the expression of osteocalcin. Only Fe³⁺ treatment at 300 μM for 72 hours significantly increased osteocalcin mRNA level (Figure 16G); whereas, 24 and 48-hour treatments of both iron species did not significantly affect osteocalcin expression (Figure 16G–H).

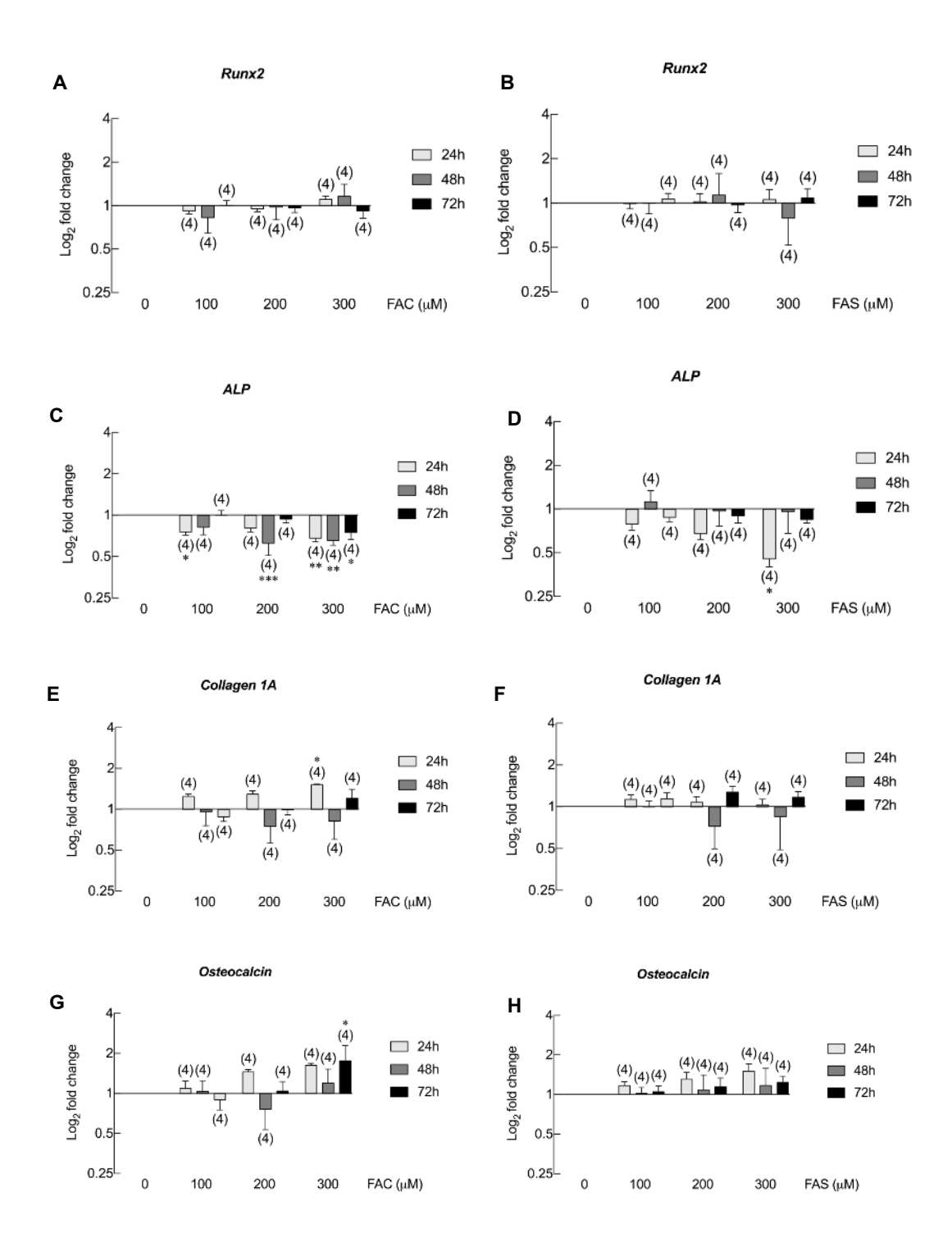


Figure 16 The expression of osteoblast differentiation markers in UMR-106 cells upon FAC and FAS exposure at 24, 48 and 72 hours was determined by qRT-PCR. (A–B) Runx2, (C–D) alkaline phosphatase (ALP), (E–F) collagen I alpha (1A), and (G–H) osteocalcin expression upon FAC and FAS exposure. **P* < 0.05, ***P* < 0.01, ****P* < 0.001 as compared to control group (0 μM).

Objective 15: To elucidate the effects of exogenous calcium treatment on iron-induced osteoblast cell death

15.1 Rationale

Hypocalcemia has been reported in thalassemia, which could worsen thalassemia and iron overload-induced osteoporosis. Giving that calcium supplement could be one of the therapeutic agents for thalassemia and iron overload-induced osteoporosis, the direct effects of extracellular calcium on osteoblast cell viability under iron overload have not been elucidated.

15.2 Experiment procedures

In this experiment, osteoblast UMR-106 cell viability was determined in osteoblasts treated with FAC at 0, 30, 100 and 200 µM in the presence or absence of CaCl₂. At the end of the treatment period, cell viability was determined by MTT assay by adding 0.5 mg/mL thiazolyl blue tetrazolium bromide (MTT dye) (Sigma Chemical Co., St. Louis, MO, USA) in culture media and incubating at 37 °C for 3 hours. After incubation, MTT solvent (5% (w/v) Sodium dodecyl sulfate (SDS) (Vivantis Technologies Sdn. Bhd., Malaysia) in 50% (v/v) N, N-dimethylformamide (VWR international, LLC, OH, USA) in purified water was added in each well. The absorbance was measured with microplate reader (Metertech Inc., Taiwan) at 540 nm according to Riss et al. (2016). An absorbance was subtracted from culture medium background and normalized to control group (vehicle control without iron treatment). Then the absorbance was calculated as a percentage of cell viability.

15.3 Results

Similar to results from previous experiments, this experiment also showed that FAC significantly reduced osteoblast cell viability in dose dependent manner. When extracellular calcium in a form of $CaCl_2$ was applied, deleterious effect of ferric on osteoblast was subsided in a dose-dependent manner of $CaCl_2$ (Figure 17). $CaCl_2$ at 1 mM was able to rescue osteoblasts from FAC-induced osteoblast cell death by 17.63% and 16.31% in 100 and 200 μ M FAC, respectively. More profound effects were shown in a higher concentration of $CaCl_2$. Our results showed that osteoblast cell death was recovered by 25.38%, 32.61% and 25.43% in 30, 100 and 200 μ M FAC treated groups in the presence of 2.5 mM $CaCl_2$ (Figure 17).

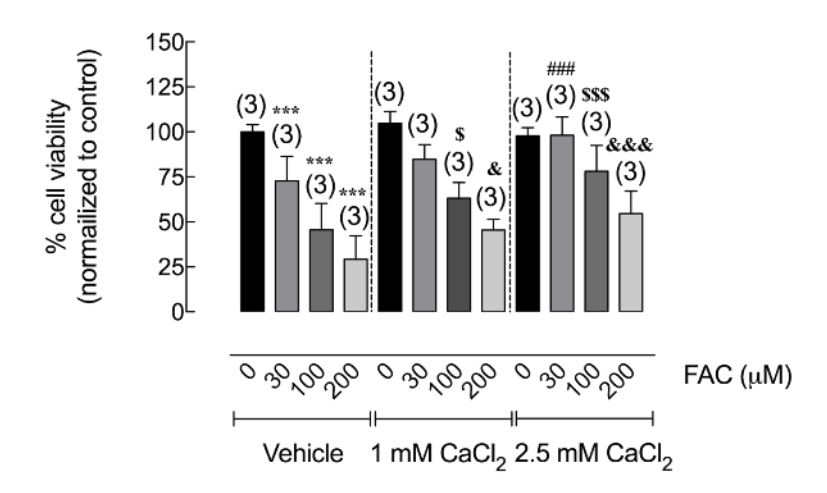


Figure 17 Effects of extracellular CaCl₂ on UMR-106 osteoblast cell survival under iron overload with FAC were illustrated. Osteoblast cell viability was significantly improved ***P < 0.001 as compared to control group (0 μM) with vehicle control; **P < 0.001 as compared to 30 μM FAC in vehicle control group; *P < 0.05, ***P < 0.001 as compared to 100 μM FAC in vehicle control group; *P < 0.05, ***P < 0.001 as compared to 200 μM FAC in vehicle control group.

Objective 16: To examine the effects of ferric and ferrous on osteoblast cell cycle progression

16.1 Rationale

Many studies showed the correlation between ROS production and cell cycle arrest in osteoblast MC3T3-E1cells. In addition, our previous published data showed that both ferric and ferrous suppressed osteoblast cell viability and proliferation. Therefore, this experiment aimed to elucidate the potential effects of these iron species on cell cycle progression in osteoblasts.

16.2 Experimental procedures

UMR-106 cells were seeded at 1.0×10^5 cells/well in 6-well tissue culture plate (Corning, NY, USA). After 24 hours, the cells were treated with 0, 30, 100, 200 and 300 μ M of FAC and FAS (Sigma Chemical Co., St. Louis, MO, USA) for 72 hours. The treatments were refreshed every day. Then, the cells were harvested by trypsinization and fixed in cold 70% ethanol overnight at -20°C. Subsequently, each cell suspension was centrifuged at 800 rpm for 3 minutes and incubated with propidium iodide (PI) DNA staining solution (20 μ g/mL PI)(Life Technologies, CA, USA) and 200 μ g/mL DNAse-free RNAse A (Life Technologies, CA, USA) for 30 minutes at room temperature in the dark. Cell cycle distribution was analyzed using a FACScan flow cytometer (FACSCanto; BD Biosciences, USA).

16.3 Results

To investigate the involvement of iron-induced cell growth inhibition in osteoblast cells, cell cycle distribution of iron-treated UMR-106 cells was analyzed by flow cytometry. UMR-106 cells were treated with 0 (control), 30, 100, 200 and 300 μ M of FAC or FAS for 72 hours. The results showed that the percentage cell population in the G0/G1 phase was significantly increased in 200 and 300 μ M FAC-treated groups as compared to the control (Figure 18). Similar results could be seen in osteoblasts treated with 200 μ M FAS (Figure 19). Whereas, no significant change was observed in the S and G2/M phases. Therefore, these results suggested that FAC and FAS could induce cell cycle arrest in G0/G1 phase resulting in cell growth inhibition in osteoblasts.

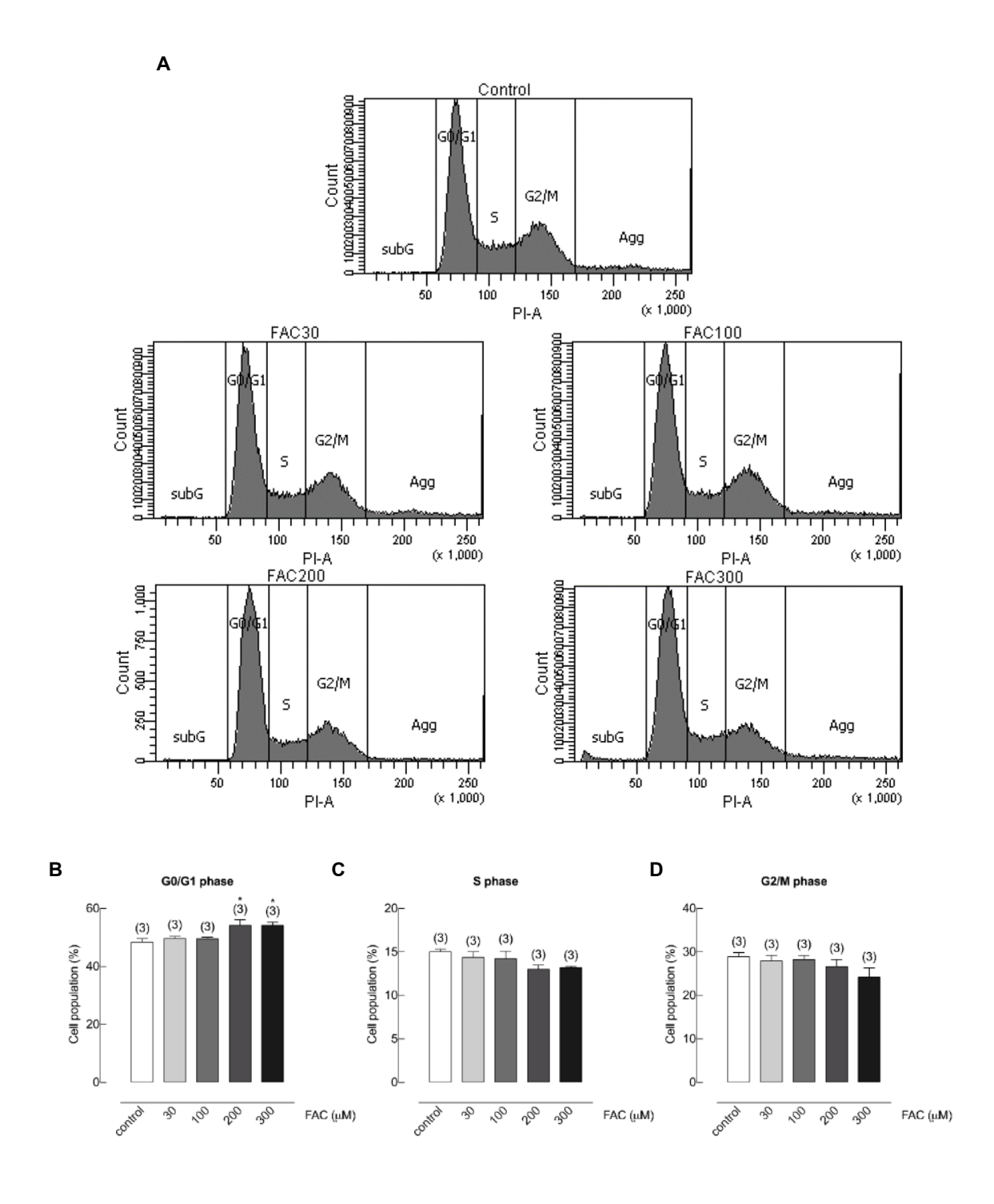


Figure 18 Cell cycle distribution of UMR-106 cells treated with FAC (A) representative figures of cell cycle distribution from flow cytometry, Quantified data showing percent cell distribution in G0/G1 phases (B), S phase (C) and G2/M phases (D), *P < 0.05 as compared to control group (0 μ M)

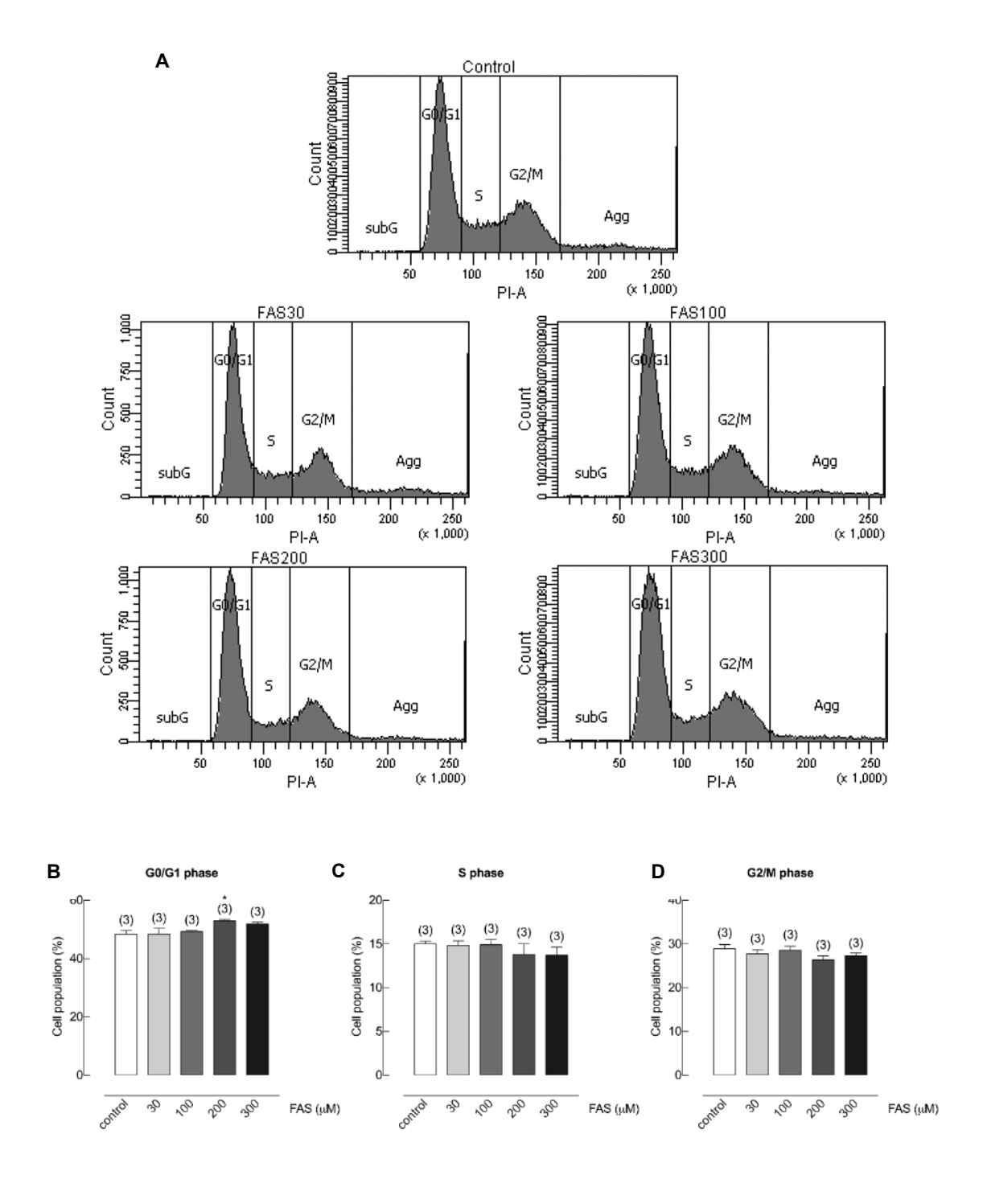


Figure 19 Cell cycle distribution of UMR-106 cells treated with FAS (A) representative figures of cell cycle distribution from flow cytometry, Quantified data showing percent cell distribution in G0/G1 phases (B), S phase (C) and G2/M phases (D), *P < 0.05 as compared to control group (0 μ M)

Research Output

International publication

Results from this project has been published in 1 international peer-reviewed article in Biometals (impact factor 2.478, Q1), and another manuscript is accepted to be published in PLoS One (impact factor 2.776, Q1). (Table 2).

Lertsuwan K, Nammultriputtar K, Nanthawuttiphan S, Phoaubon S, Lertsuwan J, Thongbunchoo J, Wongdee K, Charoenphandhu N (2018) Ferrous and ferric differentially deteriorate proliferation and differentiation of osteoblast-like UMR-106 cells. Biometals 31(5):873-889. (Attached document)

Lertsuwan K, Nammultriputtar K, Nanthawuttiphan S, Tannop N, Teerapornpuntakit J, Thongbunchoo J, Charoenphandhu N (2020) Differential effects of Fe2+ and Fe3+ on osteoblasts and the effects of 1,25(OH)2D3, deferiprone and extracellular calcium on osteoblast viability under iron-overloaded conditions. PLoS One (Accepted) (Attached document)

Other activities

1 Presentation in international and national conferences

- 1.1 Being a speaker in the topic: "Targeting Molecular Mechanism for Osteoporosis in Thalassemia and Iron Overload" in COCAB-moving forward for food and drug translational research, Bangkok, Thailand (August 2018)
- 1.2 Parts of results from this project has been presented and published (conference proceeding) in the topic: "Comparative Effects of Ferric and Ferrous on Osteoblast Cell Survival and Function" in Pure and Applied Chemistry International Conference 2019 (February 2019).

Nanthawuttiphan S, Charoenphandhu N, **Lertsuwan**, **K**. (2019, February) *Comparative Effects of Ferric and Ferrous on Osteoblast Cell Survival and Function* presented at Pure and Applied Chemistry International Conference 2019, Bangkok, Thailand.

- 1.3 Parts of results from this project has been presented as a poster in a topic of:
- "Differential effects of Fe²⁺ and Fe³⁺ on the proliferation and differentiation of osteoblasts" in the 9th Federation of the Asian and Oceanian Physiological Societies Congress (FAOPS), Kobe, Japan. (March 2019)
- Nammultriputtar K., **Lertsuwan K.** and Charoenphandhu N. (2019, March) Differential effects of Fe2+ and Fe3+ on the proliferation and differentiation of osteoblasts. Poster presented at the 9th Federation of the Asian and Oceanian Physiological Societies Congress (FAOPS), Kobe, Japan.
- 1.4 Oral presentation in a topic of "Unveiling underlined molecular mechanisms of Thalassemia-induced osteoporosis" at 27th FAOBMB & 44th MSBMB Conference and IUBMB Special Symposia, Kuala Lumpur, Malaysia (August 2019)

Lertsuwan K, Nammultriputtar K, Nammultriputtar K, Phoaubon S and Charoenphandhu N. (2019, August) Unveiling underlined molecular mechanisms of Thalassemia-induced osteoporosis. Oral presentation at

27th FAOBMB & 44th MSBMB Conference and IUBMB Special Symposia, Kuala Lumpur, Malaysia

1.5 Parts of results from this project has been presented and published (conference proceeding) in the topic: "Investigating the Involvement of Ferroptosis in Osteoblast Cell Death under Iron Overload" at Pure and Applied Chemistry International 2020 (PACCON 2020), Bangkok, Thailand (February 2020).

Tannop N, Charoenphandhu N. and **Lertsuwan K.** (2020, February) Investigating the Involvement of Ferroptosis in Osteoblast Cell Death under Iron Overload. Poster presented at Pure and Applied Chemistry International 2020 (PACCON 2020), Bangkok, Thailand

2 Collaboration with other researchers

- 2.1 Associate professor Dr. Kannikar Wongdee (Burapha University) in her suggestions and expertise in iron transport and regulation
- 2.2 Dr. Jomnarong Lertsuwan (Chulabhorn Research Institute) in his suggestions and expertise in apoptotic and non-apoptotic cell death mechanisms

Table 2 Outputs from this project were illustrated as follows

Output	Detail First / Corresponding		sponding author
		First author	Corresponding
			author
Research articles			
Lertsuwan K, Nammultriputtar K, Nanthawuttiphan S,	manuscript is under preparation	Lertsuwan K.	Charoenphandhu N
Phoaubon S, Lertsuwan J, Thongbunchoo J, Wongdee	manuscript is submitted.		
K, Charoenphandhu N (2018) Ferrous and ferric	manuscript is under revision.		
differentially deteriorate proliferation and differentiation	manuscript is accepted/ in		
of osteoblast-like UMR-106 cells. Biometals 31(5):873-	Press.		
889. (IF 2.478, Q1)	☑ manuscript is published.		
Lertsuwan K, Nammultriputtar K, Nanthawuttiphan S,	☐ manuscript is under preparation	Lertsuwan K	Charoenphandhu N
Tannop N, Teerapornpuntakit J, Thongbunchoo J,	manuscript is submitted.		·
Charoenphandhu N (2020) Differential effects of Fe ²⁺	manuscript is under revision.		
and Fe ³⁺ on osteoblasts and the effects of	manuscript is accepted/ in		
1,25(OH)2D3, deferiprone and extracellular calcium on	Press.		
osteoblast viability under iron-overloaded conditions.	manuscript is published.		
PLoS One (IF 2.776, Q1) (Accepted)			
International conference			
Nanthawuttiphan S, Charoenphandhu N and	results are presented.	Nanthawuttiphan S	Lertsuwan K.
Lertsuwan, K. (2019, February) Comparative Effects of	I	ramiawataphan	Lortouwan It.
Ferric and Ferrous on Osteoblast Cell Survival and	proceeding is published.		
Function presented at Pure and Applied Chemistry	Exproceeding is published.		
International Conference 2019, Bangkok, Thailand.			
Nammultriputtar K., Lertsuwan K . and	☑ results are presented.	Nammultriputtar K	Charoenphandhu N
Charoenphandhu N. (2019, March) Differential effects	proceeding is accepted.		
of Fe ²⁺ and Fe ³⁺ on the proliferation and differentiation	proceeding is published		
of osteoblasts. Poster presented at the 9th Federation			
of the Asian and Oceanian Physiological Societies			
Congress (FAOPS), Kobe, Japan.			
Lertsuwan K, Nammultriputtar K, Nammultriputtar K,	☑ results are presented.	Lertsuwan K	Charoenphandhu N
Phoaubon S and Charoenphandhu N. (2019, August)	proceeding is accepted.		
Unveiling underlined molecular mechanisms of	proceeding is published		
Thalassemia-induced osteoporosis. Oral presentation a			
27th FAOBMB & 44th MSBMB Conference and IUBMB			
Special Symposia, Kuala Lumpur, Malaysia			
Tannop N, Charoenphandhu N. and Lertsuwan K.	☑ results are presented.	Tannop N	Lertsuwan K
(2020, February) Investigating the Involvement of	proceeding is accepted.		
Ferroptosis in Osteoblast Cell Death under Iron	☑ proceeding is published.		
Overload. Poster presented at Pure and Applied			
Chemistry International 2020 (PACCON 2020),			
Bangkok, Thailand			

5. Budget details

	Year 1 (Baht)	Year 2 (Baht)	Sum (Baht)
1. Honorarium	156,000	156,000	312,000
- Honorarium for principal investigator			
2. Materials			
- Chemicals and disposables for cells tissue culture and	35,000	35,000	70,000
treatments			
- Chemicals and consumables for molecular techniques,	99,000	89,000	188,000
such as qRT-PCR, Western blot, ROS assay, glutathione			
assay, CRIPSR/Cas9 construction			
- Experimental animals and related chemicals and			
consumables	10,000	20,000	30,000
3. Expenses	-	-	-
4. Hiring	-	-	-
Total	300,000	300,000	600,000

OUTPUTS

Publication in international peer-reviewed journals

orate Proliferation and Differentiation of UMR-106 Cells



Ferrous and ferric differentially deteriorate proliferation and differentiation of osteoblast-like UMR-106 cells

Kornkamon Lertsuwan · Ketsaraporn Nammultriputtar · Supanan Nanthawuttiphan · Supathra Phoaubon · Jomnarong Lertsuwan · Jirawan Thongbunchoo · Kannikar Wongdee · Narattaphol Charoenphandhu

Received: 14 May 2018/Accepted: 10 July 2018 © Springer Nature B.V. 2018

Abstract The association between iron overload and osteoporosis has been found in many diseases, such as hemochromatosis, β-thalassemia and sickle cell anemia with multiple blood transfusion. One of the contributing factors is iron toxicity to osteoblasts. Some studies showed the negative effects of iron on osteoblasts; however, the effects of two biological available iron species, i.e., ferric and ferrous, on osteoblasts are elusive. Since most intracellular ionized iron is ferric, osteoblasts was hypothesized to be more responsive to ferric iron. Herein, ferric ammonium citrate (FAC) and ferrous ammonium sulfate (FAS) were used as ferric and ferrous donors. Our results showed that both iron species suppressed cell survival and proliferation. Both also induced osteoblast cell death consistent with the higher levels of cleaved caspase 3 and caspase 7 in osteoblasts, indicating that iron induced osteoblast apoptosis. Iron treatments led to the elevated intracellular iron in osteoblasts as determined by atomic absorption spectrophotometry, thereby leading to a decreased expression of genes for cellular iron import and increased expression of genes for cellular iron export. Effects of FAC and FAS on osteoblast differentiation were determined by the activity of alkaline phosphatase (ALP). The lower ALP activity from osteoblast with iron exposure was found. In addition, ferric and ferrous differentially induced osteoblastic and osteoblast-derived osteoclastogenic gene expression alterations in osteoblast. Even though both iron species had

K. Lertsuwan · S. Nanthawuttiphan · S. Phoaubon Department of Biochemistry, Faculty of Science, Mahidol University, Bangkok, Thailand

K. Lertsuwan · K. Nammultriputtar · J. Thongbunchoo · K. Wongdee · N. Charoenphandhu Center of Calcium and Bone Research (COCAB), Faculty of Science, Mahidol University, Bangkok, Thailand

K. Nammultriputtar · J. Thongbunchoo · N. Charoenphandhu (🖂) Department of Physiology, Faculty of Science, Mahidol University, Rama VI Road, Bangkok 10400, Thailand e-mail: naratt@narattsys.com

N. Charoenphandhu Institute of Molecular Biosciences, Mahidol University, Nakhon Pathom, Thailand

Published online: 16 July 2018

Chonburi, Thailand

Laboratory of Chemical Carcinogenesis, Chulabhorn Research Institute, Bangkok, Thailand

K. Wongdee Faculty of Allied Health Sciences, Burapha University,

N. Charoenphandhu The Academy of Science, The Royal Society of Thailand, Dusit, Bangkok 10300, Thailand

፟ Springer

similar effects on osteoblast cell survival and differentiation, the overall effects were markedly stronger in FAC-treated groups, suggesting that osteoblasts were more sensitive to ferric than ferrous.

Keywords Alkaline phosphatase · Ferric · Ferrous · Iron overload · Osteoblast

Introduction

Iron is one of the most essential elements found in organisms. It functions as the crucial components in many biochemical molecules, such as in iron-sulfur cluster containing proteins and in the heme group of oxygen transporting-storing proteins, hemoglobin and myoglobin. Iron enters our body in one of the two forms, i.e., ferrous (Fe²⁺) and ferric (Fe³⁺). In enterocytes, heme-coupled ferrous can be transported into the cell via heme carrier protein (HCP1), and the free ferrous can be transported via divalent metal transporter 1 (DMT1). In contrast to a straightforward transport mechanism for ferrous, ferric from vegetables and grains needs to be reduced by ferric reductase, duodenal cytochrome b (Dcytb), to ferrous before being imported to the cell via DMT1. Ferrous can be exported out of enterocyte via ferroportin (Fpn), and is later oxidized back to ferric by the activity of oxidase enzyme, ceruloplasmin (Cp), and transported in circulation with transferrin. When transferrin-coupled iron reaches the target cells, it can be taken up by the cells via transferrin receptor-mediated endocytosis. Ferric will be released, reduced back to ferrous by ferric reductase Steap3 and exported out of the endocytic vesicle via DMT-1, respectively (MacKenzie et al. 2008; McKie et al. 2001). While the mechanism of iron uptake has been well elucidated in enterocytes and some other cell types, such as macrophages, an ability to import iron and the transport mechanism for osteoblasts are largely unknown.

Regardless to their vital roles in biological systems, excess amount of iron can become toxic to cells. For bone cells, it has been shown that iron negatively affected osteoblast survival, differentiation and mineralization, but had stimulatory effects on osteoclast development (Chen et al. 2015; Tian et al. 2016; Tsay

et al. 2010; Zarjou et al. 2010; Zhao et al. 2014). Not surprisingly, osteoporosis is a common complication in several diseases with iron overload including βthalassemia and hemochromatosis. Disease-associated osteoporosis may worsen patients' conditions, leading to immobility or even mortality from severe fracture. Therefore, knowing the potential factor governing iron-overload-induced osteoporosis would be highly beneficial for specialized drug development for this condition. Even though some investigators have reported the adverse effects of ferric on osteoblast survival and differentiation, the differential effects of ferrous and ferric on bone microenvironment have not been illustrated. High dose of ferric nitrate has been shown to suppress rat osteoblast cell (UMR-106) proliferation, protein synthesis and ALP activity (Diamond et al. 1991). Ferric in a form of ferric ammonium citrate (FAC) was also widely used to test the effects of ferric on osteoblasts. Several groups reported that FAC treatment decreased cell viability, collagen I expression and ALP activity in mouse osteoblast (MC3T3-E1) and human osteoblast (hFOB1.19) cells (He et al. 2013; Tian et al. 2016; Yamasaki and Hagiwara 2009). On the other hand, the negative effects of iron on osteoblast were also found from ferrous exposure. Another study showed that ferrous in a form of ferrous sulfate also inhibited osteoblastic gene expression and induced cell apoptosis in fetal rat-derived calvarial culture (Messer et al. 2009). In addition, another investigator showed that FAC and ferritin ferroxidase suppressed osteoblast differentiation and extracellular matrix calcium deposition in human osteosarcoma 143-B cells, suggesting the potential mechanism of iron-mediated osteoblast suppression via ferritin ferroxidase activity (Zarjou et al. 2010). Interestingly, the comparative studies of the two iron species on osteoblast have not been elucidated.

Since there are two major iron species in biological system, i.e., ferrous and ferric, our comparative study is crucial for specialized therapy targeting the iron specie that causes more detrimental effects on iron overload-induced osteoporosis. Accordingly, this study is the very first study to compare the effects of ferric and ferrous on osteoblast cell proliferation and differentiation. Specifically, the effects of the two iron forms on osteoblast survival, proliferation, function as well as the expression of osteoblastic genes,



osteoclastogenic genes and genes for iron transporters upon ferric and ferrous exposure were investigated.

Materials and methods

Cell culture and reagents

UMR-106 cells (American Type Culture Collection, ATCC, no. CRL-1661) were purchased from ATCC, and were maintained in Dulbecco's modified Eagle's medium (DMEM) (Sigma, MO, USA) supplemented with 10% fetal bovine serum (FBS) (PAA Laboratories, Pasching, Austria), and 100 U/ml penicillinstreptomycin (Gibco, NY, USA). They were grown at 37 °C with 5% CO₂ and subcultured according to ATCC's protocol. Ferric ammonium citrate (FAC) (Sigma) was used as ferric treatment, and ferrous ammonium sulfate (FAS) (Sigma) was used as ferrous treatment. Unless otherwise specified, the treatments were refreshed everyday by half changing the treatment containing media.

Cell viability assay

Osteoblastic UMR-106 cells were plated at 2500 cells/well in 96-well tissue culture plate (Corning, NY, USA). Twenty-four hours after plating, the cells were treated with escalating concentration of FAC or FAS ranging from 0 to 800 μM for 24, 48 or 72 h. After the treatment period, cell viability was measured by using MTT (3-(4,5-dimethylthiazol-2-yl)-2,5-diphenyltetrazolium bromide) assay. In short, MTT (Sigma Aldrich, MO, USA) was added to each well to achieve a final concentration of 1 mg/ml. The cells were then incubated at 37 °C for 3 h. After that, formazan dissolving solution containing 10% SDS (Sigma Aldrich, MO, USA) in 50% N,N-dimethylformamide (DaeJung, Gyeonggi-do, South Korea) to dissolve MTT product, formazan. The absorbance of each well representing cell viability was determined at 590 nm by a microplate reader (Model 1420; Wallac, MA, USA).

BrdU assay

Cell proliferation was determined by BrdU Cell Proliferation Assay Kit (Cell signaling technology, Inc., MA, USA). UMR-106 cells were plated in

96-well plate (Corning, NY, USA) by seeding density 2500 cells/well. After plating for 24 h, cells were treated with 5-bromo-2'-deoxyuridine (BrdU) in culture media containing iron treatment (FAC or FAS) at concentrations of 0, 1, 3, 10, 30, 100, 300 and 1000 µM for 24 h. During cell proliferation, BrdU acts as pyrimidine analog incorporated into the newly synthesized DNA of proliferating cells by replacing thymidine. After being treated, cells were fixed with fixing solution and followed by adding BrdU mouse antibody and anti-mouse IgG HRP-linked antibody to detect the incorporated BrdU. Then, the HRP-substrate, TMB (3,3',5,5'-tetramethylbenzidine) was added to develop color, the intensity of which was quantified at 450 nm to determine the proportional BrdU incorporation that could directly indicate cell proliferation.

Live/dead cell viability assay

UMR-106 cells were plated at 1×10^5 cells/well in 6-well tissue culture plate (Corning, NY, USA). After plating for 24 h, cells were treated with 0, 100, 200 or 300 µM of FAC or FAS for 72 h. After that, the cells were simultaneously labeled with calcein AM and ethidium homodimer using Live/dead viability/cytotoxicity kit for mammalian cells (Invitrogen, CA, USA) to stain live and dead cells, respectively. The labeled cells were incubated at 37 °C for 30 min. After 30 min incubation, the pictures from seven different fields in each treatment were visualized and captured under fluorescent microscope (model BX53; Olympus Corporation, Tokyo, Japan). The quantification was done by using cellSens software (Olympus Corporation, Tokyo, Japan) to measure pixel coverage and fluorescent intensity for green (living cells) and red (dead cells) to obtain average dead/live ratio in each treatment.

Western blot analysis

Cells were plated at 4.2×10^5 cells/well in 6-well tissue culture plate (Greiner, Kremsmünster, Austria). Cells were treated with 0, 100, 200 or 300 μ M of FAC and FAS for 72 h before collecting cell pellets by scraping. Cell pellets were lysed for 45 min in modified radioimmunoassay precipitation (RIPA) buffer containing 50 mM Tris–HCl (DaeJung, Gyeonggi-do, South Korea) pH 7.4, 1% Triton



X-100, 0.25% deoxycholate, 150 mM NaCl (DaeJung, Gyeonggi-do, South Korea) supplemented with Roche complete Minitabs (Roche, IN, USA) at supplier's recommended concentration. Protein concentration of the samples was measured by using BCA protein assay kit (Thermo scientific, MA, USA). Twenty-five micrograms of proteins were subjected to SDS-PAGE using 4-20% Bis-Tris polyacrylamide gels. The proteins were transferred to nitrocellulose membrane (GE, Little Chalfont, United Kingdom). Membranes were blocked for 1.5 h at room temperature in blocking buffer containing 4% w/v bovine serum albumin (BSA) in 0.1% v/v Tween 20 in Tris buffer saline (TBST). All blots were incubated in primary antibody and secondary antibody diluted in blocking buffer at 4 °C overnight and at room temperature for 75 min, respectively. Primary antibodies used in this experiment included rabbit anti-cleaved caspase-3 (Asp175) monoclonal antibody (9964, Cell Signaling Technology, MA, USA), rabbit anti-cleaved caspase-7 (Asp198) monoclonal antibody (8438, Cell Signaling Technology, MA, USA), rabbit anti-actin monoclonal antibody (A2066, Sigma Aldrich, MO, USA). Secondary antibody was goat anti-rabbit IgG conjugated with horseradish peroxidase (7074, Cell Signaling Technology, MA, USA). Proteins were visualized by enhanced chemiluminescence (ECL) (Millipore, MA, USA) and exposed to Hyperfilm (GE Healthcare, Boston, MA, USA).

Intracellular iron concentration measurement

Measurement intracellular iron concentration was done by flame atomic absorption spectroscopy (FAAS). UMR-106 cells were plated in 12-well plate (Corning, NY, USA) by seeding density 210,000 cells/ well; 24 hafter plating, cells were treated FAC or FAS at the concentration of 0, 100, 200 and 300 µM for 24 h. The cells were collected by washing twice in 1× phosphate buffer saline (PBS) before gently scraped with cell scraper (Corning, NY, USA) in PBS. After centrifugation at 7000 rpm for 15 min, the pellet was resuspended in 500 µL of ultrapure water for a brief sonication (Li et al. 2016). Then the samples were digested with 65% nitric acid (HNO₃) and hydrogen peroxide (H2O2) by Ethos UP MAXI-44 microwave digester (Milestone, CT, USA). After digestion, iron concentration was measured by FAAS (PinAAcle 900T Atomic Absorption Spectrometer, PerkinElmer, Waltham, MA, USA). In addition, the protein content of the samples was measured by bicinchoninic acid assay and was used to normalize intracellular iron concentration, as described by Noble and Bailey (2009) (Noble and Bailey 2009).

Quantitative reverse transcription polymerase chain reaction (qRT-PCR)

UMR-106 cells were plated at 4.2×10^5 cells/well in 6-well tissue culture plate (Greiner, Kremsmünster, Austria). Unless otherwise stated, cells were treated with either FAC or FAS at their half maximal inhibitory concentration (IC50; determined by the experiments in Fig. 1) for 24 h before collecting cell pellets by scraping. Total cellular RNA from cell lysates was extracted by using TRIzol reagent (Invitrogen, CA, USA) according to manufacturer's instruction. Following extraction, RNA was treated with RNAse-free DNase I (Roche, IN, USA) according to manufacturer's protocol. RNA quality and quantity were analyzed spectrophotometrically by using Nano-Drop-2000c spectrophotometer (Thermo Scientific, MA, USA) and electrophoretically by using 0.8% v/w agarose gel in 0.5x Tris-acetate (TAE) buffer. One microgram of RNA was converted to cDNA by using iScript cDNA synthesis kit (Bio-rad, CA, USA) with the thermal cycler (model MyCycler; Bio-rad, CA, USA). qRT-PCR was operated by Bio-rad MiniOpticon using SsoFast EvaGreen Supermix (Bio-rad, CA, USA) according to manufacturer's recommendation. PCR was performed at 95 °C for 40 s (enzyme activation and DNA denaturation), annealing temperature (Table 1) for 30 s (annealing), 65 °C for 5 s and 95 °C for 30 s (melting curve construction). Relative expression levels of the genes mentioned in Table 1 were calculated from $2^{-\Delta Ct}$ values to the housekeeping gene [hypoxanthine phosphoribosyltransferase 1 (Hprt1) or β -actin], and normalized by control to obtain $2^{-\Delta\Delta Ct}$.

Alkaline phosphatase activity assay (ALP assay)

UMR-106 cells were plated in 12-well plate (Corning, NY, USA) at seeding density 210,000 cells/well. Twenty-four hours after plating, cells were treated with FAC or FAS at concentration 0, 100, 200, 300 μM for 24 h and collected by washing twice in PBS before gently scraped with cell scraper (Corning,

Springer

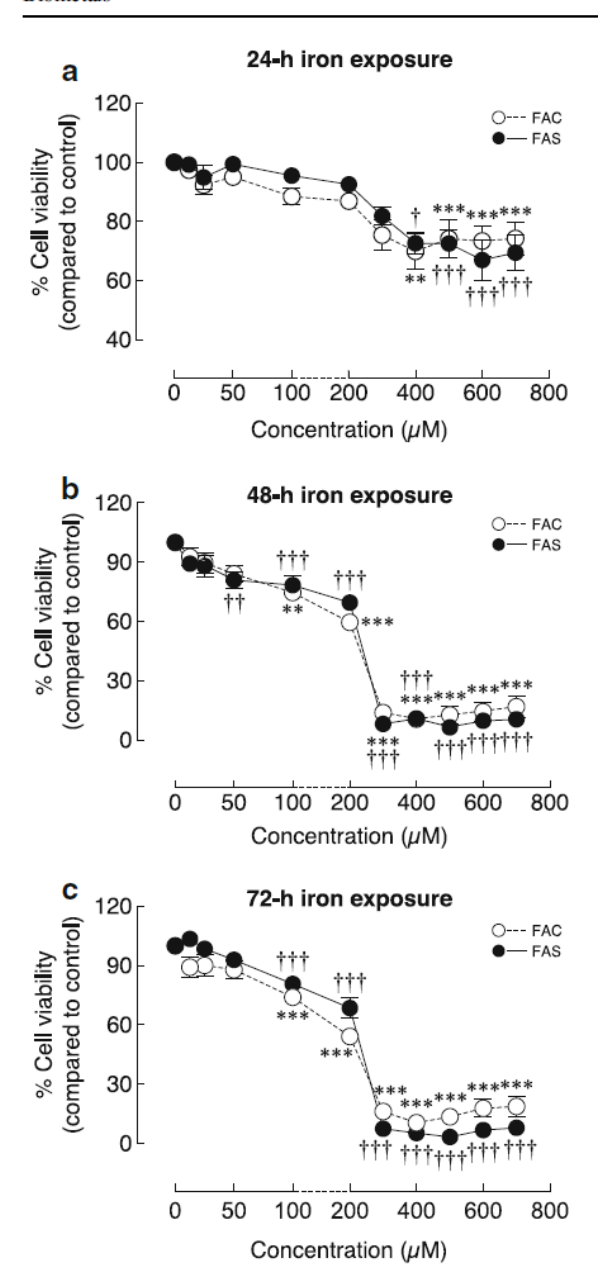


Fig. 1 Effects of FAC and FAS on osteoblast cell survival after iron exposure for 24 h (a), 48 h (b) and 72 h (c). Both FAC and FAS treatments led to decreased osteoblast cell survival in dose dependent manner. (**P < 0.01, ***P < 0.001 as compared to control in FAC treated groups; $^{\dagger}P < 0.05$, $^{\dagger\dagger}P < 0.01$, $^{\dagger\dagger\dagger}P < 0.001$, as compared to control in FAS treated group; experiments were performed in 4 biological replicates each with 3 technical repeats)

NY, USA) in PBS. After centrifugation at 7000 rpm for 15 min, the pellet was resuspended in 250 μ L of lysis buffer (1% Triton X-100 in 50 mM Tris–HCl pH

7.6) for a brief sonication. In addition, the protein content of samples was measured by BCA assay (Noble and Bailey 2009) to normalize ALP activity.

To determine effects of iron on osteoblast differentiation by measurement alkaline phosphatase activity (ALP activity), 100 μL of the sample content was added into 96 well plate and incubated with 20 μL of 40 nM p-nitrophenyl phosphate (phosphatase substrate) (Sigma Aldrich, MO, USA) for 10–30 min at 37 °C. To stop reaction, 0.5 M NaOH 20 μL was added and mixed briefly before measurement the OD at 405 nm shortly after the mixing. The proportion of ALP activity was determined by the color changed from the reduction of phosphatase substrate from colorless to yellow. The quantitative of ALP activity was normalized to protein content and control.

Results

Ferrous and ferric iron differentially inhibited osteoblast cell survival

UMR-106 cells were used to determine the effects of ferric and ferrous iron on osteoblastic cell growth. The cells were treated with ferrous (FAS) or ferric (FAC) at the final concentration of iron at 0, 25, 50, 75, 100, 200, 400, 600 or 800 µM. Cells were treated with different iron species for 24, 48 or 72 h, after which the cell viability of each group was determined by MTT assay normalized to control (0 μ M of treatment). Our results showed that both ferric and ferrous had a negative effect on osteoblast cell survival in a dosedependent manner (Fig. 1). After 24-h treatment, all conditions could not suppress UMR-106 cell growth more than 50%. Even with the highest dose used in these experiments (800 µM), cell viability of UMR-106 dropped by 25.74 and 30.56% for FAC and FAS, respectively (Fig. 1a). At 48 and 72 h after treatment, UMR-106 cells responded to FAS and FAC in a similar pattern. UMR-106 cell survival reduced drastically with the treatment concentration higher than 200 µM to achieve the half maximal inhibitory concentration (IC50) at 221.64 and 232.35 µM of FAC and FAS treatment after 48 h (Fig. 1b). The cells showed slightly lower IC50 after 72 h of iron treatments for both iron species. The IC₅₀ of iron on UMR-106 cell survival at 72 h was 211.45 and 229.76 μM



Table 1 Rattus norvegicus primers used in the qRT-PCR experiments

Gene	Accession no.	Primer (forward/reverse)	Annealing temperature (°C)
Iron transport			
Transferrin receptor 1 (TfR1)	NM_022712	5'-ATACGTTCCCCGTTGTTGAGG-3' 5'- GGCGGAAACTGAGTATGGTTGA-3'	52.00
Transferrin receptor 2 (TfR2)	NM_001105916	5'-AGCTGGGACGGAGGTGACTT-3' 5'-TCCAGGCTCACGTACACAACA- 3'	55.00
Divalent metal transporter 1 (DMT1)	NM_013173	5'-GCTGAGCGAAGATACCAGCG-3'	53.00
Ferroportin (Fpn)	XM_017596804	5'-TGTGCAACGGCACATACTTG-3' 5'-TTCCGCACTTTTCGAGATGG-3' 5'- TACAGTCGAAGCCCAGGACTGT- 3'	52.00
Duodenal cytochrome B1 (DCytb1)	NM_001011954	5'-TCCTGAGAGCGATTGTGTTG-3' 5'-TTAATGGGGCATAGCCAGAG-3'	50.00
Ceruloplasmin (Cp)	XM_008760859	5'-TCCACTGCCATGTGACTGAC-3' 5'-AACAACGTCATTGTGCTCGT-3'	51.00
Hephaestin (Heph)	XM_006257049	5'-CACATTTTTCCAGCCACCTT-3' 5'-TGACGAACTTTGCCTGTGAG-3'	50.00
Homeostatic iron regulator (HFE)	NM_010424	5'-CAGCCTCTCACTGCCACT-3' 5'-AGTGTGTCCCCTCCAAGT-3'	51.00
Osteogenic differentiation factor			
Runt-related transcription factor 2 (Runx2)	NM_053470	5'-TAACGGTCTTCACAAATCCTC- 3'	54.00
		5′-GGCGGTCAGAGAACAAACTA- 3′	
Osteocalcin (OCN)	J04500	5'-CACAGGGAGGTGTGAG-3' 5'-TGTGCCGTCCATACTTTC-3'	57.00
Ephrin type-B receptor 4 (EphB4)	NM_010144	5'-GTGTATGCCACGATACGCTT-3' 5'- ACTGTGTCCACCTTGATGTAGG- 3'	50.85
Ephrin B2 (Ephrin B2)	NM_001107328	5'-AACACTCTCCACAGCACACG-3' 5'-TGGGCAGAAGACACTGTCTG-3'	52.30
Osteoprotegerin (OPG)	NM_012870	5'-ATTGGCTGAGTGTTCTGGT-3' 5'-CTGGTCTCTGTTTTGATGC-3'	50.28
Cyclooxygenase2 (COX2)	NM_017232	$5'\!-\!TATCAGGTCATCGGTGGAGAG\!-\!3'$	53.50
		5′-CGAAGCCAGATGGTAGCATAC- 3′	
Osteoclastogenic differentiation factor Receptor activator of nuclear factor κB ligand (RANKL)	NM_057149	5'-TCGCTCTGTTCCTGTACT-3' 5'-AGTGCTTCTGTGTCTTCG-3'	47.35



Table 1 continued

Gene	Accession no.	Primer (forward/reverse)	Annealing temperature (°C)
Macrophage colony-stimulating factor (MCSF)	NM_023981	5′–ATCCAGGCAGAGACTGACAGA–3′	54.29
		5'-CGCAGTGTAGATGAACCATCC-3'	
Monocyte Chemoattractant Protein-1 (MCP-	NM_031530	5'-TGAGTCGGCTGGAGAACTA-3'	51.53
1)		5'-ATTGGGGTCAGCACAGAT-3'	
Interleukin 1β (IL-1β)	NM_031512	5'-TCAAGCAGAGCACAGACCTGT- 3'	56.07
		5'-TGAGAGACCTGACTTGGCAGA-3'	
Interleukin 6 (IL-6)	NM_012589	5'-GCAAGAGACTTCCAGCCAGT-3'	54.97
		5'-AGCCTCCGACTTGTGAAGTG-3'	
Housekeeping gene			
Hypoxanthine phosphoribosyltransferase 1 (Hprt1)	NM_012583	5'-GGCCAGACTTTGTTGGATTTG-3'	53.00
		5'- CTTTCGCTGATGACACAAACAT- 3'	

for FAC and FAS, respectively (Fig. 1c). Generally, FAC showed slightly higher inhibitory effects on UMR-106 than FAS.

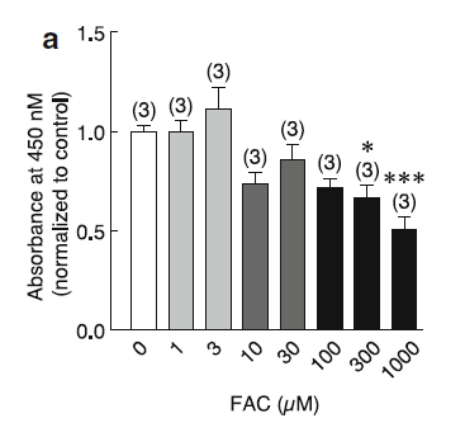
Both iron species suppressed UMR-106 cell proliferation

UMR-106 osteoblast cells were treated with different concentration of either FAS or FAC at 0, 1, 3, 10, 30, 100, 300 or 1000 μM. Cell proliferation rate was determined by BrdU assay after 24 h of FAC or FAS treatments. The incorporation of BrdU into the newly synthesized DNA represented the ability of cells to proliferate under the treatment of FAS and FAC. FAC showed a more severe effect on UMR-106 cell proliferation (Fig. 2). FAC significantly suppressed UMR-106 cell proliferation by 33.44 and 49.48% at 300 and 1000 µM, respectively (Fig. 2a). On the other hand, FAS significantly inhibited UMR-106 cell proliferation by 26.55% at 100 μM and by 28.53% at 1000 µM. Even though the results were not statistically significant, cells treated with FAS also showed a markedly reduced cell proliferation by 23.43% at 300 μM (Fig. 2b) Corresponding to the results from cell survival assay in Fig. 1, FAC showed the overall greater suppression effects on UMR-106 cell proliferation than FAS.

Ferric and ferrous induced osteoblast cell death

Membrane integrity as well as intracellular enzyme activity can be used to determine cell death and cell viability. In this experiment, cell membrane integrity was assessed by using ethidium homodimer, which penetrated cell and nuclear membrane of the dead cells. After entering the cell, the red-fluorescent ethidium homodimer can bind to DNA inside the cell giving a red fluorescent signal of dead cells. On the other hand, the activity of intracellular esterase to change calcein-AM into the green-fluorescent calcein indicated the viability of living cells. UMR-106 cells were treated with different concentrations of FAC or FAS including 0, 100, 200 and 300 µM for 72 h. After that, the cells were labeled simultaneously with ethidium homodimer and calcein-AM. The intensity of red/green fluorescent signals and the area coverage of green and red fluorescent positive cells were evaluated to get dead/live ratio of each group. Our





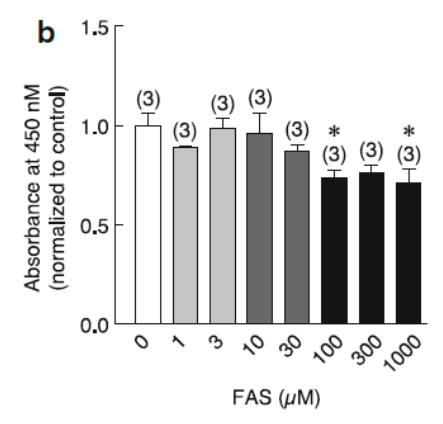


Fig. 2 Both FAC (a) and FAS (b) suppressed osteoblast cell proliferation as shown by BrdU assay. (*P < 0.05, ***P < 0.001 as compared to control; experiments were performed in 3 biological replicates each with three technical repeats)

results showed that both iron species induced cell death as indicated by the increased death/live ratio in all treatment groups (Fig. 3a, b). Fluorescent intensity ratios between the red ethidium homodimer (from dead cells) and the green calcein product were 33.50, 34.07 and 35.29 in UMR-106 cells treated with 100, 200 and 300 µM FAS, respectively. Even though the intensity ratios from FAC treated cells were lower than those from FAS treated cells at 28.47 and 24.50 after treated with 100 and 200 µM FAC, respectively, the dead/live intensity ratio was significantly higher to 54.09 with 300 µM FAC (Fig. 3c). The lost of cell membrane integrity of dead cells and the activity of intracellular enzyme of living cells were also measured by the ratios between red fluorescent positive to green fluorescent positive cells representing the ratio between area coverage of the dead cells to living cells. The dead/live ratios were 70.28, 97.43 and 171.32 for cells treated with 100, 200 and 300 µM FAC, respectively. The dead/live ratios were slightly lower for FAS treatment at 65.77, 93.33 and 140.44 for 100, 200 and 300 µM of FAS (Fig. 3d). Taken together, FAC still showed a higher ability to induce osteoblast cell death as indicated by the greater dead/live intensity and dead/live area coverage than FAS.

FAC and FAS induced osteoblast cell death via apoptosis

To investigate the effects of both ferrous and ferric on apoptotic markers level, UMR-106 cells were treated with FAC and FAS for 72 h before collecting protein samples. The samples were used for western blot analysis of apoptotic markers including cleaved caspase 3 and cleaved caspase 7 to evaluate the protein level of these apoptotic markers after exposing to both iron species (Fig. 4a). Our results showed that the level of cleaved caspase 3 increased drastically after UMR-106 was treated with FAC in a dose-dependent manner (Fig. 4a, b). Although the results were not statically significant, similar trend could be seen in the groups treated with FAS (Fig. 4b). These results suggested that both iron species induced osteoblast cell death via apoptosis pathway. To confirm this speculation, the level of another executioner caspase, cleaved caspase 7, upon the exposure of FAC and FAS was evaluated (Fig. 4a, c). After exposing to FAC, UMR-106 also had a dramatically elevated level of cleaved caspase 7. A slight increase of cleaved caspase 7 could be observed in FAS treated cells (Fig. 4c). Taken together, our results indicated that both ferric and ferrous iron induced osteoblast cell apoptosis with a higher degree from ferric.

FAC and FAS treatments led to increased intracellular iron and gene expression alteration in iron transporters

To determine whether the exposure of both iron treatments led to increased intracellular iron, intracellular iron after 24 h of FAC or FAS treatment was determined by using FAAS. Results from FAAS showed that intracellular iron significantly elevated after FAC treatment from 0.18 mg iron/mg proteins in the control to 0.43, 0.65 and 1.03 mg iron/mg proteins after treated with 100, 200 and 300 µM of FAC.

Springer

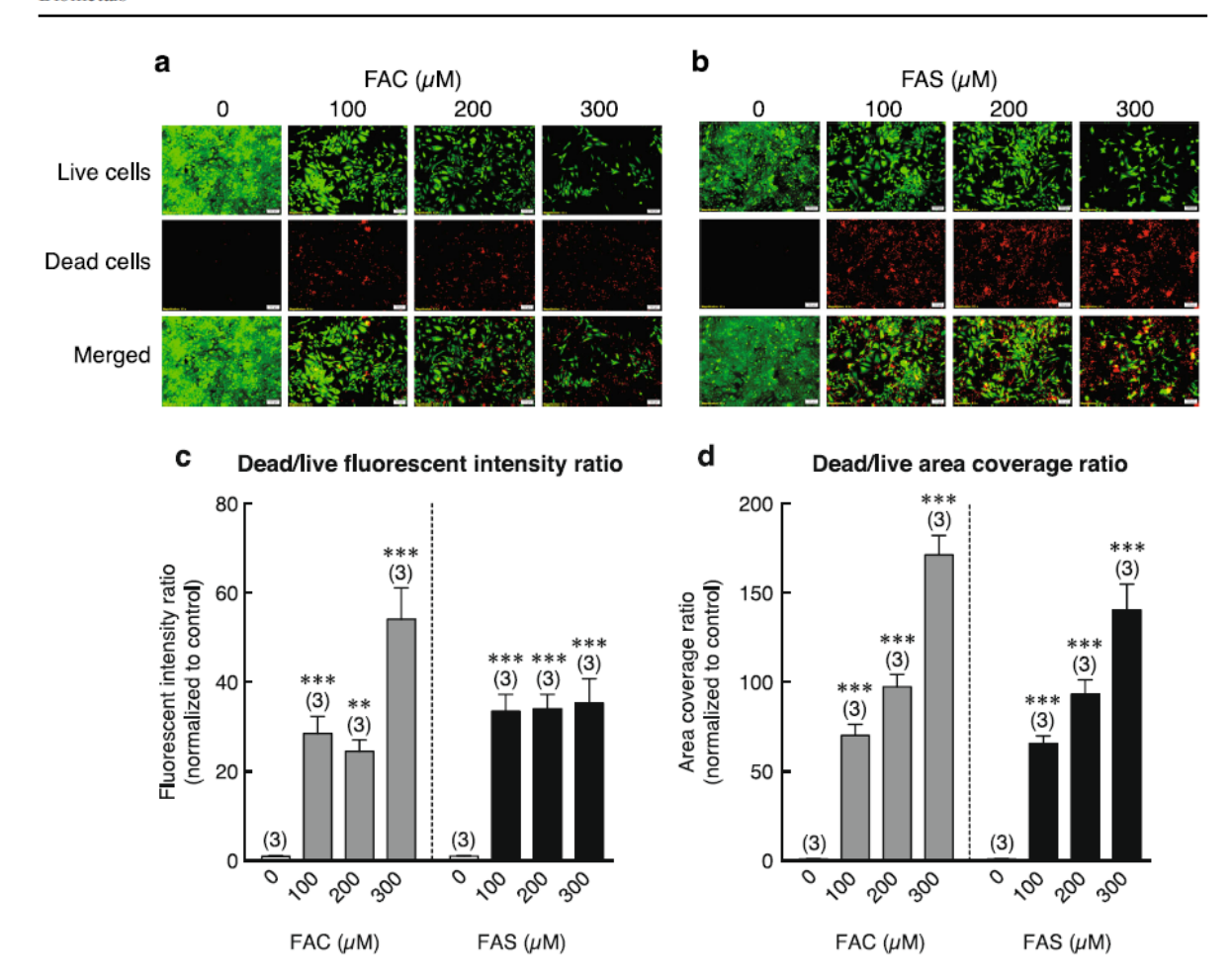


Fig. 3 The dead-inducing activity from FAC and FAS on osteoblast UMR-106 was tested by live/dead assay. Green fluorescent signal from calcein stained live cells, and red fluorescent signal from ethidium homodimer stained dead cells. UMR-106 cells treated with FAC (a) and FAS (b) showed decreased live cells and increased dead cells in dose-dependent manner. The quantified data from dead/live fluorescent intensity

ratio (c) and dead/live area coverage ratio (d) confirmed the elevation of dead cell population and the reduction of live cell population in UMR-106 cells treated with FAC and FAS. (**P < 0.01, ***P < 0.001 as compared to control; experiments were performed in 3 biological replicates each with 7–8 technical repeats). (Color figure online)

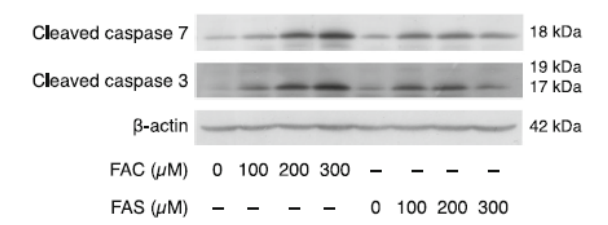
Likewise, intracellular iron increased from 0.17 mg iron/mg proteins in the control group to 0.56, 0.50, 0.51 for 100, 200 and 300 μ M FAS treated cells (Fig. 5a). Our results indicated that FAC induced higher intracellular iron uptake in osteoblast cells as compared to FAS.

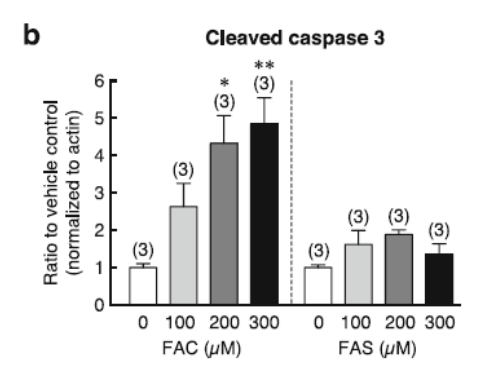
To examine the potential transporter(s) responsible for cellular transport of iron in osteoblasts, the expression level of iron transport machineries upon FAC and FAS treatment was investigated by qRT-PCR. After 72-h iron treatment, iron transporters and its associated genes showed gene expression alterations after iron exposure (Fig. 5b-i). Results showed

that the DMT1 levels were reduced by 56 and 45% after FAC and FAS treatment, respectively (Fig. 5b). Similar trend could be seen in genes for transferrin receptor 1 and 2 (TfR1 and TfR2) with approximately 70 and 20% reduction for TfR1 and TfR2 after both iron treatments (Fig. 5c, d). Only minor reduction was observed in Dcytb gene expression after FAC and FAS treatment (Fig. 5e). On the other hand, the opposite trend was observed for hephaestin (Heph) and Fpn. Specifically, Heph expression was upregulated by 1.38- and 1.18-fold for FAC and FAS (Fig. 5f), while the expression levels of Fpn were increased significantly by 1.71- and 1.36-fold as compared to control









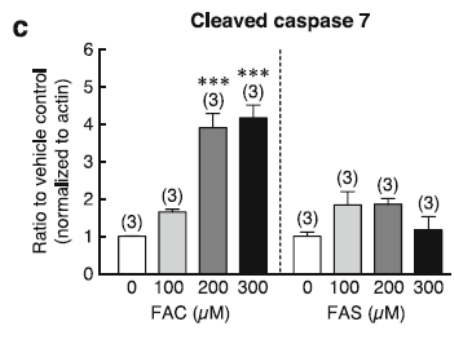


Fig. 4 The representative blot showed the elevation of cleaved caspase 3 and cleaved caspase 7 in UMR-106 exposed to FAC and FAS (a). The quantified data showed a significant increase in cleaved caspase 3 (b) and cleaved caspase 7 (c) in UMR-106 treated with FAC. Even though the results were not statistically significant, similar trend could be seen in UMR-106 treated with FAS. (*P < 0.05, **P < 0.01, ***P < 0.001 as compared to control; experiments were performed in three biological replicates)

(Fig. 5h). There were no significant changes in hemochromatosis protein (HFE) and Cp (Fig. 5g, i), but the latter of which showed a tendency of upregulation.

Both iron species decreased alkaline phosphatase (ALP) activity

Comparative effects of FAS and FAC on osteoblast differentiation and activity were determined by the

activity of ALP. After treated with either FAC or FAS at 100, 200 or 300 μM for 24 h, ALP activity from UMR-106 cells was assessed. The activity of ALP and the activity of ALP normalized to protein content were evaluated. Our results showed a significant decrease in ALP activity from UMR-106 treated with FAC (Fig. 6a). Similar trend could be found in UMR-106 treated with FAS (Fig. 6b). When the activity of ALP was normalized to protein content of each sample, the results were quite fluctuated. However, the reduction of ALP in UMR-106 treated with 300 μM of FAC and FAS were clearly seen (Fig. 6c, d). Our overall results showed that both FAC and FAS, especially the high dose treatment, suppressed ALP activity in UMR-106 cells.

Ferrous and ferric differently affected osteoblastic and osteoclastogenic genes expression

In addition to the expression of osteoblastic genes that directly promote osteoblast differentiation itself, osteoblast also regulates osteoclast differentiation and activity through the interaction and secretion of several osteoblastic and osteoclastogenic factors. Here, the expression levels of osteoblastic genes that promote osteoblast differentiation, but inhibit osteoclast differentiation were determined (Fig. 7). Results showed that the expression levels of erythropoietinproducing human hepatocellular receptor-interacting protein B2 (Ephrin B2), Cyclooxygenase 2 (Cox-2) and osteoprotegerin (OPG) were 1.06, 1.70 and 1.44 fold increased after FAC treatment relative to control (Fig. 7a, c-d). While there was no significant change in erythropoietin-producing human hepatocellular receptors B4 (Eph B4) after FAC treatment, FAS treatment led to a downregulation of Ephrin B2 and Eph B4 by 16 and 25% as compared to control (Fig. 7a, b). The small increase in COX-2 and OPG expression was seen after FAS treatment (Fig. 7c, d). Additional experiments were performed for 2 early differentiation markers, i.e., Runt-related transcription factor 2 (Runx2) and osteocalcin (OCN) using rat βactin as a housekeeping gene. However, when UMR-106 cells were treated with 100 μM of FAC and FAS, the expression of the two markers was not significantly altered (P > 0.05; n = 6/group). Specifically, the expression showed only 1.01 ± 0.16 (P = 0.998) and 1.04 \pm 0.14 (P = 0.99) fold as compared to control in FAC- and FAS-treated groups,



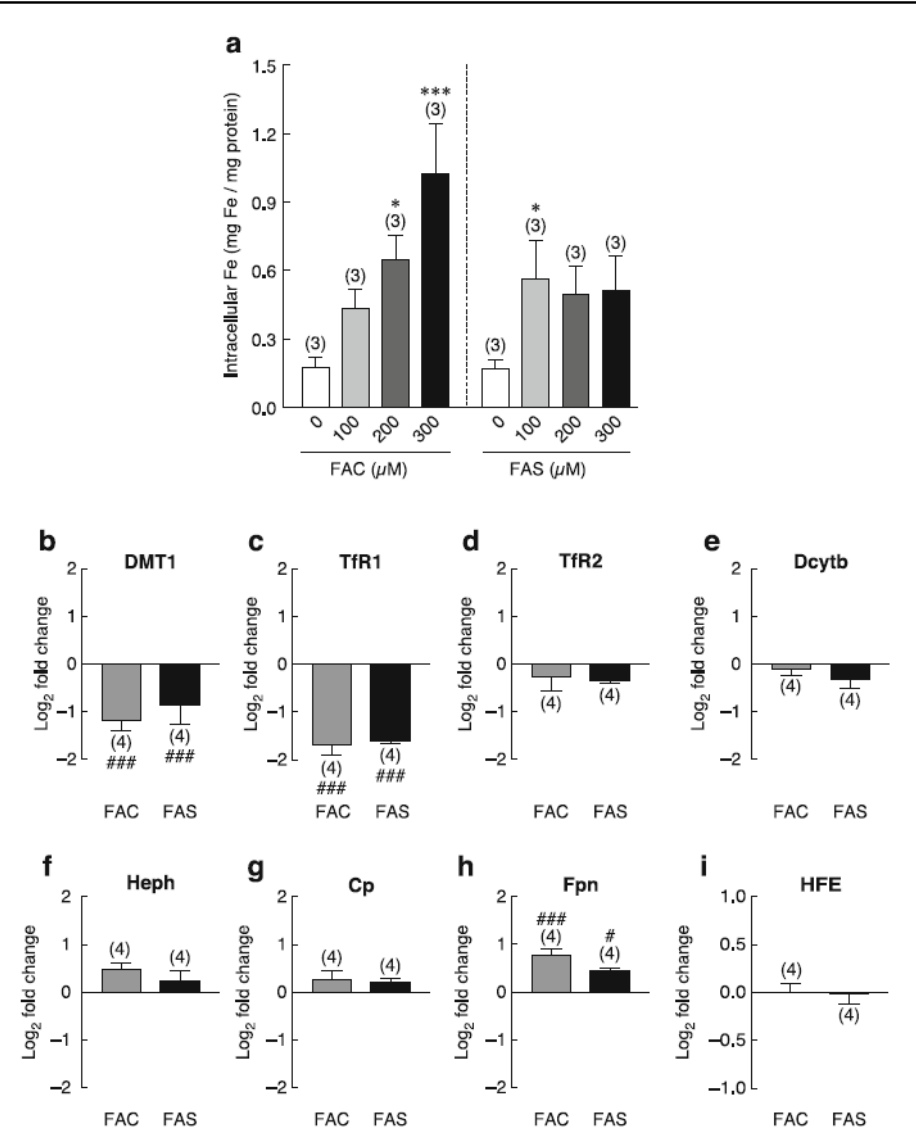


Fig. 5 a FAC and FAS treatment on UMR-106 cells led to elevated intracellular iron in dose-dependent manner. *P < 0.05, ***P < 0.001 as compared to control; experiments were performed in 3 biological replicates each with three technical repeats. b—i Gene expression alteration of iron transporters and proteins functioning in cellular iron transport after iron exposure at the IC $_{50}$ obtained from Fig. 1 (221.64 μ M for FAC and 232.35 μ M for FAS) compared with the control

group. The expression of DMT1 (b), TfR1 (c), TfR2 (d) and Dcytb (e) in UMR-106 was reduced after both FAC and FAS exposure. The expression of Heph (f), Cp (g), Fpn (h) was induced with FAC and FAS treatment; while HFE was unaffected (i). $^{\#}P < 0.05$, $^{\#\#}P < 0.001$ as compared to control group; experiments were performed in four biological replicates each with three technical repeats

respectively. The OCN expression levels were 1.13 ± 0.25 (P = 0.467) and 1.25 ± 0.19 (P = 0.539) fold in FAC and FAS treated groups as compared to the control group. On the other hand, expression levels of osteoclastogenic genes, which promote osteoclast differentiation, were also tested.

Our data showed that FAC treatment led to a significantly increase in monocyte chemotactic protein 1 (MCP-1) and interleukin 6 (IL-6) to 2.80 and 2.14 fold change normalized to control (Fig. 7e, f). FAC showed only a minimal effect on macrophage colony-stimulating factor (M-CSF) and interleukin-1β



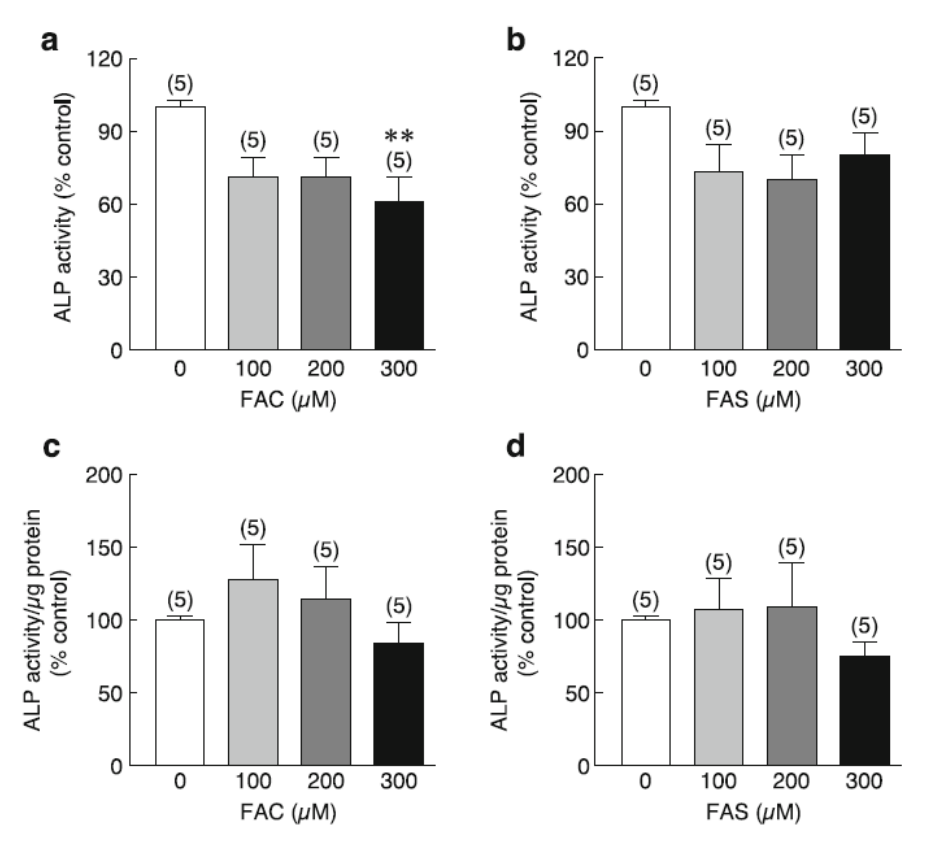


Fig. 6 ALP activity from UMR-106 cells treated with FAC and FAS was determined. ALP activity in UMR-106 cells was significantly reduced after 24 h of FAC treatment (a). Similar trend was observed in UMR-106 cells treated with FAS (b). When ALP activity was normalized to protein content of each

sample, the decreased ALP activity in UMR-106 treated was seen in cells treated with 300 μ M FAC and FAS (c, d). (**P < 0.01 as compared to control; experiments were performed in 5 biological replicates each with three technical repeats)

(IL-1 β) (Fig. 7g, h). Interestingly, FAC significantly suppressed Receptor activator of nuclear factor κB ligand (RANKL) expression (Fig. 7i). On the other hand, FAS induced an increased expression of MCP-1 and IL-6 to 1.87 and 1.378 fold change relative to control (Fig. 7e, f). The expression of MCSF, IL-1 β and RANKL was minimally altered after FAS treatment.

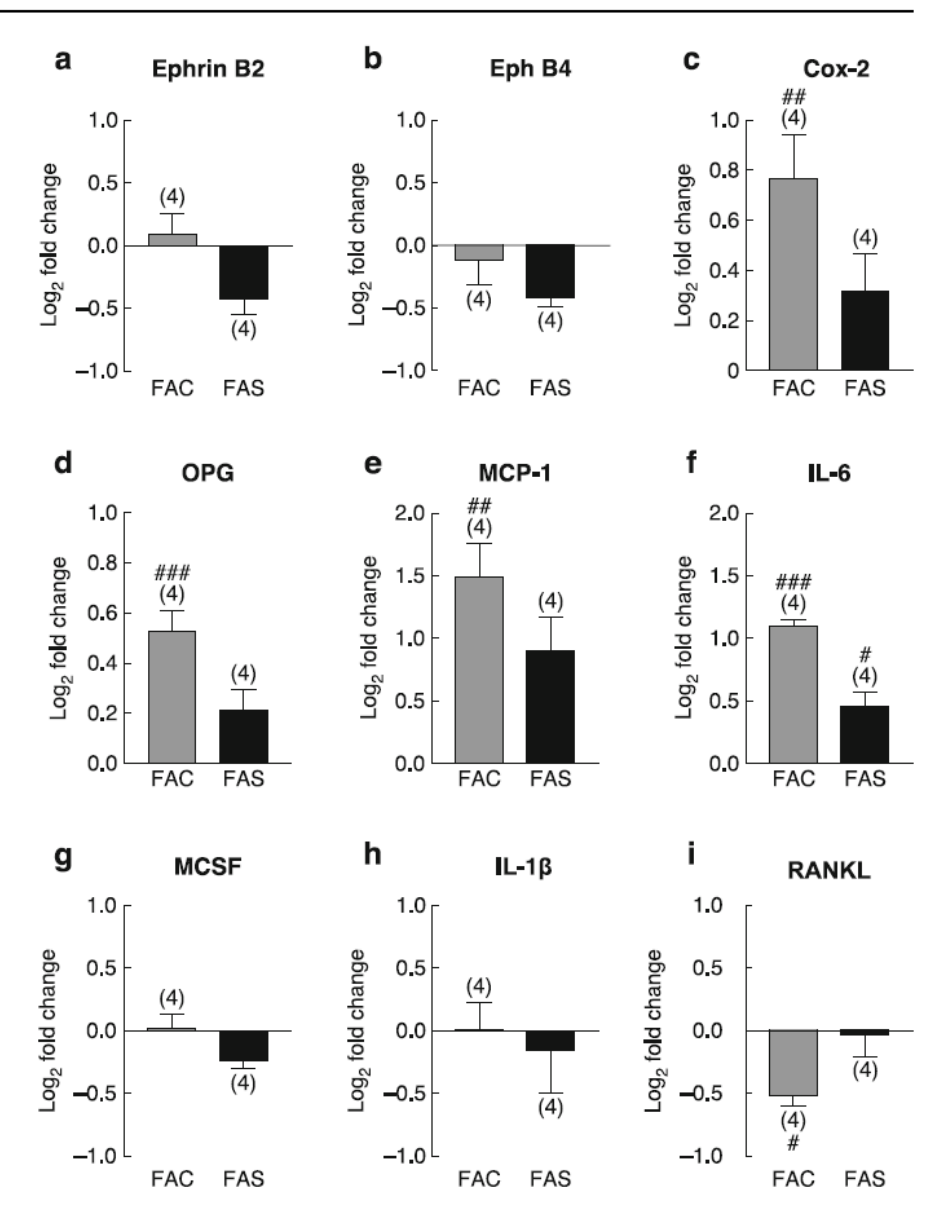
Discussion

As a pivotal element for human body, excess amount of iron or iron overload can be deleterious to many organs including bone. Iron overload could come from uncontrollable iron absorption as in hemochromatosis as well as from increased iron absorption or repeated blood transfusion to compensate with ineffective

erythropoiesis in several blood diseases, such as βthalassemia. It has been demonstrated that iron had negative effects on bone structure and calcium homeostasis, presumably by enhancing bone resorption and suppressing bone formation, the latter of which might be related to the ferroxidase activity of ferritin (Chen et al. 2015; Tian et al. 2016; Tsay et al. 2010; Zarjou et al. 2010; Zhao et al. 2014). Bone formation was found to have an inverse correlation with degree of iron overload (Diamond et al. 1991; Tsay et al. 2010). Iron overload was also associated with reduced osteoblast recruitment and collagen synthesis in osteoporotic pig (de Vernejoul et al. 1984). While the normal serum iron levels range from 10 to 30 µM, the concentration can be elevated to $> 50 \mu M$ in ironoverloaded patients (Ganz 2007; Zhao et al. 2014). In addition, serum iron > 89.5 µM can cause serious systemic toxicity, and mortality rate is high when



Fig. 7 Gene expression levels of osteoblastic and osteoclastogenic genes in UMR-106 after being treated with FAC and FAS at the IC50 obtained from Fig. 1 (221.64 μM for FAC and 232.35 µM for FAS) compared with the control group. The osteoblastic genes including Ephrin B2 (a), Eph B4 (b), Cox-2 (c), OPG (d) MCP-1 (e), IL-6 (f), MCSF (g), IL-1 β (h) and RANKL (i) were studied. OPG, Cox-2, MCP-1 and IL-6 were significantly increased with FAC treatment. IL-6 expression was also induced by FAS. RANKL expression was suppressed by FAC. $^{\#}P < 0.05, \,^{\#\#}P < 0.01,$ ###P < 0.001 as compared to control; experiments were performed in four biological replicates each with three technical repeats



serum iron > 179 μ M (Bregstein et al. 2011). Thus, the investigation of effects of iron on osteoblasts in the present study was performed in the broad range of iron concentration (0–1 mM) to investigate the effects of both physiological and supra-physiological concentrations, some of which (e.g., 100 μ M) could be observed in iron-overloaded conditions.

Two major forms of iron exist in biological systems, i.e., ferrous (Fe²⁺) and ferric (Fe³⁺). In this study, FAS and FAC were used to study the differential effects of the two iron species on osteoblast cell survival and proliferation. The results showed that

both FAC and FAS suppressed osteoblast cell survival in dose and time-dependent manner (Fig. 1a-c). Similarly, data from BrdU assay indicated that high dosage of both iron species significantly decreased osteoblast cell proliferation even within 24 h (Fig. 2). Our results corresponded to previous studies showing negative effects of iron on osteoblast cells (Balogh et al. 2016; Diamond et al. 1991; He et al. 2013; Messer et al. 2009; Tian et al. 2016; Yamasaki and Hagiwara 2009; Zhang et al. 2017). It has been shown that ferrous sulfate treatment caused osteoblast cell death in fetal rat-derived calvarial culture (Messer



et al. 2009). In addition, a high-dose ferric nitrate and FAC suppressed osteoblast cell proliferation and decreased cell viability of mouse osteoblast-like MC3T3-E1 cells (Diamond et al. 1991; Yamasaki and Hagiwara 2009). In addition to the similar antiproliferative effects of iron on osteoblasts as reported before and in this study, this is the very first study to compare the effects of ferrous and ferric iron on osteoblast cell survival and proliferation. Our results have suggested that ferric from FAC has more detrimental effects on osteoblast cell survival and cell proliferation than ferrous from FAS (Figs. 1, 2).

To verify whether both iron species also induced osteoblast cell death, the measurement of the lost of membrane integrity and the activity of intracellular esterase representing dead and live cells were performed. Our results showed the dramatically elevated dead/live intensity ratio and dead/live area coverage in UMR-106 after both iron treatments with the stronger effects from FAC than FAS (Fig. 3). This indicated that both iron species induced osteoblastic cell death with the higher death-inducing effect from ferric than ferrous. Thus, in the presence of high circulating iron from intestinal iron hyperabsorption as in thalassemia and hemochromatosis, it could potentially cause a deleterious effect on osteoblasts, leading to iron overload-associated osteopathy.

While both iron species could induce osteoblast cell death, the mechanism behind this phenomenon is still unknown. Since the cleavage of executioner caspases, i.e., caspase 3 and 7, is widely accepted as a hallmark for apoptosis (Bressenot et al. 2009), protein levels of these apoptotic markers were investigated (Fig. 4). In this study, the level of cleaved caspase 3 was markedly elevated in osteoblasts treated with FAC and slightly increased in osteoblasts treated with FAS. This confirmed that both iron species induced osteoblast apoptosis with a stronger effect from ferric. These results were consistent with the previous studies reported the effects of FAC to induce osteoblast apoptosis (Ke et al. 2017; Liu et al. 2017; Tian et al. 2016). Our data revealed notable changes in cleaved apoptotic markers from ferric treatment versus the slight changes from ferrous treatment. However, the two iron species showed similar IC50 and had relatively resembling dead/live cell ratio for UMR-106 cells, suggesting that the two iron species might use different pathways to induce osteoblast cell death.

To demonstrate whether these iron treatments led to an increase in intracellular iron in osteoblasts, intracellular iron was measured after each iron exposure. Our results showed that upon the exposure of both ferric and ferrous treatments, the intracellular iron was remarkably increased (Fig. 5a). It is worth mentioning that FAC induced significantly higher intracellular iron in osteoblast treated with FAS at the same concentration. In other words, the transport of ferric iron across the plasma membrane of osteoblasts might be easier than that of ferrous iron. In contrast to the well-known mechanisms in enterocytes, iron transport mechanism in osteoblasts remains unclear. Gene expression of some iron-transporting proteins was thus verified in this study. Our results showed that osteoblast-like UMR-106 cells strongly expressed DMT1, TfR1, TfR2, Dcytb, Fpn, Heph, Cp and HFE. As we tested for the gene expression alteration of iron transporter genes in osteoblasts after FAC and FAS treatments, the results were consistent between the two iron species. Interestingly, our data showed that iron transporters, which are responsible for iron uptake mechanisms including DMT1, DCytb, TfR1 and TfR2, were significantly downregulated. In contrast, the expression of iron transporters involving in iron export mechanism, including Fpn1, HEph and Cp was upregulated. Our results are different from the previous study that showed an increase in DMT1 expression in 24-h FAC-treated hFOB1.19 fetal osteoblasts (Liu et al. 2017). Corresponding to our data, results from another group also showed that FAC treatment induced the iron exporter, Fpn1 expression in human hFOB1.19 osteoblasts (Zhao et al. 2014). Since our study and others showed that iron induced osteoblast cell death with the strong correlation with increased intracellular iron (Fig. 5a) (Tian et al. 2016), such adaptation to increase iron export but decrease iron import could potentially provide the survival advantages to iron-overloaded osteoblasts. Although a downregulation of ferrous-transporting DMT1 expression may explain as to why ferrous was less toxic than ferric, more investigation is required to reveal how osteoblasts uptake ferric into the cytoplasm and why ferric accumulation is more robust.

Furthermore, the possible effects of both ferrous and ferric on osteoblast differentiation were tested in this study. Our results showed a marked decrease in ALP activity after treatment with ferric or ferrous for 24 h (Fig. 5). Similar to previous characteristics, the



higher significant effects could be seen from ferric treatment (FAC) than from ferrous treatment (FAS). Our findings corresponded to previous studies that illustrated the negative effects of ferric on osteoblastderived ALP activity (Diamond et al. 1991; He et al. 2013; Jeney 2017; Yamasaki and Hagiwara 2009; Zhao et al. 2012). Furthermore, FAC and ferritin ferroxidase have been shown to inhibit osteoblast differentiation and extracellular matrix calcium deposition in human osteosarcoma 143-B cells, indicating the potential mechanism of iron-mediated osteoblast differentiation and suppression of matrix mineralization by ferritin ferroxidase activity (Zarjou et al. 2010). Herein, we reported similar phenomenon and the comparative effects of ferric and ferrous on rat osteoblast-like UMR-106 cells.

Under normal conditions, bone homeostasis is regulated by the process called bone-remodeling process, which is governed by the activity of boneforming cells (osteoblasts) and bone-resorbing cells (osteoclasts). To keep the balance remodeling process, the development and functionalities of these cells are determined by the signals from itself as well as the interplay signals from another cell type. The combinations of the intracellular signals and extracellular signals will determine whether the bone will be formed or removed by the responsible cells (Proff and Romer 2009; Raggatt and Partridge 2010). Normally, several systems, e.g., RANKL-OPG, Ephrin-Eph and Cox-2, plays important roles in this bone-remodeling process. The expression alterations of osteoblast-derived osteoblastic genes that facilitate bone formation by osteoblast and osteoblast-derived osteoclastogenic genes that regulate bone resorption by osteoclast upon iron exposure was also determined (Fig. 7). Osteoblastic gene markers used in this study included Cox-2, OPG, Ephrin B2 and Eph4. Our results showed that both iron species moderately increased the expression of Cox-2 and OPG. Since Cox-2 also plays an important role in inflammatory responses of the cells under stress, an enhanced expression of Cox-2 was also found in several cell types in response to iron-induced stress, such as hepatocytes and brain cells (Lee et al. 2010; Lukiw and Bazan 1998; Salvador et al. 2010). However, both iron forms led to a decrease in Eph B4 expression, whereas only FAS suppressed the expression of Ephrin B2. Therefore, differential expression alterations of several osteoblastic genes in osteoblast cell treated with iron were found in our study. It is worth mentioning that ferrous and ferric showed different degree of gene expression induction/suppression with an opposite effect on Ephrin B2. As many studies reported about the direct effects of iron on osteoclast differentiation, the effects on osteoblast-derived osteoclastogenic factor expression are still limited (Guo et al. 2015; Xiao et al. 2015, 2018; Xie et al. 2016). In this study, the expression change of the osteoclastogenic genes including MCSF, MCP-1, IL-1β and IL-6 after iron exposure to osteoblast was determined in this study. While the slightly reduced expression of MCSF and IL-1β and moderately lower expression of RANKL were observed in osteoblast treated with iron, both iron species markedly induced the expression of MCP-1 and IL-6 in osteoblast cells. Osteoblast is known to secrete these cytokines to facilitate osteoclast differentiation and activity (Boyle et al. 2003; Cappellen et al. 2002; Matsuo and Irie 2008). As mentioned earlier, the combination of osteoblastic factors and osteoclastogenic factors would determine the phase of bone remodeling process. Even though iron treatments induced the expression of a few osteoblastic genes in osteoblast UMR-106 cells, the opposite effects were also seen in some other osteoblastic genes. Additionally, the greater enhancement was observed in some osteoclastogenic genes after iron exposure in this study. These gene expression alterations implied the shifting role of osteoblast to induce bone resorption rather than bone formation during iron overload. Taken together, our results explained the direct effects of iron on osteoblast cells itself and the indirect effects on osteoblast-mediated osteoclast differentiation during overload-induced osteoporosis. Similar to other experiments in this study, ferric still showed the overall stronger effects on osteoblast gene expression alterations than ferrous (Fig. 7).

Our data suggested the differential contribution of the two iron species in iron overload-induced osteoporosis as ferric showed the overall greater effects on osteoblasts than ferrous. Fenton reaction has been used to explain iron toxicity in many cells. In this reaction, ferrous and ferric react with hydrogen peroxide to generate reactive oxygen species including hydroxyl radical (♠OH) and hydroperoxyl radical (HO₂♠) causing DNA and cell structural damage (Djordjevic 2004; Salgado et al. 2013; Winterbourn 1995). It has been shown that hydroxyl radical produced from Fenton



reaction of ferrous or copper is the most reactive radical known (Djordjevic 2004). With this principle, ones might assume that ferrous should be more toxic than ferric for the cells. However, our results showed that ferric treatment caused significantly higher intracellular iron in osteoblast than ferrous treatment (Fig. 5a). These results indicated that osteoblasts have the greater sensitivity to ferric than ferrous potentially by the higher level of iron transported into the cytoplasm. Accordingly, our study implied that ferric iron from the increased iron absorption (as observed in thalassemia) has greater deleterious impact on osteoblasts than ferrous iron from blood transfusion in ironoverloaded thalassemic patients. The results from this study would be beneficial for the development of interventions and iron chelation treatment for ironinduced osteoporosis.

Acknowledgments This work was supported by Grants from the Thailand Research Fund (TRF) through the TRF Senior Research Scholar Grant (RTA6080007 to N. Charoenphandhu), TRF International Research Network Program (IRN60W0001 to K. Wongdee and N. Charoenphandhu), Research Grant for New Scholar from TRF, Office of the Higher Education Commission and Mahidol University (MRG6180268 to K. Lertsuwan), RD&E funding (SCH-NR2016-141) from National Science and Technology Development Agency, Thailand, and the CIF grant, Faculty of Science, Mahidol University.

Compliance with Ethical Standards

Conflict of interest The authors declare that there is no conflict of interest.

References

- Balogh E, Tolnai E, Nagy B Jr, Nagy B, Balla G, Balla J, Jeney V (2016) Iron overload inhibits osteogenic commitment and differentiation of mesenchymal stem cells via the induction of ferritin. Biochim Biophys Acta 1862:1640–1649. https:// doi.org/10.1016/j.bbadis.2016.06.003
- Boyle WJ, Simonet WS, Lacey DL (2003) Osteoclast differentiation and activation. Nature 423:337–342. https://doi. org/10.1038/nature01658
- Bregstein J, Roskind CG, Sonnett FM (2011) CHAPTER 5 emergency medicine A2—Polin, Richard A. In: Ditmar MF (ed) Pediatric secrets, 5th edn. Mosby, Philadelphia, pp 154–196. https://doi.org/10.1016/B978-0-323-06561-0. 00005-7
- Bressenot A, Marchal S, Bezdetnaya L, Garrier J, Guillemin F, Plenat F (2009) Assessment of apoptosis by immunohistochemistry to active caspase-3, active caspase-7, or cleaved PARP in monolayer cells and spheroid and subcutaneous xenografts of human carcinoma. J Histochem

- Cytochem 57:289–300. https://doi.org/10.1369/jhc.2008. 952044
- Cappellen D, Luong-Nguyen NH, Bongiovanni S, Grenet O, Wanke C, Susa M (2002) Transcriptional program of mouse osteoclast differentiation governed by the macrophage colony-stimulating factor and the ligand for the receptor activator of NFkappa B. J Biol Chem 277:21971–21982. https://doi.org/10.1074/jbc.M200434200
- Chen B, Li GF, Shen Y, Huang XI, Xu YJ (2015) Reducing iron accumulation: a potential approach for the prevention and treatment of postmenopausal osteoporosis. Exp Ther Med 10:7–11. https://doi.org/10.3892/etm.2015.2484
- de Vernejoul MC, Pointillart A, Golenzer CC, Morieux C, Bielakoff J, Modrowski D, Miravet L (1984) Effects of iron overload on bone remodeling in pigs. Am J Pathol 116:377–384
- Diamond T, Pojer R, Stiel D, Alfrey A, Posen S (1991) Does iron affect osteoblast function? Studies in vitro and in patients with chronic liver disease. Calcif Tissue Int 48:373–379
- Djordjevic VB (2004) Free radicals in cell biology. Int Rev Cytol 237:57–89. https://doi.org/10.1016/S0074-7696(04)37002-6
- Ganz T (2007) Molecular control of iron transport. J Am Soc Nephrol: JASN 18:394–400. https://doi.org/10.1681/ASN. 2006070802
- Guo JP, Pan JX, Xiong L, Xia WF, Cui S, Xiong WC (2015) Iron chelation inhibits osteoclastic differentiation in vitro and in Tg2576 mouse model of Alzheimer's disease. PLoS ONE 10:e0139395. https://doi.org/10.1371/journal.pone.0139 395
- He YF et al (2013) Iron overload inhibits osteoblast biological activity through oxidative stress. Biol Trace Elem Res 152:292–296. https://doi.org/10.1007/s12011-013-9605-z
- Jeney V (2017) Clinical impact and cellular mechanisms of iron overload-associated bone loss. Front Pharmacol 8:77. https://doi.org/10.3389/fphar.2017.00077
- Ke JY, Cen WJ, Zhou XZ, Li YR, Kong WD, Jiang JW (2017) Iron overload induces apoptosis of murine preosteoblast cells via ROS and inhibition of AKT pathway. Oral Dis 23:784–794. https://doi.org/10.1111/odi.12662
- Lee FP, Jen CY, Chang CC, Chou Y, Lin H, Chou CM, Juan SH (2010) Mechanisms of adiponectin-mediated COX-2 induction and protection against iron injury in mouse hepatocytes. J Cell Physiol 224:837–847. https://doi.org/ 10.1002/jcp.22192
- Liu F, Zhang WL, Meng HZ, Cai ZY, Yang MW (2017) Regulation of DMT1 on autophagy and apoptosis in osteoblast. Int J Med Sci 14:275–283. https://doi.org/10.7150/ijms. 17860
- Lukiw WJ, Bazan NG (1998) Strong nuclear factor-kappaB-DNA binding parallels cyclooxygenase-2 gene transcription in aging and in sporadic Alzheimer's disease superior temporal lobe neocortex. J Neurosci Res 53:583–592. https://doi.org/10.1002/(SICI)1097-4547(19980901)53:5 <583::AID-JNR8>3.0.CO;2-5
- MacKenzie EL, Iwasaki K, Tsuji Y (2008) Intracellular iron transport and storage: from molecular mechanisms to health implications. Antioxid Redox Signal 10:997–1030. https://doi.org/10.1089/ars.2007.1893



- Matsuo K, Irie N (2008) Osteoclast-osteoblast communication. Arch Biochem Biophys 473:201–209. https://doi.org/10. 1016/j.abb.2008.03.027
- McKie AT et al (2001) An iron-regulated ferric reductase associated with the absorption of dietary iron. Science 291:1755–1759. https://doi.org/10.1126/science.1057206
- Messer JG, Kilbarger AK, Erikson KM, Kipp DE (2009) Iron overload alters iron-regulatory genes and proteins, downregulates osteoblastic phenotype, and is associated with apoptosis in fetal rat calvaria cultures. Bone 45:972–979. https://doi.org/10.1016/j.bone.2009.07.073
- Noble JE, Bailey MJ (2009) Quantitation of protein. Methods Enzymol 463:73–95. https://doi.org/10.1016/S0076-6879(09)63008-1
- Proff P, Romer P (2009) The molecular mechanism behind bone remodelling: a review. Clin Oral Investig 13:355–362. https://doi.org/10.1007/s00784-009-0268-2
- Raggatt LJ, Partridge NC (2010) Cellular and molecular mechanisms of bone remodeling. J Biol Chem 285:25103–25108. https://doi.org/10.1074/jbc.R109.041087
- Salgado P, Melin V, Contreras D, Moreno Y, Mansilla HD (2013) Fenton reaction driven by iron ligands. J Chil Chem Soc 58:2096–2101. https://doi.org/10.4067/S0717-97072013000400043
- Salvador GA, Uranga RM, Giusto NM (2010) Iron and mechanisms of neurotoxicity. Int J Alzheimers Dis 2011:720658. https://doi.org/10.4061/2011/720658
- Tian Q, Wu S, Dai Z, Yang J, Zheng J, Zheng Q, Liu Y (2016) Iron overload induced death of osteoblasts in vitro: involvement of the mitochondrial apoptotic pathway. PeerJ 4:e2611. https://doi.org/10.7717/peerj.2611
- Tsay J et al (2010) Bone loss caused by iron overload in a murine model: importance of oxidative stress. Blood 116:2582–2589. https://doi.org/10.1182/blood-2009-12-260083

- Winterbourn CC (1995) Toxicity of iron and hydrogen peroxide: the Fenton reaction. Toxicol Lett 82–83:969–974
- Xiao W, Beibei F, Guangsi S, Yu J, Wen Z, Xi H, Youjia X (2015) Iron overload increases osteoclastogenesis and aggravates the effects of ovariectomy on bone mass. J Endocrinol 226:121–134. https://doi.org/10.1530/JOE-14-0657
- Xiao W et al (2018) Iron-induced oxidative stress stimulates osteoclast differentiation via NF-kappaB signaling pathway in mouse model. Metabolism. https://doi.org/10.1016/ j.metabol.2018.01.005
- Xie W, Lorenz S, Dolder S, Hofstetter W (2016) Extracellular iron is a modulator of the differentiation of osteoclast lineage cells. Calcif Tissue Int 98:275–283. https://doi.org/10. 1007/s00223-015-0087-1
- Yamasaki K, Hagiwara H (2009) Excess iron inhibits osteoblast metabolism. Toxicol Lett 191:211–215. https://doi.org/10. 1016/j.toxlet.2009.08.023
- Zarjou A, Jeney V, Arosio P, Poli M, Zavaczki E, Balla G, Balla J (2010) Ferritin ferroxidase activity: a potent inhibitor of osteogenesis. J Bone Miner Res 25:164–172. https://doi. org/10.1359/jbmr.091002
- Zhang D, Wong CS, Wen C, Li Y (2017) Cellular responses of osteoblast-like cells to 17 elemental metals. J Biomed Mater Res A 105:148–158. https://doi.org/10.1002/jbm.a. 35805
- Zhao GY, Zhao LP, He YF, Li GF, Gao C, Li K, Xu YJ (2012) A comparison of the biological activities of human osteoblast hFOB1.19 between iron excess and iron deficiency. Biol Trace Elem Res 150:487–495. https://doi.org/10.1007/ s12011-012-9511-9
- Zhao GY, Di DH, Wang B, Zhang P, Xu YJ (2014) Iron regulates the expression of ferroportin 1 in the cultured hFOB 1.19 osteoblast cell line. Exp Ther Med 8:826–830. https://doi.org/10.3892/etm.2014.1823



Differential effects of Fe ²⁺ and Fe ³	[:] on osteoblasts and	the effects of 1,25(OH) $_2$ D $_3$,
deferiprone and extracellular calciu	um on osteoblast vial	bility under iron-overloaded

----- Forwarded message ------

From: **PLOS ONE** < <u>em@editorialmanager.com</u>>

Date: Thu, 21 May 2563 at 02:34

Subject: Notification of Formal Acceptance for PONE-D-20-08025R1 -

[EMID:1e19cd2ea6e42fee]

To: Kornkamon Lertsuwan < kornkamon.ler@mahidol.edu>

You are being carbon copied ("cc:'d") on an e-mail "To" "Narattaphol Charoenphandhu" naratt@narattsys.com;narattaphol.cha@mahidol.ac.th

CC: "Kornkamon Lertsuwan" kornkamon.ler@mahidol.edu, "Ketsaraporn Nammultriputtar" cocabsubmit@gmail.com, "Supanan Nanthawuttiphan" cocab.lab@gmail.com, "Natnicha Tannop" cocabthalassemia@yahoo.com, "Jarinthorn Teerapornpuntakit" jarintee@gmail.com, "Jirawan Thongbunchoo" cocabpresuckling@gmail.com

PONE-D-20-08025R1

Differential effects of Fe²⁺ and Fe³⁺ on osteoblasts and the effects of 1,25(OH)₂D₃, deferiprone and extracellular calcium on osteoblast viability under iron-overloaded conditions

Dear Dr. Charoenphandhu:

I am pleased to inform you that your manuscript has been deemed suitable for publication in PLOS ONE. Congratulations! Your manuscript is now with our production department.

If your institution or institutions have a press office, please notify them about your upcoming paper at this point, to enable them to help maximize its impact. If they will be preparing press materials for this manuscript, please inform our press team within the next 48 hours. Your manuscript will remain under strict press embargo until 2 pm Eastern Time on the date of publication. For more information please contact onepress@plos.org.

For any other questions or concerns, please email plosone@plos.org.

Thank you for submitting your work to PLOS ONE.

With kind regards,

PLOS ONE Editorial Office Staff on behalf of

Prof. Gianpaolo Papaccio Academic Editor PLOS ONE In compliance with data protection regulations, you may request that we remove your personal registration details at any time. (Use the following URL:

https://www.editorialmanager.com/pone/login.asp?a=r). Please contact the publication office if you have any questions.

--

Kornkamon Lertsuwan, Ph.D.
Assistant Professor of Biochemistry
Department of Biochemistry
Center of Calcium and Bone Research
Faculty of Science, Mahidol University
kornkamon.ler@mahidol.edu

1	
2	
3	Differential effects of Fe ²⁺ and Fe ³⁺ on osteoblasts and the effects of
4	1,25(OH) ₂ D ₃ , deferiprone and extracellular calcium on osteoblast viability
5	under iron-overloaded conditions
6	
7	Kornkamon Lertsuwan ^{1,2} , Ketsaraporn Nammultriputtar ^{2,3} , Supanan Nanthawuttiphan ¹ ,
8	Natnicha Tannop ¹ , Jarinthorn Teerapornpuntakit ^{2,4} , Jirawan Thongbunchoo ² ,
9	Narattaphol Charoenphandhu ^{2,3,5,6}
10	1 Donator of CD's 1 and 4 and Fronte of Colors M. 1 (1.11) in the Donate 1.0400 The land
11 12 13	 Department of Biochemistry, Faculty of Science, Mahidol University, Bangkok 10400, Thailand Center of Calcium and Bone Research (COCAB), Faculty of Science, Mahidol University, Bangkok 10400, Thailand
14	³ Department of Physiology, Faculty of Science, Mahidol University, Bangkok 10400, Thailand
15	⁴ Department of Physiology, Faculty of Medical Science, Naresuan University, Phitsanulok 65000,
16	Thailand
17	⁵ Institute of Molecular Biosciences, Mahidol University, Nakhon Pathom 73170, Thailand
18	⁶ The Academy of Science, The Royal Society of Thailand, Dusit, Bangkok 10300, Thailand
19	
20	
21	
22	Type of article: Research article
23	
24	Short title: Differential effects of ferric and ferrous on osteoblast viability under iron-overloaded
25	conditions
26	
27	
28	*To whom correspondence should be addressed:
29	Narattaphol Charoenphandhu, M.D., Ph.D.
30	Department of Physiology,
31	Faculty of Science, Mahidol University,
32	Rama VI Road, Bangkok 10400, Thailand
33	Tel & Fax: +66-2-201-5629
34 35	Email: narattaphol.cha@mahidol.ac.th
	Wayyyandar Familia Famaya Iran ayarlaad Ostocklast
36	Keywords: Ferric, Ferrous, Iron overload, Osteoblast
37	

Abstract

38

39

40

41

42

43

44

45

46

47

48

49

50

51

52

53

54

55

56

57

58

59

60

One of the potential contributing factors for iron overload-induced osteoporosis is the iron toxicity on bone forming cells, osteoblasts. In this study, the comparative effects of Fe³⁺ and Fe²⁺ on osteoblast differentiation and mineralization were studied in UMR-106 osteoblast cells by using ferric ammonium citrate and ferrous ammonium sulfate as Fe³⁺ and Fe²⁺ donors, respectively. Effects of 1,25 dihydroxyvitamin D₃ [1,25(OH)₂D₃] and iron chelator deferiprone on iron uptake ability of osteoblasts were examined, and the potential protective ability of 1,25(OH)₂D₃, deferiprone and extracellular calcium treatment in osteoblast cell survival under iron overload was also elucidated. The differential effects of Fe³⁺ and Fe²⁺ on reactive oxygen species (ROS) production in osteoblasts were also compared. Our results showed that both iron species suppressed alkaline phosphatase gene expression and mineralization with the stronger effects from Fe³⁺ than Fe²⁺. 1,25(OH)₂D₃ significantly increased the intracellular iron but minimally affected osteoblast cell survival under iron overload. Deferiprone markedly decreased intracellular iron in osteoblasts, but it could not recover iron-induced osteoblast cell death. Interestingly, extracellular calcium was able to rescue osteoblasts from iron-induced osteoblast cell death. Additionally, both iron species could induce ROS production and G0/G1 cell cycle arrest in osteoblasts with the stronger effects from Fe³⁺. In conclusions, Fe³⁺ and Fe²⁺ differentially compromised the osteoblast functions and viability, which can be alleviated by an increase in extracellular ionized calcium, but not 1,25(OH)₂D₃ or iron chelator deferiprone. This study has provided the invaluable information for therapeutic design targeting specific iron specie(s) in iron overload-induced osteoporosis. Moreover, an increase in extracellular calcium could be beneficial for this group of patients.

Introduction

61

62 Iron overload could be a result from an increase in iron absorption, ineffective erythropoiesis and 63 regular blood transfusion [1,2]. These conditions are commonly found in several diseases, e.g., 64 β-thalassemia, hereditary hemochromatosis and sickle cell anemia [3–5]. Because the body has 65 no active mechanism for effective iron excretion [2,6], excess iron often leads to iron toxicity in 66 a number of organs, such as heart, liver and bone [2,7,8], the latter of which could lead to 67 massive calcium loss, osteoporosis, pathological fracture and deformity. Thus, many patients with iron overload have been reported to exhibit signs of osteopenia or osteoporosis [9–11]. 68 Two forms of ionized iron exist in the biological systems—i.e., ferrous (Fe²⁺) and ferric 69 iron (Fe³⁺) [12]. Regarding intestinal absorption, free-ionized non-heme Fe³⁺ iron must be 70 reduced to Fe²⁺ by ferric reductase duodenal cytochrome b (DcytB) before being transported into 71 72 cells, mostly via divalent metal transporter (DMT)-1. Once inside the cells, iron is either stored 73 in iron storage protein, ferritin or entering mitochondria to be used for heme and iron-sulfur cluster synthesis. Fe²⁺ is exported from the intestinal cells by ferroportin-1 and oxidized back to 74 75 Fe³⁺ by copper-dependent ferroxidase hephaestin before binding to transferrin and circulated 76 through the body [13-15]. Excess free iron in the cells could participate in redox reaction for reactive oxygen species (ROS) production through interconverting between Fe³⁺ and Fe²⁺, 77 leading to organ damage and a number of diseases, e.g., fibrosis, liver injury, heart failure, 78 79 diabetes mellitus, neurodegenerative diseases and bone loss [5,16,17]. 80 Cellular iron metabolism in bone cells is largely unclear. For example, the principle route for osteoblast iron uptake is controversial, but it might be related to DMT1, some calcium 81 channels and/or transferrin receptor-mediated endocytosis. Nevertheless, ROS from iron 82 83 overload has been reported to inhibit osteoblast differentiation and stimulate osteoclast differentiation, so bone loss could be the consequence [18,19]. Previously, we reported that Fe³⁺ was a dominant iron specie that inhibited osteoblast by decreasing osteoblast survival, proliferation and activity [20]. Although it is known that iron overload can disturb bone homeostasis causing bone loss, it is not known whether Fe³⁺ and Fe²⁺ have similar effects on osteoblast differentiation. Moreover, the effects of deferiprone (DFP) as a potential therapeutic agent for osteoblast cell suppression under iron overload were also tested in this study.

Human bone marrow derived-mesenchymal stem cells (hBMSCs) can differentiate into multiple committed cell types, e.g., chondrocytes, cardiomyocytes and osteoblasts. Osteoblast differentiation is regulated epigenetically and genetically by different proteins, cytokines and miRNAs [21,22]. Previous studies showed that an inhibition of histone deacetylases (HDACs), especially HDAC2, could facilitate hBMSC osteogenic differentiation [22]. Moreover, bone morphogenetic protein (BMP)-2 and miR-29c-3p were also shown to regulate osteoblast differentiation through Wnt/β-catenin pathway [21,23].

Osteoblast differentiation is driven by the sequential expression of multiple proteins classified as early, intermediate and late osteoblast differentiation markers responsible for osteoblast proliferation, maturation and mineralization, respectively. *Runt*-related transcription factor (Runx)-2 is the principal transcription factor, which further regulates other early differentiation markers including osterix (OSX) and alkaline phosphatase (ALP). Later on, intermediate osteoblast differentiation markers including collagen type 1 and osteopontin are expressed during pre-osteoblast development into mature osteoblasts. Osteocalcin is then expressed marking the stage of mature osteoblasts [22,24]. However, the differential effects of Fe³⁺ and Fe²⁺ on osteoblast differentiation marker expression have never been studied or compared. Additionally, 1,25 dihydroxyvitamin D₃ (1,25(OH)₂D₃)—a potent enhancer for

intestinal calcium absorption—profoundly benefits bone homeostasis, in part by increasing calcium availability for bone formation and delaying bone resorption. Furthermore, 1,25(OH)₂D₃ was also shown to directly modulate osteoblast proliferation, differentiation and mineralization of osteoblasts (for reviews, please see [25–27]). It is possible that 1,25(OH)₂D₃ is able to help protect against adverse effects of iron overload on bone homeostasis. Our previous study illustrated that osteoblasts expressed similar iron transporters as found in enterocytes (e.g., the presence of DMT1 expression), and extracellular iron exposure enhanced iron transport into osteoblasts [20]. However, the effects of 1,25(OH)₂D₃ on iron uptake capacity of osteoblasts remained elusive, and the effects of 1,25(OH)₂D₃ and extracellular calcium on osteoblast viability under iron overload has never been elucidated.

Accordingly, this study is aimed to examine the effects of two different iron species, including Fe³⁺ and Fe²⁺, on osteoblast differentiation markers and osteoblast mineralization ability in UMR-106 cells by using ferric ammonium citrate (FAC) and ferrous ammonium sulfate (FAS) as Fe³⁺ and Fe²⁺ donors, respectively. As the known calcium absorption enhancer, effects of 1,25(OH)₂D₃ on iron uptake and cell survival of osteoblasts under iron overload with the two iron species were determined. Moreover, effects of extracellular calcium supplement on osteoblast cell survival under iron overload were also examined. Because deferiprone (DFP) has been used as an iron chelator to protect iron excess in iron overload patients [28,29], effects of DFP on iron uptake ability and osteoblast cell survival under iron overload with FAC and FAS were determined. Last but not least, the comparative effects of Fe³⁺ and Fe²⁺ on ROS production and cell cycle progression in osteoblasts under iron overload were elucidated.

Due to the ability to retain cell proliferation, several osteoblast models derived from osteosarcoma or stem cells were used. Several osteosarcoma-derived osteoblast cells were

widely used to represent osteoblasts or cells committed to osteoblast linage, such as MG-63, Saos-2, U-2 OS and UMR-106 cell lines [30,31]. Therefore, this study provided the critical information for the development of treatment for iron overload-induced osteoporosis using specific therapeutic agents targeting specific iron specie(s) or mechanism underlies iron overload-induced osteoblast cell death in UMR-106 cells derived from rat osteosarcoma. UMR-106 cells have similar phenotypic characteristics to those found in primary osteoblasts, such as morphological appearance, high ALP activity, expression of vitamin D receptors and in vitro mineralization within 6 days after seeding [32–37].

Materials and Methods

Cell culture and reagents

UMR-106 cells were obtained from American Type Culture Collection (ATCC no. CRL-1661). Cells were maintained and propagated at the Department of Physiology and Department of Biochemistry, Faculty of Science, Mahidol University, Thailand. UMR-106 cells were grown in Dulbecco's modified Eagle's medium (DMEM; Sigma Chemical CO., St. Louis, MO, USA) supplemented with 10% (v/v) fetal bovine serum (FBS; PAA Laboratories, Pasching, Austria) and 100 U mL⁻¹ penicillin-streptomycin (Gibco, Grand Island, NY, USA). Cells were incubated at 37 °C with 5% CO2 and sub-cultured according to manufacturer's instruction. The medium was replaced every other day.

Ferric ammonium citrate (FAC) and ferrous ammonium sulfate (FAS) were used as donors of Fe³⁺ and Fe²⁺, respectively (Sigma). Our previous study from viability assay (MTT assay) as well as cell proliferation assay (BrdU assay) at varied concentration of FAC and FAS showed that <30 μ M of Fe²⁺ and Fe³⁺ affected neither viability nor proliferation of UMR-106

153 cells [20]. Thus, we used \geq 30 μ M Fe²⁺ and Fe³⁺ in the present study as we aimed to investigate 154 the effects of iron on osteoblast viability. Moreover, we have shown that the short-term <300 μ M 155 Fe²⁺ and Fe³⁺ exposure did not significantly affect osteoblast cell viability [20]. Thus, 200 μ M 156 and 300 μ M FAC and FAS were used in some experiments for a short period of time without 157 affecting osteoblast viability. In this study, deferiprone (3-hydroxy-1,2-dimethyl-4(1H)-pyridone; 158 DFP) (Sigma) was used as an iron chelator. Calcium chloride (CaCl₂) (Merck, Kenilworth, NJ, 159 USA) was used as extracellular calcium treatment.

Quantitative real-time PCR (qRT-PCR)

Cells were plated at 4.2×10^5 cells/well in 6-well plate (Corning, NY, USA). After seeding, cells were exposed to Fe³⁺ or Fe²⁺ iron donors (FAC and FAS) at 0, 100, 200 and 300 μM for 24, 48, and 72 h. Several studies showed that the expression alteration of osteoblast differentiation markers in different osteoblast cell lines including UMR-106 cells could be observed from 12 to 96 h of treatments, and the alteration of mRNA and protein expression was well correlated [38–42]. After incubation, the cells were collected by washing twice with phosphate buffered saline (PBS) solution and dissolved in TRIzol reagent (Invitrogen, Carlsbad, CA, USA) to extract total RNA. RNA was purified then measured the OD with NanoDrop-2000c spectrophotometer (Thermo Fisher Scientific, Waltham, MA, USA) at 260 and 280 nm. The ratio of which ranged between 1.8 and 2.0 was considered acceptable. Then, 1 μg of RNA was converted to complementary DNA (cDNA) with iScript cDNA synthesis kit (Bio-rad, Hercules, CA, USA) according to the manufacturer's instruction.

The quantitative real-time PCR (qRT-PCR) was performed by QuantStudio 3D Digital PCR System with SsoFast EvaGreen Supermix (Bio-rad) for 40 cycles at 95 °C for 60 seconds,

- 55–60 °C annealing temperature (S1 Table) for 30 seconds and 72 °C for 30 seconds. Fold
 change values were calculated from the threshold cycles (C_T) based on the standard ΔC_T method.
- 178 Relative expression was expressed as the $2^{-\Delta\Delta CT}$ method.

Bone mineralization determination by alizarin red staining

Twenty-four hours after cell seeding, bone nodule formation of UMR-106 cells were induced by adding 50 mM β-glycerophosphate (Sigma) and 50 μg/mL L-ascorbate 2-phosphate (Sigma) with or without FAC or FAS (0–300 μM) for 6 days. It was previously reported that mineralization in UMR-106 cells occurred as early as 20 h after seeding, presumably due to high ALP activity [37,43], and alizarin red staining could be observed on day 4–5 [9,39]. The media was changed every other day. On day 6, cells were stained for calcium mineralization by alizarin red staining. The culture media was removed, and cells were gently washed with PBS for 3 times. Then, cells were fixed with 70% cold ethanol for 1 h at 4 °C. After fixing, cells were washed with deionized water 3 times. The water was completely removed, and cells were stained with 40 mM alizarin red S (Sigma) for 5–10 minutes on the shaker at room temperature. Alizarin red S was removed by washing 5 times with PBS or until the solution came out clear. Osteoblasts were inspected under a light microscope (Nikon, Melville, NY, USA), and the pictures were taken for further analysis. The total area of red nodule formation was quantified by Image J software (National Institutes of Health, USA).

Flame atomic absorption spectrometry (FAAS)

- Osteoblasts were seeded at 1×10^5 cells/well in 12-well plates (Corning) and incubated for 24 h.
- 198 UMR-106 cells were pre-treated with 10 nM 1,25(OH)₂D₃ (Cayman Chemical, Ann Arbor, MI,

199	USA) without iron for 72 h. Then, cells were exposed to iron treatments (FAC or FAS) at 0, 100
200	200 and 300 μM together with 10 nM 1,25(OH) ₂ D ₃ or vehicle control for 24 h.
201	To determine the effects of deferiprone (DFP) on intracellular iron of osteoblasts under
202	iron overload, after 1,25(OH) ₂ D ₃ treatment mentioned above, cells were washed twice in cold
203	PBS. Then, 100 μM DFP (Sigma) in PBS was added and incubated with slowly shaker at 4 $^{\circ}$ C
204	for 30 minutes.
205	After the treatments, the solution was removed, and cells were washed again with PBS
206	before gently scraped with cell scraper (Corning) in PBS. After centrifugation at 7,000 rpm for
207	15 minutes, the pellet was re-suspended and briefly sonicated in 250 μL of ultrapure water
208	Then, the samples were digested in 65% nitric acid (HNO ₃) and 30% hydrogen peroxide (H ₂ O ₂)
209	by Ethos UP MAXI-44 microwave digester (Milestone, CT, USA) as mentioned previously
210	After digestion, the samples were adjusted the volume to 25 mL with ultrapure water.
211	Intracellular iron was measured by FAAS. The system was calibrated with blank solution
212	(2% HNO ₃), and the working standard in optimum range was used. Data analysis for intracellular
213	iron concentration was normalized to protein concentration measured by bicinchoninic acid
214	assay (BCA assay).
215	
216	Cell viability assay
217	To study the effects of 1,25(OH) ₂ D ₃ on osteoblast cell viability under iron overload, UMR-106
218	cells were plated in 24-well plates at 2×10^4 cells/well. Twenty-four hours after plating, cells
219	were treated with 10 nM 1,25(OH) ₂ D ₃ (Cayman Chemical, Ann Arbor, MI, USA) or 9:1

propylene glycol-ethanol as a vehicle control for 72 h. Then iron treatments (FAC or FAS) at 0,

100, 200 and 300 μM were introduced to the cells together with 10 nM 1,25(OH)₂D₃ or vehicle
 control for 24 h.

To study the effects of deferiprone (DFP) and CaCl₂ on osteoblast cell viability under iron overload, the cells were plated at 1,000 cells/well on 96-well plates and allowed to attach to the plates for 24 h. After that, cells were treated with either FAC or FAS at 0, 30, 100 and 200 μ M in the presence or absence of 100 μ M DFP for 72 h. Similarly, the cells will be exposed to FAC or FAS at 0, 30, 100 and 200 μ M with or without 1mM and 2.5 mM CaCl₂ for 72 h.

At the end of the treatment period, cell viability was determined by MTT assay by adding 0.5 mg/mL thiazolyl blue tetrazolium bromide (MTT; Sigma) in culture media and incubating at 37 °C for 3 h. After incubation, MTT solvent (5% (w/v) Sodium dodecyl sulfate (SDS) (Vivantis Technologies Sdn. Bhd., Malaysia) in 50% (v/v) N, N-dimethylformamide (VWR international, LLC, OH, USA) in purified water was added in each well. The absorbance was measured with microplate reader (Metertech Inc., Taiwan) at 540 nm according to Riss et al. (2016) [44]. An absorbance was subtracted from culture medium background and normalized to control group (vehicle control without iron treatment). Then the absorbance was calculated as a percentage of cell viability.

Cellular reactive oxygen species (ROS) assay

UMR-106 cells were seeded at 2.5×10^4 cells/well in 96-black well plate (Corning). After 24 h, ROS production was measured by using DCFDA cellular ROS detection assay kit (Abcam, Cambridge, UK). The cells were washed with $1\times$ buffer solution. Then, DCFDA solution was added 100 μ L/well, and the cells were incubated for 45 minutes. After incubation, they were washed with $1\times$ buffer again, then iron treatments were added at 0, 30, 100 and 200 μ M and

244	incubated for 6 h. ROS production was measured with fluorescence microplate reader (Spark TM
245	10M multimode microplate reader, Switzerland) at Ex/Em: 485/535 nm. Fold of ROS production
246	was normalized to control groups.
247	
248	Cell cycle analysis
249	UMR-106 cells were seeded at 1.0×10^5 cells/well in 6-well tissue culture plate (Corning). After
250	24 h, the cells were treated with 0, 30, 100, 200 and 300 μ M of FAC and FAS (Sigma) for 72 h.
251	The treatments were refreshed every day. Then, the cells were harvested by trypsinization and
252	fixed in cold 70% ethanol overnight at -20 °C. Subsequently, each cell suspension was
253	centrifuged at 800 rpm for 3 minutes and incubated with propidium iodide (PI) DNA staining
254	solution (20 $\mu g/mL$) (Life Technologies, CA, USA) and 200 $\mu g/mL$ DNAse-free RNAse A (Life Polymer RNAse) (Life Technologies) (Life Technologi
255	Technologies, CA, USA) for 30 minutes at room temperature in the dark. Cell cycle distribution
256	was analyzed using a FACScan flow cytometer (FACSCanto; BD Biosciences, USA).
257	
258	Statistical analysis
259	The results were expressed as Mean \pm standard error of mean (SEM). The mean values were
260	from at least 3 biological replicates with at least 3 internal repeats. The treatment groups were
261	analyzed by the multiple comparison of one-way analysis of variance (ANOVA). The difference
262	between pairs of means was analyzed by Tukey all pair comparison. The level of significance for
263	all statistical tests was $P < 0.05$, and all data were analyzed by GraphPad Prism 5.0 (GraphPad
264	Software Inc., San Diago, CA, USA).
265	

Results

267

287

288

Ferric (Fe³⁺) and ferrous (Fe²⁺) altered osteoblast differentiation markers 268 269 Osteoblast differentiation was determined by the expression of osteoblast differentiation factors, 270 and iron overload has been reported to contribute to osteoblast differentiation impairment [9,45,46]. This study aimed to investigate the effects of two iron species, ferric (Fe³⁺) and ferrous 271 (Fe²⁺), on the expression of osteoblast differentiation factors including runt-related transcription 272 273 factor 2 (Runx2), alkaline phosphatase (ALP), collagen type 1A and osteocalcin by qRT-PCR. 274 UMR-106 cells were exposed to ferric ammonium citrate (FAC) of ferrous ammonium sulfate (FAS) as Fe³⁺ and Fe²⁺iron donors, respectively. Twenty-four, 48 and 72 h treatments of Fe³⁺ or 275 Fe²⁺ did not significantly change Runx2 mRNA expression level (Fig 1A–B). On the other hand, 276 277 high concentration of both iron treatments significantly decreased ALP mRNA level at 24 h (Fig. 278 1C-D). For 48- and 72-h exposure, the significant reduction of ALP mRNA level was found in only Fe³⁺ iron treatment but not Fe²⁺ (Fig 1C-D). Ferric treatment also had stronger effects on 279 the expression of collagen type 1A at 24 h than Fe²⁺ iron. Interestingly, Fe³⁺ treatment at 200 and 280 300 µM triggered collagen type 1A mRNA expression (Fig 1E), but neither Fe³⁺ nor Fe²⁺ 281 282 changed collagen type 1A mRNA level at 48 and 72 h (Fig 1E-F). Similar trend could be seen in the expression of osteocalcin. Only Fe³⁺ treatment at 300 µM for 72 h significantly increased 283 284 osteocalcin mRNA level (Fig 1G); whereas, 24- and 48-h treatments of both iron species did not 285 significantly affect osteocalcin expression (Fig 1G–H). 286

Ferric (Fe³⁺) had higher deleterious effects on osteoblast mineralization than

ferrous (**Fe**²⁺)

Previous experiments showed that both iron forms could suppress the activity and expression of alkaline phosphatase (ALP), which is the key marker for bone mineralization ([20] and Fig 1C–D). Therefore, this experiment was hypothesized that iron overload from both iron species could also impair bone mineralization. Osteoblasts (UMR-106 cells) were incubated with 50 mM β-glycerophosphate and 50 μg/mL of L-ascorbate 2-phosphate to induce bone nodule formation in the presence or absence of Fe³⁺ or Fe²⁺ treatments for 6 days. After that, alizarin red staining was used to determine calcium deposition referred to bone mineralization after treatment either with Fe³⁺ or Fe²⁺. Quantified data showed that both Fe³⁺ and Fe²⁺ treatments significantly reduced the mineralization of bone nodule in a dose-dependent manner (Fig 2). Fe³⁺ significantly reduced osteoblast mineralization down to 51.04%, 29.27%, 21.79% and 17.49% at 100, 200, 250 and 300 μM, respectively (Fig 2A). On the other hand, osteoblast mineralization was slightly decreased to 71.29% and 66.79% in osteoblasts treated with 250 and 300 μM of Fe²⁺ (Fig 2B). Fe³⁺ treatment had stronger inhibitory effects on bone mineralization than Fe²⁺. This study confirmed that both forms of iron impaired bone mineralization, and the more drastic effects were observed in ferric treatments (S1 Fig).

1,25(OH)₂D₃ enhanced iron uptake in osteoblasts

1,25(OH)₂D₃ is an essential hormone for bone formation by inducing intestinal calcium transport. Interestingly, vitamin D deficiency and hypocalcemia were found in thalassemic patients with iron overload condition [47,48]. Therefore, 1,25(OH)₂D₃ might be beneficial for bone homeostasis of these patients. In addition, osteoblasts were also shown to express similar

set of iron transporters found on enterocytes [20,49]. Accordingly, the relationship between 1,25(OH)₂D₃ and iron uptake in osteoblast is still needed to be uncovered. This experiment aimed to determine the effects of 1,25(OH)₂D₃ on iron uptake into osteoblasts upon Fe³⁺ and Fe²⁺ exposure. After treatment, intracellular iron concentration in osteoblast UMR106 cells were measured by flame atomic absorption spectrometry (FAAS). 1,25(OH)₂D₃ significantly increased intracellular iron concentration in osteoblasts treated with FAC and FAS as compared to vehicle treated groups. As shown in Fig 3A, intracellular iron increased in 1,25(OH)₂D₃ treated osteoblasts from 0.11 to 0.16 mg/mg proteins in cells treated with 100 µM FAC, from 0.12 to 0.20 mg/mg proteins with 200 μ M FAC and from 0.14 to 0.22 mg/mg proteins with 300 μM FAC exposure. Likewise, treatment with 1,25(OH)₂D₃ also facilitated iron uptake into osteoblast treated with Fe²⁺ iron more than vehicle treated groups at the comparable doses of Fe²⁺ iron treatment. As shown in Fig 3B, intracellular iron increased from 0.10 to 0.16 mg/mg proteins with 100 µM FAS, from 0.11 to 0.18 mg/mg proteins with 200 µM FAS and from 0.11 to 0.17 mg/mg proteins with 300 μM FAS treatments with the presence of 1,25(OH)₂D₃. Our results showed that 1,25(OH)₂D₃ facilitated iron uptake of both iron species into osteoblasts, and we also found that Fe³⁺ was still a prefer form that was transported into osteoblasts.

328

329

330

331

332

333

334

312

313

314

315

316

317

318

319

320

321

322

323

324

325

326

327

1,25(OH)₂D₃ minimally affected iron-induced osteoblast cell death

Previous experiment showed that 1,25(OH)₂D₃ could enhance iron uptake leading to elevated intracellular iron in osteoblasts (Fig 3). To verify the effects of 1,25(OH)₂D₃ on osteoblast viability in the presence of iron, UMR-106 cells were pre-treated with 1,25(OH)₂D₃ for 72 h, then 1,25(OH)₂D₃ coupled with Fe³⁺ (FAC) or Fe²⁺ (FAS) for 24 h. Osteoblast viability was compared between vehicle and 1,25(OH)₂D₃-treated cells with the same concentration of Fe³⁺

and Fe²⁺ treatments. As shown in Fig 4A, $1,25(OH)_2D_3$ treatment led to decreased osteoblast viability from 55.79% to 48.49% at 100 μ M, from 53.54% to 45.98% in 200 μ M and from 45.01% to 40.35% in 300 μ M of FAC treated groups. However, no statistically significant difference was found. Similar effects were also shown in FAS treated groups. Osteoblast viability was decreased from 64.88% to 56.75% in 100 μ M, from 60.86% to 55.25% in 200 μ M and from 55.92% to 52.17% in 300 μ M of FAS treated groups in the presence of 1,25(OH)₂D₃ (Fig 4B). Even though the further reduction in osteoblast viability was noted in osteoblasts treated with iron together with 1,25(OH)₂D₃, none of these results showed statistically different between the vehicle control and 1,25(OH)₂D₃ treatments.

Deferiprone diminished 1,25(OH)₂D₃-induced intracellular iron in osteoblasts

To further verify whether intracellular iron level relates to iron-induced osteoblast cell death under iron overload or not, effects of iron chelator on intracellular iron in osteoblasts under iron overload with FAC and FAS were tested. Deferiprone (DFP) was an iron chelator used to protect the excess iron in iron overload patients [28,29]. Therefore, this experiment aimed to study effects of DFP on intracellular iron of osteoblasts under iron overload with or without 1,25(OH)₂D₃ stimulation. After cells were exposed to vehicle control or 1,25(OH)₂D₃ and iron treatments, osteoblasts were incubated with DFP prior to intracellular iron measurement by FAAS. Overall, intracellular iron in osteoblast UMR-106 cells was decreased after the incubation with 100 μM deferiprone (Fig 5). In the absence of 1,25(OH)₂D₃, only high concentration of FAC at 300 μM could significantly raise intracellular iron in osteoblasts. No significant change was observed in other FAC or FAS treated groups; hence, the effect of DFP on the level of intracellular iron in these groups was not observed (Fig 5A). However, intracellular iron level in

osteoblasts treated with 300 μ M FAC was decreased significantly from 0.14 mg/mg proteins to 0.10 mg/mg proteins in the presence of DFP (Fig 5A). On the other hand, DFP notably lowered intracellular iron under 1,25(OH)₂D₃ stimulation from 0.11 to 0.09 mg/mg proteins in control groups, from 0.16 to 0.11 mg/mg proteins in 100 μ M, from 0.20 to 0.12 mg/mg proteins in 200 μ M and from 0.22 to 0.14 mg/mg proteins in 300 μ M FAC treated groups (Fig 5B). Similarly, intracellular iron in FAS together with 1,25(OH)₂D₃ treated osteoblasts also decreased from 0.14 to 0.10 mg/mg proteins in control groups, from 0.16 to 0.12 mg/mg proteins in 100 μ M, from 0.18 to 0.12 mg/mg proteins in 200 μ M and from 0.17 to 0.12 mg/mg proteins in 300 μ M FAS treated osteoblasts (Fig 5B). These results demonstrated that iron chelator, DFP, could reduce 1,25(OH)₂D₃-induced intracellular iron in osteoblasts from both iron exposure.

Deferiprone could not recover iron-induced osteoblast cell death

As previous experiment showed that deferiprone (DFP) could reduce intracellular iron in osteoblasts treated with FAC and FAS with and without 1,25(OH)₂D₃ (Fig 5). Effects of DFP on osteoblast cell survival under iron overload, especially those under 1,25(OH)₂D₃ stimulation were investigated. As shown in Fig 6A, FAC significantly reduced osteoblast cell survival in a dose-dependent manner both in vehicle control and DFP treated groups. While osteoblast cell survival was slightly improved in DFP treated groups: from 92.75% to 99.63%, from 73.54% to 75.66%, from 46.09% to 50.94% in osteoblasts treated with 30 μM, 100 μM and 200 μM FAC, respectively, none of these changes showed statistical significance. This effect could not be seen in osteoblasts treated with 300 μM FAC (Fig 6A). Similarly, dose-dependent inhibitory effects were also seen in FAS treated osteoblasts. However, a nonsignificant improvement of osteoblast cell survival was only seen in osteoblasts cells treated with 30 μM FAS from 93.83% in vehicle

control to 97.89% in DFP treated group. It is worth to note that long-term exposure of DFP also significantly reduced osteoblast cell survival by itself. Thereby, the further reduction in osteoblasts exposed to iron together with DFP was also observed (Fig 6A–B).

Extracellular calcium treatment recovered iron-induced osteoblast cell death

Hypocalcemia has been reported in thalassemia, which could worsen thalassemia and iron overload-induced osteoporosis [50–52]. Giving that calcium supplement could be one of the therapeutic agents for thalassemia and iron overload-induced osteoporosis, the direct effects of extracellular calcium on osteoblast cell viability under iron overload have not been elucidated. In this experiment, osteoblast UMR-106 cell viability was determined in osteoblasts treated with FAC at 0, 30, 100 and 200 μM in the presence or absence of CaCl₂. Similar to results from previous experiments, this experiment also showed that FAC significantly reduced osteoblast cell viability in dose dependent manner. When extracellular calcium in a form of CaCl₂ was applied, deleterious effect of ferric on osteoblast was subsided in a dose-dependent manner of CaCl₂ (Fig 7). CaCl₂ at 1 mM was able to rescue osteoblasts from FAC-induced osteoblast cell death by 17.63% and 16.31% in 100 and 200 μM FAC, respectively. More profound effects were shown in a higher concentration of CaCl₂. Our results showed that osteoblast cell death was recovered by 25.38%, 32.61% and 25.43% in 30, 100 and 200 μM FAC treated groups in the presence of 2.5 mM CaCl₂ (Fig 7).

Both Fe³⁺ and Fe²⁺ induced cellular reactive oxygen species (ROS) production

in osteoblasts

Reactive oxygen species (ROS) were shown to be associated with iron toxicity in several organs [53–55]. In this experiment, cellular ROS production in osteoblasts treated with FAC and FAS was measured to investigate whether this activity was related to iron-induced osteoblast cell death by both iron species. As shown in Fig 8A, FAC at 30, 100, and 200 µM significantly increased osteoblast ROS production to 1.39, 1.54 and 1.68-fold, respectively as compared to the control group (0 µM). In the same way, levels of cellular ROS in osteoblasts exposed to FAS was also increased significantly to 1.30 and 1.67-fold in 100 and 200 µM FAS treated groups as compared to control (Fig 8B). Hence, ROS level was increased in osteoblasts treated with both FAC and FAS in a dose-dependent manner.

Fe³⁺ and Fe²⁺ caused G0/G1 cell cycle arrest in osteoblasts

To investigate the involvement of iron-induced cell growth inhibition in osteoblasts, cell cycle distribution of iron-treated UMR-106 cells was analyzed by flow cytometry. UMR-106 cells were treated with 0 (control), 30, 100, 200 and 300 μ M of FAC or FAS for 72 h. The results showed that the percentage of cell population in the G0/G1 phase was significantly increased in 200 and 300 μ M FAC-treated groups as compared to the corresponding control (Fig. 9F). Similar results could be seen in osteoblasts treated with 200 μ M FAS (Fig. 10F). However, no significant change was observed in the S and G2/M phases. Our results thus suggested that FAC and FAS could induce cell cycle arrest in G0/G1 phase, resulting in cell growth inhibition in osteoblasts.

Discussion

426

427

428

429

430

431

432

433

434

435

436

437

438

439

440

441

442

443

444

445

446

447

448

Osteoporosis in thalassemia and other iron overload-related diseases has been documented by many studies as reviewed in [45,56,57]. Interestingly, the information about the direct effects of iron on osteoblasts is still limited. As the two biological available forms of iron, our previous study was the first study to compare the direct deleterious effects of ferric (Fe³⁺) and ferrous (Fe²⁺) on osteoblast cell viability, proliferation and differentiation [20]. Similarly, previous studies from other groups also showed negative effects of iron on osteoblasts [9,58-61]. In this study, direct effects of Fe³⁺ and Fe²⁺ on the expression of osteoblast differentiation markers upon iron exposure were examined and compared. While both Fe³⁺ and Fe²⁺ did not significantly alter the expression of most osteoblast differentiation markers, both iron species markedly inhibited ALP expression (Fig 1). Similar to the previously reported data showing that Fe³⁺ had stronger negative effects on osteoblasts than Fe²⁺ [20], Fe³⁺ also showed the stronger suppressive effects on ALP expression in osteoblasts than Fe²⁺ in this study. These results also corresponded to the previous reports that both Fe³⁺ and Fe²⁺ could impair ALP activity [20,41,60,62,63]. A few studies also suggested the inhibitory roles of iron on the expression of osteoblast differentiation markers in C2C12 myoblast cells and human bone marrow multipotent mesenchymal stem cells (BMSCs) [9,64]. Accordingly, these results suggested that both iron species could have higher inhibitory effects on osteoblast differentiation markers in osteoblast precursor cells during osteogenic induction than in committed osteoblast cells. Interestingly, a slight induction of collagen 1A and OCN expression was observed in FAC treated groups (Fig 1E and G). Similar induction was observed in previous studies where OCN expression was non statistically increased in C2C12 cells treated with ferric sulfate [64]. Our results also showed that collagen type 1A mRNA expression was slightly increased in the presence of 300 µM FAC at 24 h, but

this induction disappeared in the later time points (Fig 1E). This corresponded to previous studies showing that collagen I protein was down-regulated in osteoblasts treated with long-term exposure of FAC [41]. Future experiments can also be done to determine protein expression of these osteoblast differentiation markers. However, previous studies reported that the alterations of mRNA and protein expression of these osteoblast differentiation markers were well correlated in iron-treated osteoblasts and BMSCs [9,41]. ALP is an enzyme functioning in osteoblast mineralization by hydrolyzing inorganic pyrophosphate to phosphate for hydroxyapatite formation [65]. Hence, the effects of Fe³⁺ and Fe²⁺ on osteoblast mineralization from the measurement of calcium deposition in osteoblasts themselves and in peripheral extracellular matrices were further investigated. Our results also confirmed that FAC (Fe³⁺) inhibited osteoblast mineralization significantly and with the stronger degree than FAS (Fe²⁺). Although long-term exposure of certain iron concentration could also affect osteoblast viability, our previous published data [20] and results from the present study (Fig. 1) showed that both Fe²⁺ and Fe³⁺ could suppress ALP activity and expression in UMR-106 cells. Therefore, a decreased ALP function may contribute to the negative effects of Fe²⁺ and Fe³⁺ on mineralization shown in this study.

449

450

451

452

453

454

455

456

457

458

459

460

461

462

463

464

465

466

467

468

469

470

471

In addition to direct effects of iron overload on bone cells that could aggravate osteoporosis, hypocalcemia and certain hormone deficiency may also contribute to osteoporosis. Interestingly, hypocalcemia and vitamin D deficiency have also been reported in thalassemia patients and animals, which could also contribute to thalassemia-induced osteoporosis [66,67]. Hypocalcemia was also evidenced in hemochromatosis [68]. Accordingly, vitamin D and/or calcium supplement may be treatment options for iron overload-induced osteoporosis. Previous study in our laboratory also demonstrated calcium absorption impairment in thalassemic mice.

Moreover, administration of iron transport inhibitor, hepcidin or vitamin D₃ could restore calcium transport in thalassemic mice [49]. These findings suggested that calcium transport had an inverse correlation with iron absorption in intestine. Our previous report also showed that both iron species could enhance intracellular iron in osteoblast exposed to FAC and FAS in a dose-dependent manner [20]. Moreover, similar set of iron transporters found in intestinal cells were also expressed in osteoblasts [20], but the direct effects of vitamin D on osteoblast iron uptake has never been elucidated. Therefore, effects of 1,25(OH)₂D₃ on intracellular iron of osteoblast and on osteoblast viability under iron overload with FAC and FAS were investigated. Our results showed that, surprisingly, 1,25(OH)₂D₃ significantly induced intracellular iron in osteoblasts treated with FAC and FAS (Fig 3). However, this increased intracellular iron in osteoblasts did not significantly alter osteoblast survival under FAC and FAS treatments (Fig 4). Since the reciprocal interaction between calcium and iron transport has been proposed in intestinal cells or in intestine of thalassemic mice, our report suggested that this phenomenon might not occur in osteoblasts. There is no previous report about the effects of 1,25(OH)₂D₃ on iron uptake in osteoblasts. However, previous study in human hepatocellular carcinoma reported that 1,25(OH)₂D₃ could mediate iron homeostasis in HepG2 cells and monocytes by suppressing hepcidin expression but promoting ferroportin and ferritin expression [69]. This report supported our hypothesis that 1,25(OH)₂D₃ could also have a non-calciotropic effects on osteoblasts leading to higher iron uptake capacity. Nevertheless, the mechanism behind 1,25(OH)₂D₃induced intracellular iron in osteoblasts under iron overload still needs to be sought. Moreover, because the increased intracellular iron in osteoblasts treated with 1,25(OH)₂D₃ under iron overload did not significantly affect osteoblast cell viability (Fig 4), our results suggested that the level of intracellular iron did not directly correlate with osteoblast cell death under iron overload.

472

473

474

475

476

477

478

479

480

481

482

483

484

485

486

487

488

489

490

491

492

493

To further verify this speculation, iron chelator, deferiprone (DFP) was selected to examine the effects on intracellular iron of osteoblasts and osteoblast viability under iron overload. Our results demonstrated that DFP effectively reduced intracellular iron in osteoblasts treated with FAC and FAS, especially under 1,25(OH)₂D₃ stimulation (Fig 5). Interestingly, DFP could not significantly rescue osteoblasts (Fig 6). These results suggested that DFP could not be use as a therapeutic or preventive agent for osteoblasts under iron overload, and the level of intracellular iron did not relate to osteoblast cell death under iron overload with FAC and FAS.

495

496

497

498

499

500

501

502

503

504

505

506

507

508

509

510

511

512

513

514

515

516

517

Hypocalcemia has been reported in iron overload patients as mentioned, and vitamin D₃ did not show the promising results in osteoblast cell survival under iron overload (Fig 4). Therefore, calcium supplement could be another alternative to improve calcium homeostasis in thalassemia and iron overload patients. Accordingly, the direct effects of extracellular calcium treatment in a form of CaCl₂ on osteoblast cell survival under iron overload has been tested in this study. Interestingly, the results showed that CaCl₂ could effectively rescue osteoblasts from iron-induced osteoblast cell death (Fig 7). Even though the reciprocal interaction between calcium and iron transport has been suggested in intestine of thalassemia mice [49], our findings have already elaborated that this might not be the underlies rescue mechanism of iron-induced osteoblast cell death by CaCl2. This is because our results demonstrated that iron-induced osteoblast cell death was independent from the level of intracellular iron in osteoblasts (Figs 3, 4, 5 and 6). Instead, a few studies recently reported the beneficial effects of extracellular calcium on osteoblast cell proliferation and development [70,71]. Accordingly, the positive signals from extracellular calcium exposure on osteoblast cells might be able to counteract the negative signals from iron overload by FAC and FAS leading to the protective properties of extracellular calcium against iron-induced osteoblast cell death. Even if the mechanism behind the protective

activity of CaCl₂ was still unknown, extracellular calcium supplement or agents that could improve serum calcium level could be a strong candidate for the therapeutic agent for iron overload-induced osteoporosis, which could protect osteoblast cells from iron toxicity and improve hypocalcemia at the same time.

518

519

520

521

522

523

524

525

526

527

528

529

530

531

532

533

534

535

536

537

538

539

540

Several studies have reported that iron overload by FAC could lead to the increase of cellular reactive oxygen species (ROS) in osteoblasts leading to iron-induced osteoblast cell death [60,61,72,73]. Previous studies showed that increased ROS production could induce cell cycle arrest in osteoblasts [74,75]. However, there is no report whether Fe²⁺ could also induce ROS production in osteoblasts, and whether the two biological available iron species, Fe³⁺ and Fe²⁺, increased a comparable level of ROS production in osteoblasts. Accordingly, ROS production in UMR-106 osteoblast cells exposed to both Fe3+ and Fe2+ was investigated and compared. The results showed that both iron species could induce ROS production in UMR-106 cells with the stronger degree from Fe³⁺ (Fig 8). Moreover, Fe³⁺ and Fe²⁺ were found to induce G0/G1 cell cycle arrest in UMR-106 cells (Figs. 9 and 10), consistent with the correlation between ROS production and G0/G1 cell cycle arrest as reported previously in MC3T3-E osteoblast-like cells [75]. Therefore, we speculated that both iron species used similar mechanism to induce osteoblast cell death via ROS production, and the use of chemical agents that could protect cells from ROS or inhibit ROS production could be another possible way to protect osteoblasts from iron-induced osteoblast cell death. More studies are needed to further elucidate this possibility.

In summary, this study provided crucial information about differential effects of two iron species, Fe³⁺ and Fe²⁺, on osteoblast cell differentiation, mineralization and ROS production as well as effects of potential therapeutic agents of osteoblast cell death under iron overload. In

addition, effects of 1,25(OH)₂D₃ on iron uptake capacity by osteoblasts and the protective property of extracellular CaCl₂ on osteoblast cell death under iron overload were firstly discovered. This study has provided the essential data for targeted therapeutic design for specific iron species contributing to osteoblast toxicity in patients with iron overload-induced osteoporosis. Last but not least we have shown that an increase in extracellular calcium by any mean may be beneficial for this group of patients.

Disclosure statement

The authors have declared that no competing interests exist.

Acknowledgments

This work was supported by the research grants from Mahidol University-Multidisciplinary Research Cluster Grant (to N. Charoenphandhu and K. Lertsuwan), the Research Grant for New Scholar from Thailand Research Fund (TRF) through the TRF, Office of the Higher Education Commission (OHEC) and Mahidol University (MRG6180268 to K. Lertsuwan), TRF International Research Network Program (IRN60W0001 to N. Charoenphandhu), TRF Senior Research Scholar Grant (RTA6080007 to N. Charoenphandhu), the CIF and CNI grant, Faculty of Science, Mahidol University (to N. Charoenphandhu and K. Lertsuwan), and the Research Assistant Grant, Faculty of Science, Mahidol University (to N. Charoenphandhu). J. Teerapornpuntakit was supported by the TRF-OHEC Research Grant for New Scholar (MRG6280198).

564 References

- 1. Franchini M. Hereditary iron overload: update on pathophysiology, diagnosis, and treatment.
- 566 Am J Hematol. 2006;81(3):202–9.
- 567 2. Kohgo Y, Ikuta K, Ohtake T, Torimoto Y, Kato J. Body iron metabolism and
- pathophysiology of iron overload. Int J Hematol. 2008;88(1):7–15.
- 3. Olynyk JK. Hereditary haemochromatosis: diagnosis and management in the gene era.
- 570 Liver. 1999;19(2):73–80.
- 4. Anderson ER, Shah YM. Iron homeostasis in the liver. Compr Physiol. 2013;3(1):315–30.
- 572 5. Raghupathy R, Manwani D, Little JA. Iron overload in sickle cell disease. Adv Hematol.
- 573 2010;2010:272940. doi: 10.1155/2010/272940
- 574 6. Anderson GJ. Mechanisms of iron loading and toxicity. Am J Hematol. 2007;82(12)
- 575 Suppl):1128–31.
- 576 7. Esposito BP, Breuer W, Sirankapracha P, Pootrakul P, Hershko C, Cabantchik ZI. Labile
- 577 plasma iron in iron overload: redox activity and susceptibility to chelation. Blood.
- 578 2003;102(7):2670–7.
- 8. Shander A, Cappellini MD, Goodnough LT. Iron overload and toxicity: the hidden risk of
- multiple blood transfusions. Vox Sang. 2009;97(3):185–97.
- 581 9. Balogh E, Tolnai E, Nagy B, Jr., Nagy B, Balla G, Balla J, et al. Iron overload inhibits
- osteogenic commitment and differentiation of mesenchymal stem cells via the induction of
- ferritin. Biochim Biophys Acta. 2016;1862(9):1640–9.
- 584 10. Jensen CE, Tuck SM, Agnew JE, Koneru S, Morris RW, Yardumian A, et al. High
- prevalence of low bone mass in thalassaemia major. Br J Haematol. 1998;103(4):911–5.

- 586 11. Panich V, Pornpatkul M, Sriroongrueng W. The problem of thalassemia in Thailand.
- Southeast Asian J Trop Med Public Health. 1992;23:1–6.
- 588 12. Sheftel AD, Mason AB, Ponka P. The long history of iron in the Universe and in health and
- disease. Biochim Biophys Acta. 2012;1820(3):161–87.
- 590 13. Evstatiev R, Gasche C. Iron sensing and signalling. Gut. 2012;61(6):933–52.
- 591 14. Ganz T, Nemeth E. Iron imports. IV. Hepcidin and regulation of body iron metabolism. Am
- J Physiol Gastrointest Liver Physiol. 2006;290(2):G199–203.
- 593 15. Papanikolaou G, Pantopoulos K. Systemic iron homeostasis and erythropoiesis. IUBMB
- 594 Life. 2017;69(6):399–413.
- 595 16. Philippe MA, Ruddell RG, Ramm GA. Role of iron in hepatic fibrosis: one piece in the
- 596 puzzle. World J Gastroenterol. 2007;13(35):4746–54.
- 597 17. Dev S, Babitt JL. Overview of iron metabolism in health and disease. Hemodial Int.
- 598 2017;21:S6–S20.
- 599 18. Tsay J, Yang Z, Ross FP, Cunningham-Rundles S, Lin H, Coleman R, et al. Bone loss
- caused by iron overload in a murine model: importance of oxidative stress. Blood.
- 601 2010;116(14):2582–9.
- 602 19. Thongchote K, Svasti S, Teerapornpuntakit J, Suntornsaratoon P, Krishnamra N,
- 603 Charoenphandhu N. Bone microstructural defects and osteopenia in hemizygous β^{IVSII-654}
- knockin thalassemic mice: sex-dependent changes in bone density and osteoclast function.
- 605 Am J Physiol Endocrinol Metab. 2015;309(11):E936–48.
- 606 20. Lertsuwan K, Nammultriputtar K, Nanthawuttiphan S, Phoaubon S, Lertsuwan J,
- Thongbunchoo J, et al. Ferrous and ferric differentially deteriorate proliferation and
- differentiation of osteoblast-like UMR-106 cells. Biometals. 2018;31(5):873–89.

- 609 21. Guo X, Bai Y, Zhang L, Zhang B, Zagidullin N, Carvalho K, et al. Cardiomyocyte
- differentiation of mesenchymal stem cells from bone marrow: new regulators and its
- 611 implications. Stem Cell Res Ther. 2018;9(1):44. doi: 10.1186/s13287-018-0773-9
- 612 22. La Noce M, Mele L, Laino L, Iolascon G, Pieretti G, Papaccio G, et al. Cytoplasmic
- interactions between the glucocorticoid receptor and HDAC2 regulate osteocalcin
- expression in VPA-treated MSCs. Cells. 2019;8(3). doi: 10.3390/cells8030217.
- 23. Huang X, Wang Z, Li D, Huang Z, Dong X, Li C, et al. Study of microRNAs targeted Dvl2
- on the osteoblasts differentiation of rat BMSCs in hyperlipidemia environment. J Cell
- 617 Physiol. 2018;233(9):6758–66.
- 618 24. Liu TM, Lee EH. Transcriptional regulatory cascades in Runx2-dependent bone
- development. Tissue Eng Part B Rev. 2013;19(3):254–63.
- 620 25. van Driel M, Pols HA, van Leeuwen JP. Osteoblast differentiation and control by vitamin D
- and vitamin D metabolites. Curr Pharm Des. 2004;10(21):2535–55.
- 622 26. van Driel M, van Leeuwen J. Vitamin D endocrinology of bone mineralization. Mol Cell
- 623 Endocrinol. 2017;453:46–51.
- 624 27. Li J, Padwa BL, Zhou S, Mullokandova J, LeBoff MS, Glowacki J. Synergistic effect of
- 625 1α,25-dihydroxyvitamin D₃ and 17β-estradiol on osteoblast differentiation of pediatric
- 626 MSCs. J Steroid Biochem Mol Biol. 2018;177:103–8.
- 28. Victor Hoffbrand A. Deferiprone therapy for transfusional iron overload. Best Pract Res
- 628 Clin Haematol. 2005;18(2):299–317.
- 29. Mobarra N, Shanaki M, Ehteram H, Nasiri H, Sahmani M, Saeidi M, et al. A Review on iron
- chelators in treatment of iron overload syndromes. Int J Hematol Oncol Stem Cell Res.
- 631 2016;10(4):239–47.

- 30. Pautke C, Schieker M, Tischer T, Kolk A, Neth P, Mutschler W, et al. Characterization of
- osteosarcoma cell lines MG-63, Saos-2 and U-2 OS in comparison to human osteoblasts.
- 634 Anticancer Res. 2004;24(6):3743–8.
- 31. Carinci F, Papaccio G, Laino G, Palmieri A, Brunelli G, D'Aquino R, et al. Comparison
- between genetic portraits of osteoblasts derived from primary cultures and osteoblasts
- obtained from human pulpar stem cells. J Craniofac Surg. 2008;19(3):616–25.
- 638 32. Atkins D, Hunt NH, Ingleton PM, Martin TJ. Rat osteogenic sarcoma cells: isolation and
- effects of hormones on the production of cyclic AMP and cyclic GMP. Endocrinology.
- 640 1977;101(2):555–61.
- 641 33. Chauhan S, Sharma A, Upadhyay NK, Singh G, Lal UR, Goyal R. In-vitro osteoblast
- proliferation and in-vivo anti-osteoporotic activity of Bombax ceiba with quantification of
- Lupeol, gallic acid and beta-sitosterol by HPTLC and HPLC. BMC Complement Altern
- 644 Med. 2018;18(1):233. doi: 10.1186/s12906-018-2299-1
- 34. Mitchell J, Rouleau MF, Goltzman D. Biochemical and morphological characterization of
- parathyroid hormone receptor binding to the rat osteosarcoma cell line UMR-106.
- 647 Endocrinology. 1990;126(5):2327–35.
- 648 35. Pacifici R, Civitelli R, Rifas L, Halstead L, Avioli LV. Does interleukin-1 affect intracellular
- calcium in osteoblast-like cells (UMR-106)? J Bone Miner Res. 1988;3(1):107–11.
- 650 36. Partridge NC, Alcorn D, Michelangeli VP, Ryan G, Martin TJ. Morphological and
- biochemical characterization of four clonal osteogenic sarcoma cell lines of rat origin.
- 652 Cancer Res. 1983;43(9):4308–14.
- 653 37. Stanford CM, Jacobson PA, Eanes ED, Lembke LA, Midura RJ. Rapidly forming apatitic
- 654 mineral in an osteoblastic cell line (UMR 106-01 BSP). J Biol Chem. 1995;270(16):9420–8.

- 655 38. Ganguly S, Ashley LA, Pendleton CM, Grey RD, Howard GC, Castle LD, et al.
- Characterization of osteoblastic properties of 7F2 and UMR-106 cultures after acclimation
- to reduced levels of fetal bovine serum. Can J Physiol Pharmacol. 2008;86(7):403–15.
- 658 39. Juhász T, Matta C, Katona É, Somogyi C, Takács R, Hajdú T, et al. Pituitary adenylate
- cyclase-activating polypeptide (PACAP) signalling enhances osteogenesis in UMR-106 cell
- line. J Mol Neurosci. 2014;54(3):555–73.
- 40. Wang BL, Dai CL, Quan JX, Zhu ZF, Zheng F, Zhang HX, et al. Parathyroid hormone
- regulates osterix and Runx2 mRNA expression predominantly through protein kinase A
- signaling in osteoblast-like cells. J Endocrinol Invest. 2006;29(2):101–8.
- 41. Zhao GY, Zhao LP, He YF, Li GF, Gao C, Li K, et al. A comparison of the biological
- activities of human osteoblast hFOB1.19 between iron excess and iron deficiency. Biol
- 666 Trace Elem Res. 2012;150(1–3):487–95.
- 42. Zhou J, Chen KM, Zhi DJ, Xie QJ, Xian CJ, Li HY. Effects of pyrite bioleaching solution of
- 668 Acidithiobacillus ferrooxidans on viability, differentiation and mineralization potentials of
- rat osteoblasts. Arch Pharm Res. 2015;38(12):2228–40.
- 43. Abuna RPF, Oliveira FS, Ramos JIR, Lopes HB, Freitas GP, Souza ATP, et al. Selection of
- 671 reference genes for quantitative real-time polymerase chain reaction studies in rat
- osteoblasts. J Cell Physiol. 2018;234(1):749–56.
- 44. Riss TL, Moravec RA, Niles AL, Duellman S, Benink HA, Worzella TJ, et al. Cell Viability
- Assays. In: Sittampalam GS, Grossman A, Brimacombe K, Arkin M, Auld D, Austin CP, et
- al., editors. Assay Guidance Manual. Bethesda (MD)2004.
- 45. Balogh E, Paragh G, Jeney V. Influence of iron on bone homeostasis. Pharmaceuticals
- 677 (Basel). 2018;11(4). doi: 10.3390/ph11040107

- 678 46. Yamasaki K, Hagiwara H. Excess iron inhibits osteoblast metabolism. Toxicol Lett.
- 679 2009;191(2–3):211–5.
- 47. Soliman A, Salama H, Alomar S, Shatla E, Ellithy K, Bedair E. Clinical, biochemical, and
- radiological manifestations of vitamin D deficiency in newborns presented with
- hypocalcemia. Indian J Endocrinol Metab. 2013;17(4):697–703.
- 48. Sultan S, Irfan SM, Ahmed SI. Biochemical markers of bone turnover in patients with β-
- 684 thalassemia major: A single center study from Southern Pakistan. Adv Hematol.
- 685 2016;2016:5437609. doi: 10.1155/2016/5437609
- 49. Kraidith K, Svasti S, Teerapornpuntakit J, Vadolas J, Chaimana R, Lapmanee S, et al.
- Hepcidin and 1,25(OH)₂D₃ effectively restore Ca²⁺ transport in β-thalassemic mice:
- reciprocal phenomenon of Fe²⁺ and Ca²⁺ absorption. Am J Physiol Endocrinol Metab.
- 689 2016;311(1):E214–23.
- 690 50. De Sanctis V, Borsari G, Brachi S, Gubellini E, Gamberini MR, Carandina G. A rare cause
- of heart failure in iron-overload thalassaemic patients-primary hypoparathyroidism.
- 692 Georgian Med News. 2008;(156):111–3.
- 51. Tangngam H, Mahachoklertwattana P, Poomthavorn P, Chuansumrit A, Sirachainan N,
- 694 Chailurkit L, et al. Under-recognized hypoparathyroidism in thalassemia. J Clin Res Pediatr
- 695 Endocrinol. 2018;10(4):324–30.
- 52. Aleem A, Al-Momen AK, Al-Harakati MS, Hassan A, Al-Fawaz I. Hypocalcemia due to
- hypoparathyroidism in β-thalassemia major patients. Ann Saudi Med. 2000;20(5–6):364–6.
- 698 53. Bystrom LM, Guzman ML, Rivella S. Iron and reactive oxygen species: friends or foes of
- 699 cancer cells? Antioxid Redox Signal. 2014;20(12):1917–24.

- 700 54. Galaris D, Pantopoulos K. Oxidative stress and iron homeostasis: mechanistic and health
- 701 aspects. Crit Rev Clin Lab Sci. 2008;45(1):1–23. doi: 10.1080/10408360701713104
- 702 55. Formanowicz D, Radom M, Rybarczyk A, Formanowicz P. The role of Fenton reaction in
- ROS-induced toxicity underlying atherosclerosis modeled and analyzed using a Petri net-
- 704 based approach. Biosystems. 2018;165:71–87.
- 705 56. Jeney V. Clinical impact and cellular mechanisms of iron overload-associated bone loss.
- 706 Front Pharmacol. 2017;8:77. doi: 10.3389/fphar.2017.00077
- 707 57. Lertsuwan K, Wongdee K, Teerapornpuntakit J, Charoenphandhu N. Intestinal calcium
- transport and its regulation in thalassemia: interaction between calcium and iron metabolism.
- 709 J Physiol Sci. 2018;68(3):221–32.
- 710 58. Diamond T, Pojer R, Stiel D, Alfrey A, Posen S. Does iron affect osteoblast function?
- 711 Studies in vitro and in patients with chronic liver disease. Calcif Tissue Int. 1991;48(6):373–
- 712 9.
- 713 59. Messer JG, Kilbarger AK, Erikson KM, Kipp DE. Iron overload alters iron-regulatory genes
- and proteins, down-regulates osteoblastic phenotype, and is associated with apoptosis in
- 715 fetal rat calvaria cultures. Bone. 2009;45(5):972–9.
- 716 60. He YF, Ma Y, Gao C, Zhao GY, Zhang LL, Li GF, et al. Iron overload inhibits osteoblast
- 517 biological activity through oxidative stress. Biol Trace Elem Res. 2013;152(2):292–6.
- 718 61. Tian Q, Wu S, Dai Z, Yang J, Zheng J, Zheng Q, et al. Iron overload induced death of
- osteoblasts in vitro: involvement of the mitochondrial apoptotic pathway. PeerJ.
- 720 2016;4:e2611. doi: 10.7717/peerj.2611

- 721 62. Yang J, Zhang J, Ding C, Dong D, Shang P. Regulation of osteoblast differentiation and iron
- content in MC3T3-E1 cells by static magnetic field with different intensities. Biol Trace
- 723 Elem Res. 2018;184(1):214–25.
- 724 63. Zhang D, Wong CS, Wen C, Li Y. Cellular responses of osteoblast-like cells to 17 elemental
- 725 metals. J Biomed Mater Res A. 2017;105(1):148–58.
- 726 64. Yang Q, Jian J, Abramson SB, Huang X. Inhibitory effects of iron on bone morphogenetic
- protein 2-induced osteoblastogenesis. J Bone Miner Res. 2011;26(6):1188–96.
- 728 65. Orimo H. The mechanism of mineralization and the role of alkaline phosphatase in health
- 729 and disease. J Nippon Med Sch. 2010;77(1):4–12.
- 730 66. Zaino EC, Yeh JK, Aloia J. Defective vitamin D metabolism in thalassemia major. Ann N Y
- 731 Acad Sci. 1985;445:127–34.
- 732 67. Aloia JF, Ostuni JA, Yeh JK, Zaino EC. Combined vitamin D parathyroid defect in
- 733 thalassemia major. Arch Intern Med. 1982;142(4):831–2.
- 734 68. Jeong HK, An JH, Kim HS, Cho EA, Han MG, Moon JS, et al. Hypoparathyroidism and
- subclinical hypothyroidism with secondary hemochromatosis. Endocrinol Metab (Seoul).
- 736 2014;29(1):91–5.
- 69. Bacchetta J, Zaritsky JJ, Sea JL, Chun RF, Lisse TS, Zavala K, et al. Suppression of iron-
- regulatory hepcidin by vitamin D. J Am Soc Nephrol. 2014;25(3):564–72.
- 739 70. Modi PK, Prabhu A, Bhandary YP, Shenoy PS, Hegde A, Es SP, et al. Effect of calcium
- glucoheptonate on proliferation and osteogenesis of osteoblast-like cells in vitro. PLoS One.
- 741 2019;14(9):e0222240. doi: 10.1371/journal.pone.0222240

- 742 71. Mitran V, Ion R, Miculescu F, Necula MG, Mocanu AC, Stan GE, et al. Osteoblast cell
- response to naturally derived calcium phosphate-based materials. Materials (Basel).
- 744 2018;11(7). doi: 10.3390/ma11071097
- 745 72. Ke JY, Cen WJ, Zhou XZ, Li YR, Kong WD, Jiang JW. Iron overload induces apoptosis of
- murine preosteoblast cells via ROS and inhibition of AKT pathway. Oral Dis.
- 747 2017;23(6):784–94.
- 748 73. Doyard M, Fatih N, Monnier A, Island ML, Aubry M, Leroyer P, et al. Iron excess limits
- 749 HHIPL-2 gene expression and decreases osteoblastic activity in human MG-63 cells.
- 750 Osteoporos Int. 2012;23(10):2435–45.
- 751 74. Li M, Zhao L, Liu J, Liu AL, Zeng WS, Luo SQ, et al. Hydrogen peroxide induces G2 cell
- 752 cycle arrest and inhibits cell proliferation in osteoblasts. Anat Rec (Hoboken).
- 753 2009;292(8):1107–13.
- 754 75. Liu W, Zhao Z, Na Y, Meng C, Wang J, Bai R. Dexamethasone-induced production of
- reactive oxygen species promotes apoptosis via endoplasmic reticulum stress and autophagy
- 756 in MC3T3-E1 cells. Int J Mol Med. 2018;41(4):2028–36.

757

758

759

Figure captions

- 760 Fig 1. The expression of osteoblast differentiation markers in UMR-106 cells upon FAC and
- 761 FAS exposure at 24, 48 and 72 h was determined by qRT-PCR. (A-B) Runx2, (C-D) alkaline
- 762 phosphatase (ALP), (E-F) collagen I alpha (1A), and (G-H) osteocalcin expression upon FAC
- and FAS exposure. *P < 0.05, **P < 0.01, ***P < 0.001 as compared to control group (0 μ M).

765 Fig 2. Quantified data from alizarin red S staining depicting calcium deposition of UMR-106 766 cells under iron overload with (A) FAC and (B) FAS. Both FAC and FAS significantly 767 decreased osteoblast calcium deposition. **P < 0.01, ***P < 0.001 as compared to control group 768 $(0 \mu M)$. 769 770 Fig 3. Intracellular iron was measured in UMR-106 cells exposed to (A) FAC and (B) FAS in the 771 presence of 1,25(OH)₂D₃ or vehicle control. 1,25(OH)₂D₃ significantly induced intracellular iron 772 in osteoblasts treated with FAC and FAS. *P < 0.05, **P < 0.01 ***P < 0.001 as compared to control group (0 μ M) with vehicle control; $^{\#}P < 0.01$, $^{\#\#}P < 0.001$ as compared to the same 773 774 dose of iron between vehicle and 1,25(OH)₂D₃ treatment. 775 776 Fig 4. UMR-106 osteoblast cell viability was tested under the presence of (A) FAC or (B) FAS 777 together with vehicle control or 1,25(OH)₂D₃. 1,25(OH)₂D₃ did not significantly affect osteoblast cell viability under iron overload with FAC and FAS. ***P < 0.001 as compared to control 778 779 group (0 µM) with vehicle control. 780 781 Fig 5. Intracellular iron in osteoblast UMR-106 cells after treated with (A) FAC and (B) FAS 782 under the stimulation of vehicle control or 1,25(OH)₂D₃ in the presence or absence of 783 deferiprone (DFP). DFP significantly reduced intracellular iron in osteoblasts treated with FAC 784 and FAS. The more profound reduction was observed in the groups under 1,25(OH)₂D₃ stimulation. **P < 0.01 ***P < 0.001 as compared to control group (0 μ M) without DFP. $^{\#}P < 0.001$ 785 0.05, ##P < 0.01, ###P < 0.001 as compared to the same iron concentration. 786

788 Fig 6. Osteoblast cell viability under iron overload from (A) FAC and (B) FAS in the presence of 789 deferiprone (DFP). DFP could not recover iron-induced osteoblast cell death in both FAC and FAS treated groups. **P < 0.01 ***P < 0.001 as compared to control group (0 µM) without 790 791 DFP. $^{\#\#}P < 0.001$ as compared to the same iron concentration. 792 793 Fig 7. Effects of extracellular CaCl₂ on UMR-106 osteoblast cell survival under iron overload 794 with FAC were illustrated. Osteoblast cell viability was significantly improved ***P < 0.001 as 795 compared to control group (0 μ M) with vehicle control; *##P < 0.001 as compared to 30 μ M FAC in vehicle control group; ${}^{\$}P < 0.05$, ${}^{\$\$\$}P < 0.001$ as compared to 100 μ M FAC in vehicle control 796 group; $^{\dagger}P < 0.05$, $^{\dagger\dagger\dagger}P < 0.001$ as compared to 200 μ M FAC in vehicle control group. 797 798 799 Fig 8. Intracellular reactive oxygen species (ROS) production in osteoblast cells treated with (A) 800 FAC and (B) FAS was evaluated. Both FAC and FAS significantly increased ROS production in osteoblasts. ***P < 0.001 as compared to control group (0 μ M); $^{\#}P < 0.05$, $^{\#\#}P < 0.01$, $^{\#\#}P < 0.01$ 801 0.001 as compared to 30 μ M of iron; ${}^{\$}P < 0.05$, ${}^{\$\$\$}P < 0.001$, as compared to 100 μ M of iron. 802 803 804 Fig 9. Cell cycle distribution of UMR-106 cells treated with 30, 100, 200 or 300 μM FAC. (A-805 E) Representative figures of cell cycle distribution as determined by flow cytometry. Quantified 806 data showing percent cell distribution in G0/G1 phases (F), S phase (G) and G2/M phases (H). *P < 0.05 as compared to control group (0 μ M); PI, propidium iodide. 807 808 809

810	Fig 10. Cell cycle distribution of UMR-106 cells treated with 30, 100, 200 or 300 μM FAS. (A–
811	E) Representative figures of cell cycle distribution as determined by flow cytometry. Quantified
812	data showing percent cell distribution in G0/G1 phases (F), S phase (G) and G2/M phases (H).
813	* P < 0.05 as compared to control group (0 μ M); PI, propidium iodide.
814	
815	Captions for supporting information files
816	
817	S1 Table. <i>Rattus norvegicus</i> primers used in the qRT-PCR experiments.
818	
819	S1 Fig. Represent images of calcium mineralization by alizarin red staining of UMR-106 cells
820	treated with FAC (A) and FAS (B).
821	

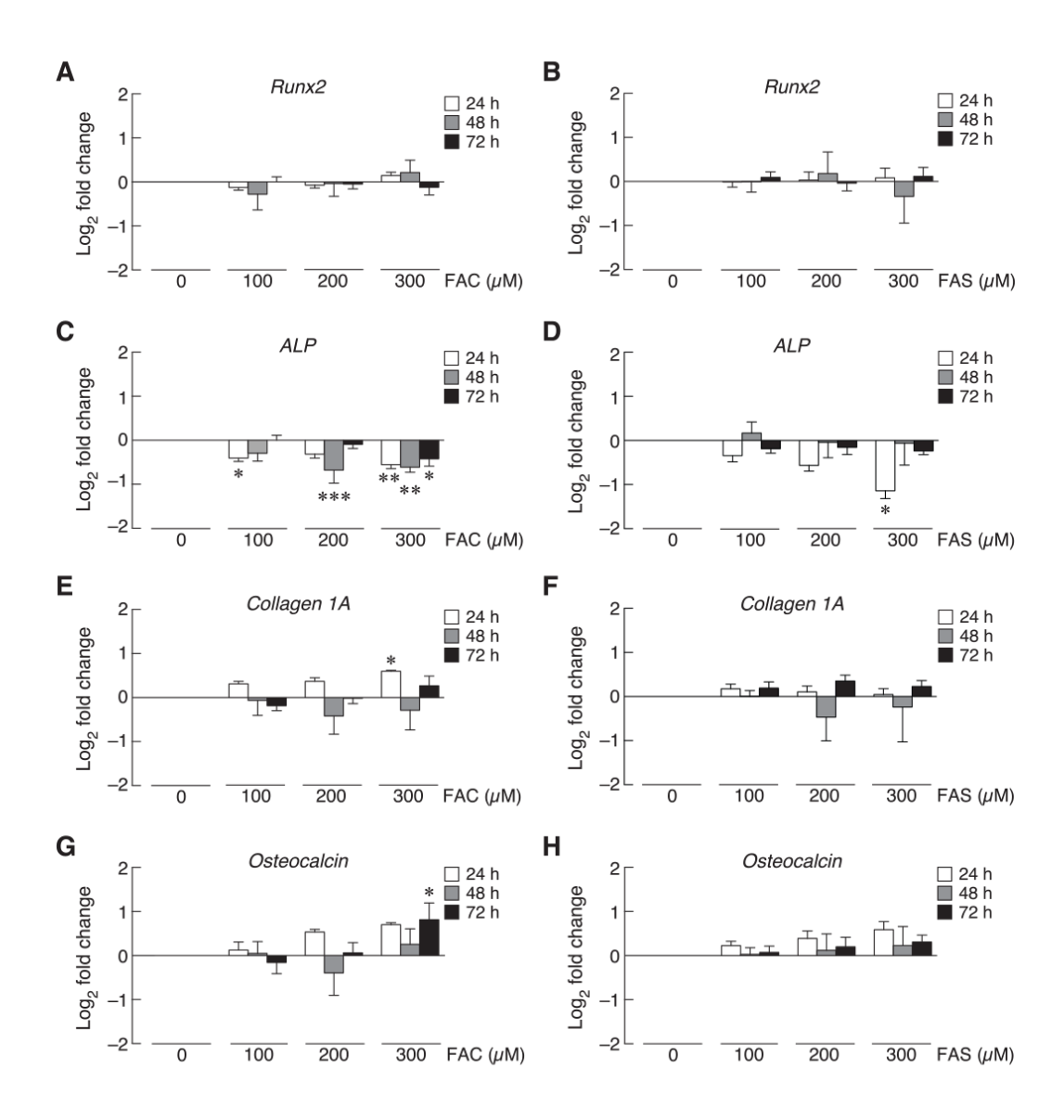


Figure 1: Lertsuwan et al.

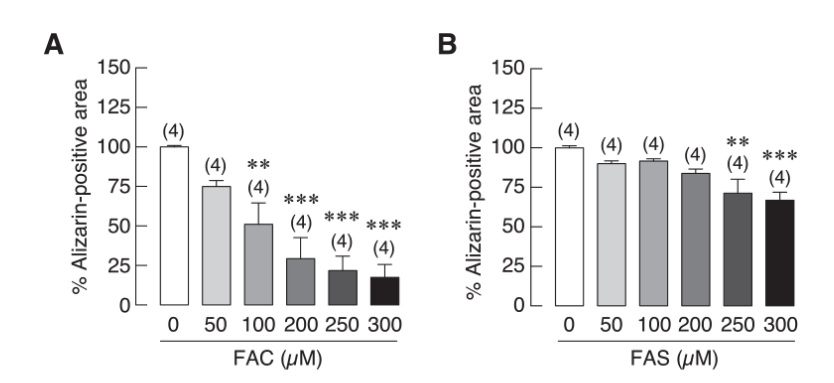
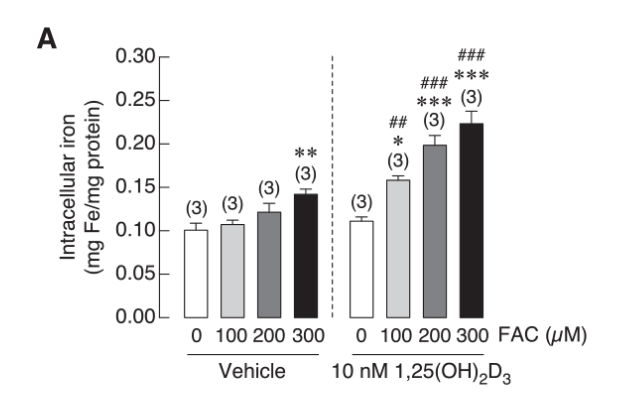


Figure 2: Lertsuwan et al.



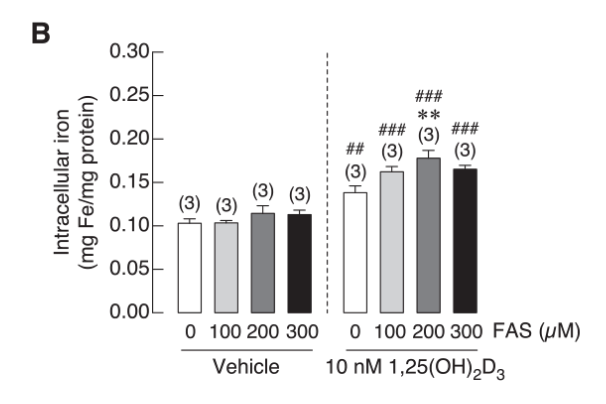


Figure 3: Lertsuwan et al.

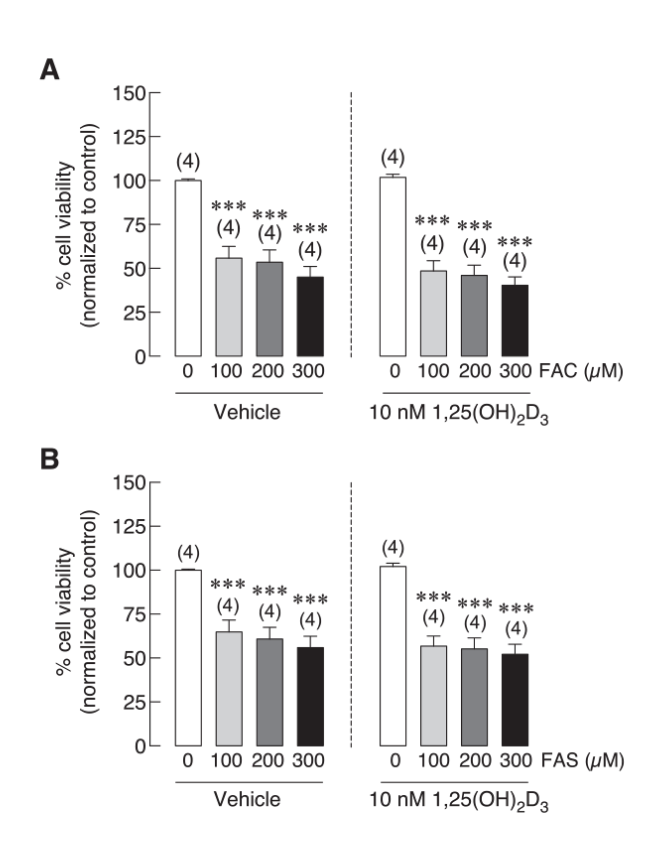


Figure 4: Lertsuwan et al.

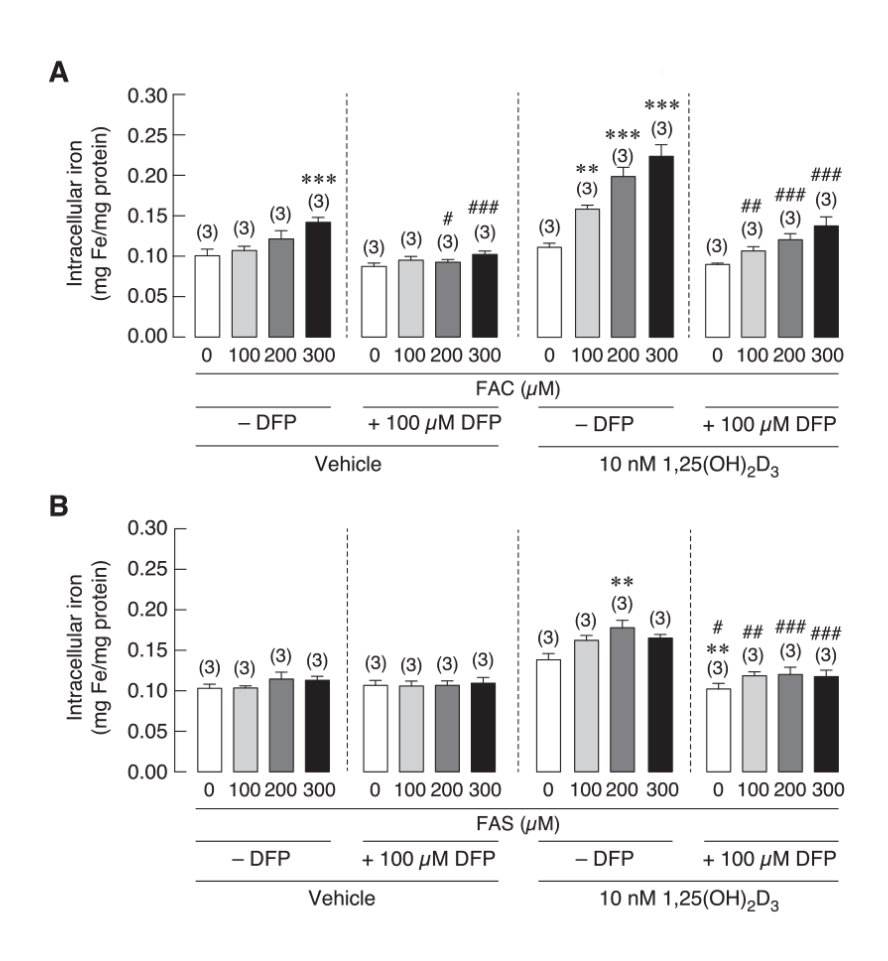


Figure 5: Lertsuwan et al.

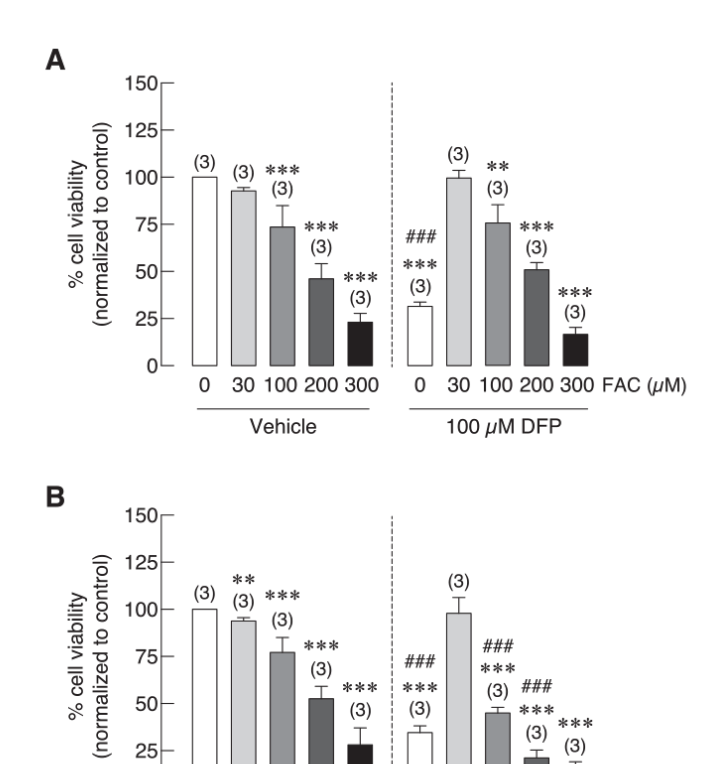


Figure 6: Lertsuwan et al.

0

0

30 100 200 300

Vehicle

0

30 100 200 300 FAS (μM)

100 μM DFP

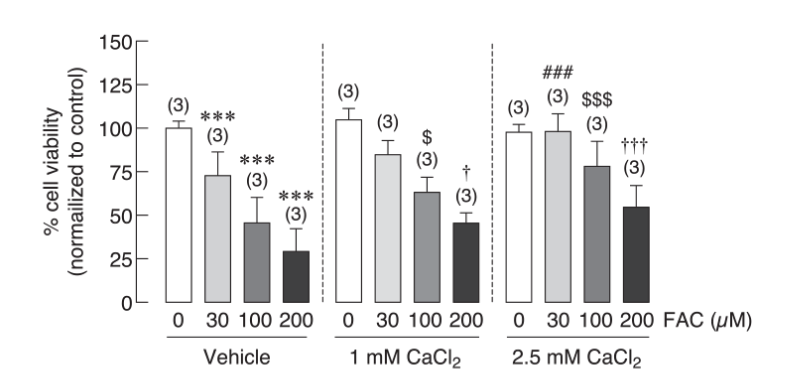


Figure 7: Lertsuwan et al.

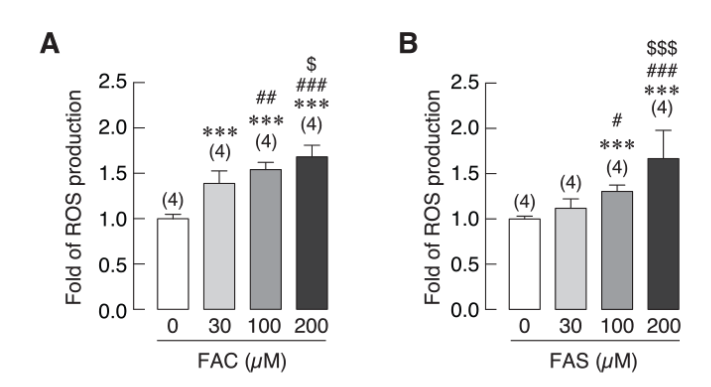


Figure 8: Lertsuwan et al.

OUTPUTS

Proceeding in an international conference

Comparative Effects of Ferric and Ferrous on
Osteoblast Cell Survival and Function





Comparative Effects of Ferric and Ferrous on Osteoblast Cell Survival and Function

Supanan Nanthawuttiphan¹, Narattaphol Charoenphandhu^{2,3,4,5}, Kornkamon Lertsuwan^{1,2*}

¹Department of Biochemistry, Faculty of Science, Mahidol University, Bangkok 10400, Thailand

²Center of Calcium and Bone research, Faculty of Science, Mahidol University, Bangkok 10400, Thailand

³Institute of Molecular Biosciences, Mahidol University, Nakhon Pathom 73170, Thailand

⁴Department of Physiology, Faculty of Science, Mahidol University, Bangkok 10400, Thailand

⁵The Academy of Science, The Royal Society of Thailand, Bangkok 10300, Thailand

*E-mail: kornkamon.ler@mahidol.edu

Abstract: Iron overload is commonly found in several diseases including hemochromatosis and thalassemia, potentially from the upregulated iron absorption and blood transfusion. Iron overload has been shown to negatively affect bone formation. Not surprisingly, osteoporosis is commonly found in these patients. There are two forms of iron existing in biological systems: ferric (Fe³⁺) and ferrous (Fe²⁺), which come from different sources. In this study, comparative effects of the two iron forms on osteoblast were studied. UMR-106 cells were treated with ferric ammonium citrate (FAC) or ferrous ammonium sulfate (FAS) representing ferric and ferrous, respectively. Our results showed that both FAC and FAS significantly decreased osteoblast cell viability. In addition, they could lead to the expression alteration of osteoblastic, osteoclastogenic and NADPH oxidases in osteoblast at different degree. Overall, FAC showed markedly stronger inhibitory effects on osteoblast cell survival and function than FAS. Lastly, ROS production from osteoblast after both iron exposure was observed. This indicated the potential mechanism of iron-mediated osteoblast cell death via ROS-mediated pathway.

1. Introduction

There are many diseases that iron overload could be found, such as thalassemia, osteoporosis, and hemochromatosis. Excess iron can damage several organs including heart, spleen, and liver. Moreover, iron negatively overload also affects metabolism by disrupting the balance of osteoblast and osteoclast cell function in bone remodeling mechanism. These two cells have the opposite functions. Osteoblast cells make new bone for bone formation, while the osteoclasts release enzyme to degrade bone¹. Osteoblasts and osteoclasts regulate each other function via the expression of

Osteoblastic and osteoclastogenic genes. Osteoblastic genes are the genes that activate osteoblast function and/or suppress osteoclast function involving in a bone generation, such as Cyclooxygenase 2 (Cox-2), Erythropoietin-producing human hepatocellular receptors B4 (Eph B4), Erythropoietin-producing human hepatocellular receptor-interacting protein B2 (Ehrin B2), and Osteoprotegerin (OPG) genes. On the other hand, osteoclastogenic genes are the genes regulating osteoclast cell function for bone resorption, such as Receptor activator of nuclear factor kappa-B ligand (RANKL), Interleukin 1 beta (IL-1β),





Monocyte Chemoattractant Protein-1 (MCP-1), Interleukin 6 (IL-6), and Macrophage colony-stimulating factor (MCSF) genes².

The human body receives 2 forms of iron including ferric (Fe3+) from vegetable and grains and ferrous (Fe2+) from meat or blood transfusion³. Even though iron is an essential component in many proteins and enzymes in the human body, excess iron can become toxic. The deposition of iron in many organs can induce oxidative stress by reactive oxygen species (ROS) production. ROS contains oxygen species, which are very active and can oxidize and damage other molecules in the body. Examples of ROS found in animal cells are hydrogen peroxide (H₂O₂), superoxide anion (O₂*-) and hydroxyl radical (HO'). ROS can be generated from the activity of several enzymes including xanthine oxidoreductase (XOR), myeloperoxidase (MPO), and nicotinamide adenine dinucleotide phosphate oxidases (NADPH oxidases or NOXs)4.

NOXs are the ROS producing enzymes located the inner-membrane mitochondria. NOXs family contains 5 subtypes including NOX1, NOX2, NOX3, NOX4, and NOX5. They are similar in function, while their structures are different. The major role of these enzymes is to transfer electron passing the membrane of mitochondria. However, excess NOXsderived ROS compounds can damage biomolecules such as nucleic acids, lipids, and proteins^{5,6}.

In previous studies, iron overload with FAC suppressed human osteoblast cells (hFOB1.19) activity through the increasing of intracellular ROS level⁷. Moreover, iron overload was accumulated in bone leading to the reduction of trabecular and cortical bones volume of 2-month-old C57/BL6 male

mice^{7,8}. In the present study, the comparative effects of ferric and ferrous on osteoblast and the correlation between NOXs and iron toxicity in osteoblast are studied.

2. Materials and Methods

2.1 Cell culture

UMR-106 osteoblast cells (American Type Culture Collection, ATCC, no. CRL-1661) were purchased from ATCC and cultured in Dulbecco's modified Eagle's medium (DMEM) (Sigma. MO, USA) supplemented with 10% fetal bovine serum (FBS) (PAA Laboratories, Pasching, Austria) and 100 U/mL penicillin-streptomycin (Gibco, NY, USA). They were maintained at 37 °C with 5% CO₂. Ferric ammonium citrate (FAC) (Sigma MO, USA) and ferrous ammonium sulfate (FAS) (Sigma MO, USA) were used as ferric and ferrous treatments, respectively.

2.2 Cell viability assay

UMR-106 cells were seeded at 2.5×10^3 cells/well in 96-well plate (Corning, NY, USA). After 24 hours, iron treatment was added at 0, 3, 10, 30, 100, 300, 1000, 3000 μM. The treatments were refreshed every day for 72 hours. After that, old media was removed; then MTT dye (3-(4,5dimethylthiazol-2-yl)-2,5-diphenyltetrazolium bromide) (Sigma Aldrich, MO, USA) was added to the final concentration of 1.2 mM. The cells were incubated for 3 hours, and stop solution (10% of SDS in 50% N, N-Dimethyl formamide) (Sigma life science, Japan and Daejung, Korea) was added 100 µL/well. Cell viability was measured at 595 nm.

2.3 Quantitative real time polymerase chain reaction (qRT-PCR)

One microgram of an RNA template from UMR-106 cells after iron exposure was mixed





with 4 μL of iScript RT super mix (Bio-rad, CA, USA) and adjusted the total volume of 20 μL with RNAse-free DNase I water (Roche, IN, USA). Then, the RNA was reverse transcribed to cDNA. The cDNA was mixed with Ssofast supermix (Bio-rad, CA, USA) and primers. The primers used in this study included NOX1 primers, NOX4 primers, and hypoxanthine phosphoribosyltransferase 1 (Hprt1) primers. The sequences of primers were listed in Table 1. The qPCR reaction was performed on Real-Time PCR machine (CFX ConnectTM, Bio-rad, USA).

Table 1 Rattus norvegicus primers used for qRT-PCR

Gene	Primer (forward/reverse)
NOX 1	5'-CCCTTTGCTTCCTTCTTGAAATC-3'
	5'-GCACCCGTCTCTCTACAAATCC-3'
NOX 4	5'-CTGCATCTGTCCTGAACCTCAA-3'
	5'-TCTCCTGCTAGGGACCTTCTGT-3'
Hprt 1	5'-GGCCAGAC <mark>TTTGTTGGATTTG-3'</mark>
	5'-CTTTCGCT <mark>G</mark> ATGACACAA <mark>A</mark> CAT-3'

2.4 Calcium deposition staining

UMR-106 cells were seeded at 2×10^4 cells/well in 24-well plate (Corning, NY, USA). After 24 hours, the cells were treated with FAC at 0, 10, 30, and 100 μM. The treatments were changed every other day. After 120 hours of treatment, old media was removed and gently washed with 1X phosphate buffer saline (PBS) for 3 times. Next, the cells were fixed with cold 70% ethanol for 1 hour. After that, ethanol was removed, and the cells were washed with DI water 3 times. Then, DI water was removed, and 40mM alizarin red s was added to stain the calcium deposition for 5 minutes. After 5 minutes, the cells were washed with 1X PBS until the buffer came out clear. The cells were then observed under a light microscope.

2.5 ROS detection assay

UMR-106 cells were seeded at 2.5×10⁴ cells/well in 96-black well plate (Corning, NY, USA). After 24 hours, ROS production was measured by using DCFDA cellular ROS detection assay kit (Abcam, USA). The cells were washed with 1X buffer. DCFDA solution was added 100 μL/well, and the cells were incubated for 45 minutes. They were washed with 1X buffer again, then iron treatment was added at 0 and 200 μM and incubated for 6 hours. ROS production was measured with a fluorescence microplate reader (SparkTM 10M multimode microplate reader, Switzerland) at Ex/Em: 485/535 nm.

3. Results & Discussion

3.1 Ferric and ferrous iron differently suppressed osteoblast cell viability

UMR-106 cells were treated with FAC or FAS at varies concentrations including 0 (control), 3, 10, 30, 100, 300, 1000 and 3000 μM. The percentage cell viability of UMR-106 cells was significantly reduced after FAC or FAS exposure with the increasing iron concentration. A half inhibitory concentration (IC₅₀) of FAC and FAS on UMR-106 cells were 250 μM (Figure 1) and 285 μM (Figure 2), respectively. These data corresponded to previous—studies—from—*Yamasaki*—and *Hagiwara* in 2009 and *Tian* et al. in 2016 showed that FAC decreased cell viability of MC3T3-E1 osteoblasts cell^{9,10}.





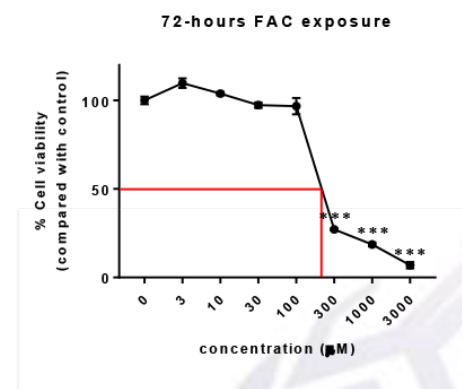


Figure 1 FAC exposure significantly reduced UMR-106 cell viability (*** $p \le 0.001$ compared with control)

After the comparison of iron IC₅₀ on UMR-106, we found that FAC has a stronger effect on UMR-106 cell viability than FAS.

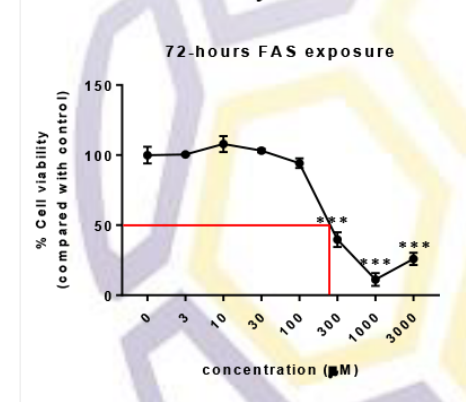


Figure 2 FAS exposure significantly reduced UMR-106 cell viability (*** $p \le 0.001$ compared with control)

3.2 Ferric and ferrous iron differently induced osteoblastic, osteoclastogenic, and NADPH oxidases (NOXs) gene expression

Our recently published data showed that the level of osteoblastic and osteoclastogenic genes expression was altered differently after FAC and FAS exposure². FAC exposure slightly increased osteoblastic OPG, Cox-2, and Ephrin B2 expression. Similarly, FAS exposure also moderately increased the

expression of OPG and Cox-2, but it decreased the expression of Eph B4 and Ephrin B2 as compared to control. On the other hand, FAC exposure led to the significant increase in osteoclastogenic IL-6 and MCP-1 expressions, and FAS exposure resulted in the increased IL-6 and MCP-1 expressions as compared with control². These results showed that iron treatment led to a more significant increase in osteoclastogenic genes expression than osteoblastic genes; hence, iron exposure could result in the higher bone resorption through the upregulated osteoclastogenic genes.

To investigate the potential mechanism of iron toxicity on osteoblast UMR-106 cells, the expression of NOXs after iron exposure was investigated. Even though the results were not statistically significant, NOX1 gene was slightly increased in UMR-106 cells after FAC or FAS exposure (Figure 3). On the other hand, NOX4 gene expression was not significantly changed after FAC or FAS exposure (Figure 4). Both iron exposures had an overall effect on the expression of NOX1 gene more than NOX4 gene.

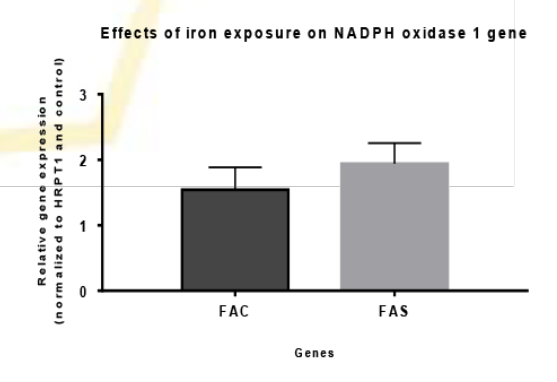


Figure 3 The expression level of NOX1 gene was slightly increased in UMR-106 cells after FAC or FAS exposure





Effects of iron exposure on NADPH oxidase 4 gene

Figure 4 The expression level of NOX4 gene was slightly increased in UMR-106 cells after FAC or FAS exposure

3.3 Ferric iron negatively affected calcium deposition activity of osteoblasts

UMR-106 cells were treated with FAC at 0 (control), 10, 30, and 100 µM. After 24 hours of iron exposure, results showed that 10 μM FAC did not significantly affect calcium deposition ability of UMR-106 the calcium deposition was However, markedly decreased after 30 and 100 µM of FAC exposure (Figure 5). Therefore, FAC exposure suppressed calcium deposition ability of osteoblast UMR106 cells. These results were similar to the previous study showed that ferrous sulfate or FAS treatment reduced extracellular matrix calcium content in human bone mesenchymal stem cells¹¹.

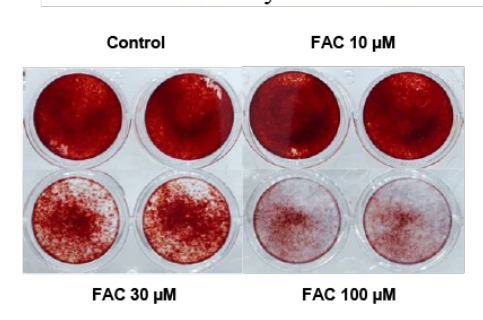


Figure 5 FAC exposure reduced calcium deposition in UMR-106 cell

3.4 Ferric and ferrous iron stimulated ROS production in osteoblasts

UMR-106 cells were treated with FAC or FAS at 200 µM for 6 hours. After FAC exposure, the intracellular ROS production in UMR-106 cells was significantly increased to approximately 1.7-fold as compared to control (Figure 6). In the same way, cellular ROS production was significantly increased to around 1.6-fold as compared with control after FAS exposure (Figure 7). These results corresponded to the previous study in mice, which showed that iron dextran treatment (a ferric oxyhydroxide complex) led to the increase of ROS production in bone marrow mononuclear cells (BMMNCs), hematopoietic progenitor cells (HPCs), and hematopoietic stem cells (HSCs) cells¹². Our results showed that both FAC and FAS could induce ROS production in osteoblast UMR-106 cells.

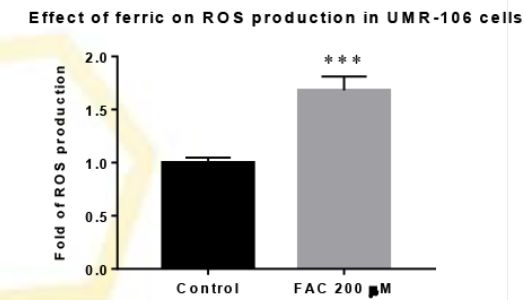


Figure 6 FAC exposure significantly induced ROS production in UMR-106 cells (*** $p \le 0.001$ compared with control)





Effect of ferrous on ROS production in UMR-106 cells

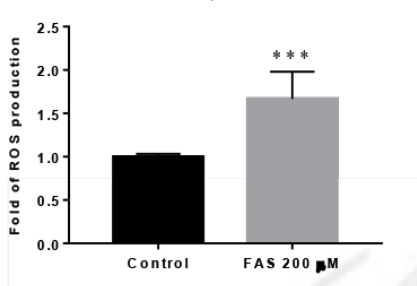


Figure 7 FAS exposure significantly increased ROS production in UMR-106 cells (*** $p \le 0.001$ compared with control)

4. Conclusion

Iron overload showed negative effects on osteoblast cells, the pivotal cells for bone formation in our body. Cytotoxicity of FAC or FAS exposure on osteoblast UMR-106 cells was shown in this study. Both iron species significantly decreased osteoblast cell viability in a dose-dependent manner. A half inhibitory concentration (IC₅₀) on UMR-106 cells were 250 µM for FAC and 285 µM for respectively. These results were consistent with the previous study that both iron species could reduce cell viability^{2,9,10}. The expression level of osteoblastic and osteoclastogenic genes was differently affected by FAC and FAS iron exposures². The expression level of NOX1 gene was increased with both iron exposures, while the expression level of NOX4 gene was not changed. The staining of calcium deposition after iron exposure showed that 100 µM of **FAC** significantly inhibited calcium deposition in UMR-106 cells. Intracellular ROS level of the UMR106 cells was significantly increased to approximately 1.7fold and 1.6-fold after FAC and FAS exposure as compared with control, respectively. In conclusion, our results were

consistent with the previous study that iron overload suppressed osteoblast cell survival and function^{7,8}. We also showed that both iron species could induce NOX1 expression and intracellular ROS production. This suggested the mechanism of iron toxicity in osteoblast is via ROS production, potentially by NOX1 activity.

Acknowledgements

This work was supported by Grants from Thailand Research Fund (TRF) through TRF International Research Network Program (IRN60W0001 to K. Wongdee and N. Charoenphandhu), the TRF Senior Research Scholar Grant (RTA6080007 Charoenphandhu), Research Grant for New Scholar from TRF, Office of the Higher Education Commission and Mahidol University (MRG6180268 to K. Lertsuwan) and the CIF grant, Faculty of Science, Mahidol University.

References

- 1. Kini, U.; Nandeesh, B., Physiology of bone formation, remodeling, and metabolism. In *Radionuclide and hybrid bone imaging*, Fogelman, I.; Gnanasegaran, G.; Van der Wall, H., Eds. Springer: 2013; Vol. 2, pp 29-57.
- 2. Lertsuwan, K.; Nammultriputtar, K.; Nanthawuttiphan, S.; Phoaubon, S.; Lertsuwan, J.; Thongbunchoo, J.; Wongdee, K.; Charoenphandhu, N., Ferrous and ferric differentially deteriorate proliferation and differentiation of osteoblast-like UMR-106 cells. *BioMetals* **2018**, *31* (5), 873-889.
- 3. Fuqua, B. K.; Vulpe, C. D.; Anderson, G. J., Intestinal iron absorption. *Journal of*





Trace Elements in Medicine and Biology **2012**, 26 (2-3), 115-119.

- 4. Bayır, H., Reactive oxygen species. *Critical Care Medicine* **2005**, *33* (12), S498-S501.
- 5. Bedard, K.; Krause, K.-H., The NOX family of ROS-Generating NADPH oxidases: physiology and pathophysiology. *Physiological reviews* **2007**, *87* (1), 245-313.
- 6. Mary, V. S.; Theumer, M. G.; Arias, S. L.; Rubinstein, H. R., Reactive oxygen species sources and biomolecular oxidative damage induced by aflatoxin B1 and fumonisin B1 in rat spleen mononuclear cells. *Toxicology* **2012**, *302* (2), 299-307.
- 7. He, Y.-F.; Ma, Y.; Gao, C.; Zhao, G.-y.; Zhang, L.-L.; Li, G.-F.; Pan, Y.-Z.; Li, K.; Xu, Y.-J., Iron overload inhibits osteoblast biological activity through oxidative stress. *Biological Trace Element Research* **2013**, *152* (2), 292-296.
- 8. Tsay, J.; Yang, Z.; Ross, F. P.; Cunningham-Rundles, S.; Lin, H.; Coleman, R.; Mayer-Kuckuk, P.; Doty, S. B.; Grady, R. W.; Giardina, P. J.; Boskey, A. L.; Vogiatzi, M. G., Bone loss caused by iron overload in a murine model: importance of oxidative stress. *Blood* 2010, *116* (14), 2582-2589.
- 9. Tian, Q.; Wu, S.; Dai, Z.; Yang, J.; Zheng, J.; Zheng, Q.; Liu, Y., Iron overload induced death of osteoblasts in vitro: involvement of the mitochondrial apoptotic pathway. *PeerJ* **2016**, *4*, e2611.
- 10. Yamasaki, K.; Hagiwara, H., Excess iron inhibits osteoblast metabolism. *Toxicology Letters* **2009**, *191*(2-3), 211-215.
- 11. Balogh, E.; Tolnai, E.; Jr., B. N.; Nagy, B.; Balla, G.; Balla, J.; Jeney, V., Iron overload inhibits osteogenic commitment and

differentiation of mesenchymal stem cells via the induction of ferritin. *Biochimica et Biophysica Acta (BBA)-Molecular Basis of Disease* **2016**, *1862(9)*, 1640-1649.

12. Chai, X.; Li, D.; Cao, X.; Zhang, Y.; Mu, J.; Lu, W.; Xiao, X.; Li, C.; Meng, J.; Chen, J.; Li, Q.; Wang, J.; Meng, A.; Zhao, M., ROS-mediated iron overload injures the hematopoiesis of bone marrow by damaging hematopoietic stem/progenitor cells in mice. *Scientific Reports* 2015, 5, 10181.

Investigating the Involvement of Ferroptosis in Osteoblast Cell Death under Iron
Overload



Investigating the Involvement of Ferroptosis in Osteoblast Cell Death under Iron Overload

Natnicha Tannop¹, Narattaphol Charoenphandhu^{2,3,4,5}, Kornkamon Lertsuwan^{1,2*}

¹Department of Biochemistry, Faculty of Science, Mahidol University, Bangkok 10400, Thailand

²Center of Calcium and Bone research, Faculty of Science, Mahidol University, Bangkok 10400, Thailand

³Institute of Molecular Biosciences, Mahidol University, Nakhon Pathom 73170, Thailand

⁴Department of Physiology, Faculty of Science, Mahidol University, Bangkok 10400, Thailand

⁵The Academy of Science, The Royal Society of Thailand, Bangkok 10300, Thailand

*E-mail: kornkamon.ler@mahidol.edu

Abstract:

Iron overload is found in many diseases including hemochromatosis and thalassemia. Previous studies showed that ferric ammonium citrate (FAC) and ferrous ammonium sulfate (FAS) induced osteoblastic cell death, leading to osteoporosis. Recently, a new form of nonapoptotic cell death called ferroptosis has been recognized as a regulated cell death characterized by the iron-dependent lipid hydroperoxides accumulation. However, the involvement of ferroptosis mechanism in osteoblast cell death under iron overload is not known. Therefore, we aim to investigate whether both forms of iron can trigger ferroptosis pathway in osteoblasts under iron overload. To pursue this goal, the protective effects of ferroptosis inhibitor (ferrostatin-1) on osteoblast cell death under iron overload were evaluated. Our results showed that increased osteoblastic cell viability was observed in osteoblast cells exposed to FAC or FAS and ferrostatin-1 as compared to the ones treated with FAC or FAS alone. In addition, lipid peroxidation in osteoblast exposed to iron was evaluated. We found that iron treatments led to the increase of lipid peroxidation in osteoblasts. Lastly, effects of FAC on the expression of ferroptosis marker, glutathione peroxidase 4 (GPX4), were also determined by western blot. Our results showed that FAC decreased GPX4 level. Together these results suggested that both ferrous and ferric iron species induced osteoblastic cell death via ferroptosis pathway.

1. Introduction

Iron is an essential element for the survival of all living organisms. It is required for maintaining normal function of many proteins, such as hemoglobin and myoglobin and enzymes containing iron-sulfur cluster involving in electron transport chain. However, free iron is extremely toxic to cells.¹

Iron overload is a condition that excess iron accumulates in the body. One of the most common causes is hereditary hemochromatosis, the stage which a person absorbs too much iron from diet. Other causes of iron overload are multiple blood transfusions and hyper iron absorption in prolonged anemia patients, such as thalassemia. Deposition of iron causes organ dysfunction in several organs including heart,

liver and spleen. Moreover, there are many evidences showing that iron overload is also associated with bone loss and osteoporosis.³

Normally, bone loss occurs when the activities of osteoblast and osteoclast in bone remodeling process are imbalance.4 Osteoblasts are specialized bone formation cells; while, osteoclasts are responsible for bone degradation.5 Previous study showed that ferric ammonium citrate; FAC (Fe³⁺) and ferrous ammonium sulfate; FAS (Fe²⁺) could induce osteoblastic cell death via apoptosis pathway, especially in FAC-treated groups that showed higher levels of cleaved caspase 3 and caspase 7. Whereas, increasing of these apoptotic markers were not statically significant in FAS-treated groups regardless of their close EC₅₀.6 Therefore, these evidences lead us to investigate whether FAC



and FAS also trigger any other mechanisms of non-apoptotic cell death.

Ferroptosis is a regulated cell death mechanism characterized by the ironaccumulation dependent of lipid hydroperoxides.⁷ Another hallmark of ferroptosis is the inactivation of glutathione peroxidase 4 (GPX4), which is the enzyme functionally reduces membrane phospholipid hydroperoxides to suppress ferroptosis. Other hallmarks availability of redox-active iron and oxidation of polyunsaturated fatty acid phospholipids.8,9 (PUFA)-containing Because ferroptosis is iron-dependent, it can be inhibited by using ferrostatin-1 (Fer-1), which blocks lipid peroxidation by trapping peroxyl radicals in lipid bilayers of cell membrane.10 Recent studies indicated that ferroptosis linked to many diseases and conditions including neurodegenerative disease, ischemic injury of the brain, heart, liver and kidney.⁷ Therefore, suppressing ferroptosis may be used as a potential therapeutic target for treating all of these diseases.

In this study, the ultimate goal is to investigate whether both forms of iron also trigger ferroptosis pathway in osteoblasts under iron overload. Understanding the underlying mechanisms would lead to the discovery of therapeutic agents for protecting the patients from iron overload-induced osteoporosis.

2. Materials and Methods2.1 Cell culture and reagents

UMR-106 osteoblast cells were provided by center of calcium and bone research (COCAB), Mahidol University. They were maintained in Dulbecco's modified Eagle's medium (DMEM) (Gibco, NY, USA) supplemented with 10% fetal bovine serum (FBS) (Gibco, NY, USA), and 100 U/mL penicillin-streptomycin (Gibco, NY, USA). They were incubated at 37°C with 5% CO₂. Ferric ammonium citrate (FAC)

(Sigma, MO, USA) was used as ferric treatment, and ferrous ammonium sulfate (FAS) (Sigma, MO, USA) was used as ferrous treatment. FAC and FAS were used at the indicated concentrations. The ferrostatin-1 (Fer-1) concentration was at 0.5 μ M (Sigma, MO, USA).

2.2 Cell viability assay

UMR-106 cells were seeded at 1,000 cells/well in 96-well plate (Corning, NY, USA). After 24 hours, cells were treated with 0, 30 or 200 µM of FAC or FAS with or without Fer-1 (0.5 µM) for 72 hours. The treatment were refreshed every day. After that, cell viability was measured by using MTT (3-(4,5-dimethylthiazol-2-yl)-2,5diphenyltetrazolium bromide) assay. In short, MTT dye (Sigma Aldrich, MO, USA) was added to each well to achieve a final concentration of 1 mg/ml. Then, the cells were incubated at 37°C for 3 hours. After that, stop solution (10% of SDS in 50% N, N-Dimethyl-formamide) (Sigma life science, Japan and Daejung, Korea) was added 100 μL/well to dissolve formazan. Cell viability was measured at 595 nm by a microplate reader (Thermo, Multiskan EX).

2.3 Lipid peroxidation measurement

UMR-106 cells were seeded at 1.0 x 10⁵ cells/well in 6-well plate (Corning, NY, USA). After 24 hours, the cells were treated with 30 and 200 µM of FAC for 72 hours. The treatment were changed every day. After the treatment period, cells were harvested and washed with 1Xcold PBS. Lipid peroxidation was measured using a lipid peroxidation (MDA) assay kit (Abcam, USA) according to the manufacturer's instructions. The cells were homogenized in lysis solution containing BHT, which stops further sample peroxidation processing, using a dounce homogenizer on ice. Next, samples were centrifuged at 13,000 x g for 10 minutes and the supernatants were collected. To generate MDA-TBA adduct, TBA reagent was added into each sample and



standard, which was incubated at 95°C for 60 minutes and cooled down to room temperature for 10 minutes. After that, supernatant containing MDA-TBA adduct was taken and added into a 96-well microplate for analysis by fluorescence microplate reader (SparkTM 10M multimode microplate reader, Switzerland) at Ex/Em: 532/580 nm.

2.4 Western blot analysis

UMR-106 cells were seeded at 1.0 x 10⁵ cells/well in 6-well plate (Corning, NY, USA). Cells were treated with 0, 30, 100, 200 and 300 µM of FAC for 72 hours. The treatment were changed every day. After that, cell pellets were collected by scraping and washed twice with 1X cold phosphate buffer saline (PBS). Proteins were extracted by radioimmunoassay precipitation buffer containing 10% protease inhibitor for 1 hour on ice. Cell lysates were centrifuged at 7,500 rpm for 30 minutes and supernatants were collected. Protein concentration was measured by using BCA protein assay kit scientific, USA). Thirty-five (Thermo microgram of protein were separated through 8-15% acrylamide gel at 100 volts for 100 minutes and transferred to nitrocellulose membrane at 12 volts for 120 minutes. Membranes were blocked for 2 hours at room temperature in blocking solution (Capricorn Scientific, USA). After that, membranes were washed 3 times with TBST and incubated with specific antibody for GPX4 (Abcam, USA) and β-actin (Abcam, USA) overnight at 4°C. Then, membranes were wash 3 times with TBST and incubated with anti-rabbit IgG secondary antibody (Cell Signaling, USA). Protein was visualized by enhanced chemiluminescence (Millipore, USA) and exposed to X-ray film (GE Healthcare, UK). The band intensity was quantified by using Image J software.

3. Results & Discussion

3.1 Ferric and ferrous induced osteoblast cell death via ferroptosis pathway

To verify the involvement of ferroptosis in iron-treated osteoblast cells, the potent and specific ferroptosis inhibitor, ferrostatin-1 (Fer-1) was used. UMR-106 cells were treated with 0 (control), 30 and 200 µM of FAC or FAS with or without Fer-1 (0.5 µM) for 72 hours. The results showed that the percentage cell viability of UMR-106 cells was significantly reduced in FAC or FAS-treated groups in a concentrationdependent manner as compared to the control. Whereas, treating cells with both FAC or FAS and Fer-1 significantly increased osteoblastic cell viability as compared to cells treated with FAC or FAS alone (Figure 1 and 2). Therefore, these results suggested that FAC and FAS could induce osteoblastic cell death via ferroptosis pathway. Moreover, ferrostatin-1 could be the potential protective agent against ironinduced cytotoxicity in osteoblasts.

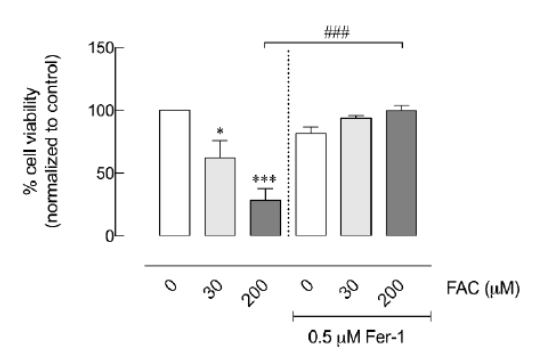


Figure 1. Ferrostatin-1 significantly increased cell viability in FAC-treated osteoblasts (* $p \le 0.05$, *** $p \le 0.001$ as compared to control, *## $p \le 0.001$ as compared to FAC-treated group)



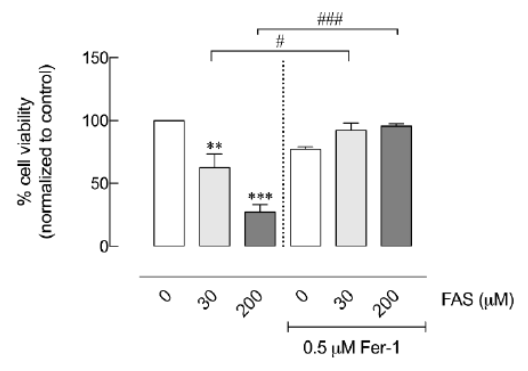


Figure 2. Ferrostatin-1 significantly increased cell viability in FAS-treated osteoblasts (** $p \le 0.01$, *** $p \le 0.001$ as compared to control, " $p \le 0.05$, "##" $p \le 0.001$ as compared to FAS-treated group)

3.2 Iron increased lipid peroxidation in osteoblasts

Ferroptosis is also characterized by the accumulation of lipid peroxides (products of lipid peroxidation) inside the cells. Lipid peroxidation leads to the oxidative degradation of lipids, especially polyunsaturated fatty acids (PUFA). The major end products of lipid peroxidation are malondialdehyde (MDA), 4-hvdroxvalkenals (4-HDA) and 2-alkenals. However, MDA has been widely used for many years as a convenient biomarker for lipid peroxidation.11

In this experiment, we firstly selected FAC for treating UMR-106 cells because previous study showed that FAC treatment had greater inhibitory effects on osteoblast viability than FAS treatment. Since FAC had a more profound effect on osteoblast cell death than FAS from our study and previous study, we expected that FAC would induce the significant level of lipid peroxides in osteoblasts. Hence, FAC was selected as a representative of iron treatment in this study.

To investigate and confirm the involvement of ferroptosis in iron-induced osteoblast cell death by measuring lipid peroxidation, the concentration of MDA in UMR-106 cells treated with 30 and 200 μ M

of FAC for 72 hours were measured. As expected, our study showed that FAC markedly increased lipid peroxidation in osteoblasts indicating that iron-induced osteoblast cell death also occurred through ferroptosis. However, this effect should also be evaluated in FAS-treated osteoblasts in the future study.

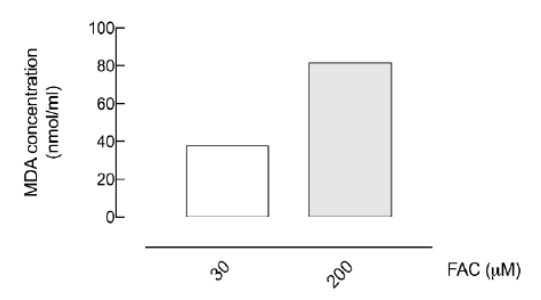


Figure 3. FAC increased MDA level in osteoblasts in a concentration-dependent manner.

3.3 Ferric treatments led to decreased glutathione peroxidase 4 (GPX4) level in osteoblasts

Inactivation of glutathione increase (GPX4) peroxidase can intracellular lipid peroxides, resulting in ferroptosis. Therefore, we would like to examine if treating osteoblast cells with FAC at different concentration would affect the level of GPX4 protein in osteoblasts. Moreover, GPX4 down-regulation is one of hallmark for ferroptosis.9 This experiment would confirm the involvement of ferroptosis in iron-induced osteoblast cell death.

To examine the effects of ferric on GPX4 level in osteoblasts, UMR-106 cells were treated with 0, 30, 100, 200 and 300 μ M of FAC for 72 hours before collecting protein samples for western blot analysis for GPX4.



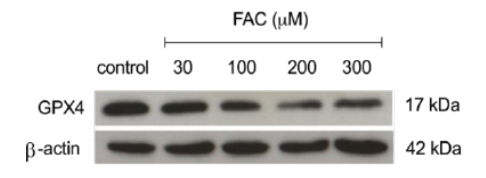


Figure 4. The expression level of GPX4 protein was slightly decreased in UMR-106 cells after FAC exposure in the representative blot.

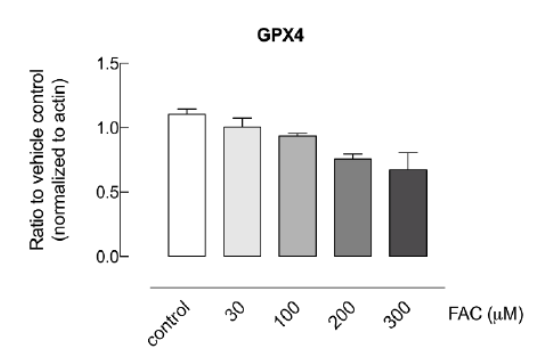


Figure 5. The quantified data showed the decreasing of GPX4 in UMR-106 cells exposed to FAC.

Even though the results were not statistically significant, the expression level of GPX4 protein was notably decreased after UMR-106 cells were treated with FAC in a dose-dependent manner (Figure 4 and 5). Our overall results showed that FAC reduced GPX4 level in osteoblasts.

4. Conclusion

Consistent with the previous study, our results also showed that both ferric and ferrous iron inhibited osteoblast cell viability in a dose-dependent manner. Moreover, previous study showed that FAC and FAS could induce osteoblast cell death via apoptosis pathway. In this study, our results suggested that both iron species also triggered other non-apoptotic cell death called ferroptosis. Ferrostation-1 (ferroptosis inhibitor) significantly increased osteoblast cell survival in FAC or FAS treated groups.

The results indicated that iron-induce osteoblastic cell death involved in ferroptosis pathway. To confirm this hypothesis, the investigation of other ferroptosis hallmarks were performed. We also showed that FAC could increase the accumulation of lipid peroxides in osteoblasts in a dose-dependent manner. The expression level of GPX4, negative regulator in ferroptosis process, also decreased after FAC exposure. In conclusion, our results were confirmed that iron overload could contribute to ferroptosis cell death in osteoblast cells. Therefore, suppression of ferroptosis can be used as a potential therapeutic target for preventing iron-induce cytotoxicity in osteoblasts.

Acknowledgements

This work was supported by Grants from Research Grant for New Scholar from TRF, Office of the Higher Education Commission and Mahidol University (MRG6180268 to K. Lertsuwan), the TRF Senior Research Scholar Grant (RTA6080007 to N. Charoenphandhu), and the CIF grant, Faculty of Science, Mahidol University.

References

- Paul, B. T.; Manz, D. H.; Torti, F. M.; Torti, S. V. Mitochondria and Iron: Current Questions. Expert Review of Hematology 2016, 10 (1), 65–79.
- Rotaru, I.; Gaman, A.; Gaman, G. Secondary Haemochromatosis in a Patient with Thalassemia Intermedia. Current health sciences journal 2014, 40 (1), 67-70.
- 3. Tsay, J.; Yang, Z.; Ross, F. P.; Cunningham-Rundles, S.; Lin, H.; Coleman, R.; Mayer-Kuckuk, P.; Doty, S. B.; Grady, R. W.; Giardina, P. J.; Boskey, A. L.; Vogiatzi, M. G. Bone Loss Caused by Iron Overload in a Murine Model: Importance of Oxidative Stress. *Blood* 2010, 116 (14), 2582–2589.



- 4. Hunter, D. J.; Sambrook, P. N. Bone Loss: Epidemiology of Bone Loss. *Arthritis Res* **2000**, *2* (6), 441–445.
- Raggatt, L. J.; Partridge, N. C. Cellular and Molecular Mechanisms of Bone Remodeling. *Journal of Biological Chemistry* 2010, 285 (33), 25103–25108.
- Lertsuwan, K.; Nammultriputtar, K.; Nanthawuttiphan, S.; Phoaubon, S.; Lertsuwan, J.; Thongbunchoo, J.; Wongdee, K.; Charoenphandhu, N. Ferrous and Ferric Differentially Deteriorate Proliferation and Differentiation of Osteoblast-like UMR-106 Cells. *BioMetals* 2018, 31 (5), 873– 889.
- Stockwell , B. R.; Friedmann, J. P. A.; Bayir , H. Ferroptosis: A Regulated Cell Death Nexus Linking Metabolism, Redox Biology, and Disease. *Cell* 2017, 171 (2), 273–285.
- 8. Yang, W. S.; Sriramaratnam, R.; Welsch, M. E.; Shimada, K.; Skouta, R.; Viswanathan, V. S.; Cheah, J. H.; Clemons, P. A.; Shamji, A. F.; Clish, C. B.; Brown, L. M.; Girotti, A. W.; Cornish, V. W.; Schreiber, S. L.; Stockwell, B. R. Regulation of Ferroptotic Cancer Cell Death by GPX4. Cell 2014, 156 (1-2), 317–331.

- 9. Dixon, J. S.; Stockwell, R. B. The Hallmarks of Ferroptosis. *Annual Review of Cancer Biology* **2019**, *3* (1), 2472–3428.
- Zilka, O.; Shah, R.; Li, B.; Angeli, J. P. F.; Griesser, M.; Conrad, M.; Pratt, D. A. On the Mechanism of Cytoprotection by Ferrostatin-1 and Liproxstatin-1 and the Role of Lipid Peroxidation in Ferroptotic Cell Death. ACS Central Science 2017, 3 (3), 232–243.
- 11. Ayala, A.; Muñoz, M. F.; Argüelles, S. Lipid Peroxidation: Production, Metabolism, and Signaling Mechanisms of Malondialdehyde and 4-Hydroxy-2-Nonenal. Oxidative Medicine and Cellular Longevity 2014, 2014, 1–31.